

DEEP BRAIN STIMULATION OF THE SUBTHALAMIC NUCLEUS INCREASES
BRAIN-DERIVED NEUROTROPHIC FACTOR IN THE CONTEXT OF
SYNUCLEINOPATHY

By

Kathryn M. Miller

A DISSERTATION

Submitted to
Michigan State University
in partial fulfillment of the requirements
for the degree of

Neuroscience – Doctor of Philosophy

2020

ABSTRACT

DEEP BRAIN STIMULATION OF THE SUBTHALAMIC NUCLEUS INCREASES BRAIN-DERIVED NEUROTROPHIC FACTOR IN THE CONTEXT OF SYNUCLEINOPATHY

By

Kathryn M. Miller

Parkinson's disease (PD) is the second most common neurodegenerative disorder behind Alzheimer's disease, and is a major burden to society. PD is a progressive disorder resulting in a variety of symptoms including dementia, autonomic, and motor dysfunction; all contributing to a diminished quality of life for afflicted individuals. Current treatments help to restore motor function, however there are no disease-modifying treatments that halt or slow the progression of PD. The question of whether deep brain stimulation (DBS) of the subthalamic nucleus (STN) can be disease-modifying in PD remains unanswered. Preclinical studies link STN DBS-mediated neuroprotection of nigrostriatal dopamine neurons to brain-derived neurotrophic factor (BDNF) signaling. However, the impact of STN DBS on α -synuclein (α -syn) aggregation, inclusion-associated neuroinflammation, and BDNF levels have yet to be examined in the context of synucleinopathy.

In this dissertation I examine the effects of STN DBS on BDNF in the preformed fibril synucleinopathy model. PFF injection resulted in accumulation of phosphorylated α -syn (pSyn) inclusions in the substantia nigra pars compacta (SNpc) and cortical areas. SNpc pSyn inclusions were associated with significantly increased major

histocompatibility complex-II immunoreactive (MHC-II-ir) microglia, and intensity, complexity, and length of astrocytes. Rats with pSyn inclusions had less tyrosine hydroxylase (THir) SNpc neurons (\approx 18-33% decrease) reflecting loss of TH phenotype. STN DBS did not alter any of these pSyn inclusion-associated effects, and also did not impact the size or intensity of individual pSyn inclusions within the SNpc. The presence of pSyn inclusions did not alter total levels of BDNF protein in any of the structures evaluated. However, the normally positive association between nigrostriatal and corticostriatal BDNF levels was negatively impacted in PFF treated rats. Despite this, rats receiving both PFF injection and STN DBS exhibited significantly increased BDNF protein in the striatum, which partially restored the normal corticostriatal BDNF relationship.

The rat α -syn PFF model provides a relevant preclinical platform to examine the impact of STN DBS on multiple potentially disease-modifying factors. Our results demonstrate that pSyn inclusions may alter anterograde BDNF transport. However, STN DBS retains the ability to increase BDNF within the context of synucleinopathy. Future studies will examine whether long-term STN DBS can prevent the nigrostriatal degeneration associated with longer post PFF injection intervals.

This dissertation is dedicated to Carol Oudsema, my advocate, confidant, and friend.
Thank you for giving me the courage to walk this path, and for supporting me every step
of the way.

And to Darwin and Curie.

ACKNOWLEDGEMENTS

I want to thank Caryl Sortwell for her unwavering support and guidance throughout my graduate career. Caryl taught me how to be a rigorous and thorough scientist, but also how to have fun in science. She has played a significant role in my scientific and personal development and I will always be grateful to her.

I would also like to thank Jack Lipton for his support and advice. I thank my thesis committee members, Brian Gulbransen, Tim Collier, and Alison Bernstein for their feedback and advice. I would also like to thank Irving Vega for his invaluable career advice and support, and for teaching me perseverance. I acknowledge with great gratitude the contributions of the Sortwell Laboratory, Chris Kemp, Joe Patterson, Anna Stoll, and Mike Kubik. Beyond the Sortwell Lab, I also thank Sudhish Mishra, Matt Benskey, Nathan Kuhn, Kathy Steece-Collier, Allyson Cole-Straus, Joe Kochmanski, and Natosha Mercado for their technical support throughout my training. I would not have made it through without the help and support of each of these individuals.

I would like to extend my sincere gratitude to the many family and friends who have enriched my life during this time – the Oudsemas, Millers, Mateckis, and LEH. I specifically want to thank Ayse Gezer and Anna Trupiano for lifting me up whenever I needed it. Your friendships have made all the difference and have truly been a pleasure. Finally, I thank my best friend and partner, James Matecki. You have steadied me, rallied me, and inspired me.

PREFACE

At the time of writing this dissertation, two chapters are in preparation for submission for July 2020.

TABLE OF CONTENTS

LIST OF TABLES	xii
LIST OF FIGURES.....	xiii
KEY TO ABBREVIATIONS	xv
Chapter 1: Introduction.....	1
Parkinson's Disease.....	2
I. Demographics	2
II. Clinical Description of Parkinson's Disease.....	2
Parkinson's Disease Neuropathology	4
I. Neuroanatomy	4
II. Nigrostriatal Degeneration	6
III. Lewy Pathology	7
Etiology of Parkinson's Disease.....	8
I. Genetics	8
II. Environmental Exposure.....	9
III. Alpha-Synuclein.....	10
IV. Aging.....	10
V. Inflammation.....	11
Current Treatment Strategies for Parkinson's Disease	12
I. Pharmacotherapies	12
II. Surgical Therapies.....	14
Deep Brain Stimulation	14
I. Clinical considerations	15
II. STN DBS	15
III. GPi DBS	16
IV. The Mechanism of STN DBS	16
Animal Models of Parkinson's Disease	17
I. Toxicants	17
II. Alpha-Synuclein.....	19
Is STN DBS Disease-Modifying?	23
Brain-Derived Neurotrophic Factor	24
I. Synthesis, Release and Signaling	25
II. BDNF in Parkinson's Disease.....	27
Goals of Current Study.....	29

Chapter 2: Synucleinopathy-Associated Pathogenesis and the Potential for STN DBS Induced Brain Derived Neurotrophic Factor 31

Abstract.....	32
Introduction	33
α -Synuclein	34
I. Normal α -Synuclein Function.....	34
II. α -Synuclein Aggregation	35
Synucleinopathy-Associated Pathogenesis	36
I. Insights Derived from Postmortem PD Tissue	36
II. Insights from the α -Synuclein PFF Model.....	41
Brain-Derived Neurotrophic Factor (BDNF)	44
Can BDNF Provide Neuroprotection from Synucleinopathy?.....	47

Chapter 3: Impact of STN DBS on Endogenous α -Syn Aggregation Triggered by Intrastratial Fibril Injection 50

Abstract.....	51
Introduction	53
I. Parkinson's Disease	53
II. STN DBS and Neuroprotection – Clinical Studies	53
III. STN DBS and Neuroprotection – Preclinical Studies	54
IV. Synucleinopathy Seeded by Injection of α -Syn Pre-Formed Fibrils (α -Syn PFFs)	54
Methods	56
I. Experimental Overview.....	56
II. Animals.....	58
III. Preparation and Quality Control of α -Syn PFFs.....	58
IV. Pre-Formed Fibril Injections	59
V. Electrode Implantation.....	60
VI. Deep Brain Stimulation.....	60
VII. Euthanasia	61
IIX. Tissue Processing	61
IX. Kluver–Barrera Histology	62
X. Proteinase K Digestion.....	64
XI. Unbiased Stereology of THir Neurons in the SNpc	65
XII. Total Enumeration of pSyn and pSyn* Immunoreactive Nigral Neurons	65
XIII. TH and pSyn Double Label Immunofluorescence	66
XIV. Fluorescent Quantification	66
XV. Statistical Analyses	67
Results	69
I. The number and Size of PFF-Induced α -Syn Inclusions in the SNpc is not Impacted by STN DBS.....	69
II. STN DBS does not Impact Nigral TH Neuron Phenotype in the Rat α -Syn PFF Model.....	71
III. STN DBS does not Alter pSyn-Associated Effects on Nigral THir Neurons.....	72

IV. STN DBS does not Impact α -Syn Inclusion Formation or Inclusion-Associated TH Phenotype in Aged Rats.	74
Discussion.....	76
I. α -Syn Aggregation in the Young SNpc	77
II. α -Syn Aggregation in the Aged SNpc.....	79
Chapter 4: Impact of Subthalamic Nucleus Deep Brain Stimulation on Synucleinopathy-Triggered Neuroinflammation in the Substantia Nigra	81
Abstract.....	82
Introduction	84
I. Present Study	85
Methods	86
I. Experimental Overview.....	86
II. Animals.....	88
III. Preparation and Quality Control of α -Syn PFFs.....	88
IV. Pre-Formed α -Syn Fibril Injections.....	89
V. Electrode Implantation.....	89
VI. Deep Brain Stimulation.....	90
VII. Euthanasia	90
IIX. Tissue Processing	91
IX. Kluver–Barrera Histology	92
X. Proteinase K Digestion.....	92
XI. Unbiased Stereology of Tyrosine Hydroxylase Immunoreactive (THir) Neurons in the Substantia Nigra pars compacta (SNpc).....	93
XII. Total Enumeration of pSyn and MHC-II Immunoreactive Cells	93
XIII. GFAP and pSyn Double Label Immunofluorescence	94
XIV. Immunofluorescence Quantification.....	94
XV. Statistical Analyses	96
Results.....	98
I. The Number of PFF-Induced α -Syn Inclusions in the SNpc is not Impacted by STN DBS.....	98
II. STN DBS does not Impact Early α -Syn PFF Associated Reductions in Nigral TH Immunoreactive Neurons.....	99
III. STN DBS does not Impact the Number of MHC-IIir Microglia in the SN Associated with α -Syn Inclusions.	100
IV. Increased GFAP Expression in the SN Associated with pSyn Inclusions is not Impacted by STN DBS.....	101
V. Astrocytic Complexity in the SN is Increased in the Presence of α -Syn Inclusions and is Unaffected by STN DBS.	104
Discussion.....	106
I. Neuroinflammation is Implicated in Clinical PD	106
II. Microglia as a Contributor to Synucleinopathy.....	107
III. Gliosis Beyond Microglia	109
IV. Can DBS Impact Neuroinflammation?.....	110
V. Summary	111

Chapter 5: Deep brain stimulation of the subthalamic nucleus increases brain-derived neurotrophic factor (BDNF) in the context of nigrostriatal synucleinopathy in the rat preformed fibril model	112
Abstract.....	113
Introduction.....	115
I. Mechanism of STN DBS-Mediated Neuroprotection – BDNF.....	115
II. α -Syn Pathology Beyond the Nigrostriatal System.....	115
III. BDNF Transport.....	116
IV. Neuroprotective potential of BDNF.....	116
V. Present Study.....	118
Methods.....	119
I. Experimental Overview.....	119
II. Animals.....	122
III. Preparation and Quality Control of α -Syn PFFs.....	122
IV. Pre-Formed Fibril Injections.....	123
V. Electrode Implantation.....	123
VI. Deep Brain Stimulation.....	124
VII. Euthanasia.....	124
IIX. Tissue Processing.....	125
IX. Kluver–Barrera Histology.....	126
X. Proteinase K Digestion.....	127
XI. Microdissections.....	127
XII. ELISA.....	128
XIII. BCA Assay.....	128
XIV. Statistical analyses.....	128
Results.....	130
I. Chapter 3 Recap: STN DBS does not Alter α -Syn Inclusions or TH Phenotype in SNpc Neurons.....	130
II. α -Syn Inclusions do not Change Total BDNF Protein Amounts.....	130
III. α -Syn Inclusions Change BDNF Structural Relationships.....	131
IV. STN DBS Increases Striatal BDNF in the α -Syn PFF Model.....	132
V. STN DBS Partially Mitigates the Corticostriatal BDNF Association Disrupted by α -Syn Inclusions.....	133
Discussion.....	136
I. Inclusion Dynamics.....	136
II. DBS Dynamics.....	138
III. Summary.....	142
Chapter 6: Conclusions and Future Directions	143
Conclusions.....	144
Clinical Implications.....	145
Future Directions.....	146
I. Does STN DBS Spare SNpc Neurons from Degeneration?.....	146
II. Do Inclusions Interfere with Anterograde Transport of BDNF?.....	147
III. Characterization of Cortical α -syn Inclusions and the Impact of STN DBS.....	147

IV. Neuroinflammation	148
Final Remarks	149
REFERENCES.....	150

LIST OF TABLES

Table 2.1: Insights into synucleinopathy-associated pathogenesis derived from postmortem PD tissue.....	40
Table 2.2: Insights into synucleinopathy-associated pathogenesis derived from in vitro PFF studies.....	43

LIST OF FIGURES

Figure 1.1: General experimental overview.....	30
Figure 3.1: Experimental overview.....	57
Figure 3.2: Distribution of sonicated α -syn PFF size prior to intrastriatal injection.....	59
Figure 3.3: Electrode placement validation.....	63
Figure 3.4: Nigral α -syn inclusions are Proteinase K-resistant.....	64
Figure 3.5: α -syn aggregates in the substantia nigra pars compacta (SNpc) of young rats are not impacted by STN DBS.....	70
Figure 3.6: STN DBS does not impact modest PFF-inclusion associated loss in TH-ir nigral neurons.....	71
Figure 3.7: STN DBS does not alter pSyn-associated effects on SNpc in rats treated with PFFs.....	73
Figure 3.8: STN DBS does not impact α -syn inclusion formation or inclusion-associated TH phenotype in aged rats.....	75
Figure 4.1: Experimental overview.....	87
Figure 4.2: Production of astrocytic rendered paths.....	96
Figure 4.3: STN DBS does not change the number of pSyn immunoreactive nigral neurons.....	98
Figure 4.4: Stereological assessment revealed no stimulation effect on the ipsilateral loss of TH phenotype in PFF treated rats 2 months after injection.....	100
Figure 4.5: α -syn inclusion-associated microgliosis in the SN is not impacted by STN DBS.....	101
Figure 4.6: STN DBS does not impact inclusion-induced increase in GFAP in the SNpc.....	103
Figure 4.7: Sholl analysis reveals that increased astrocytic process length and branching in α -syn inclusion-bearing rats that is not impacted by STN DBS.....	105
Figure 5.1: Experimental overview.....	121

Figure 5.2: Total amount of BDNF is not impacted by inclusions.....131

Figure 5.3: α -syn inclusions change BDNF structural relationships.....132

Figure 5.4: STN DBS increases striatal BDNF protein despite inclusions.....134

Figure 5.5: Schematic of possible mechanism.....141

KEY TO ABBREVIATIONS

6-OHDA	6-hydroxydopamine
AAALAC	Association for Assessment and Accreditation of Laboratory Animal Care
ANOVA	analysis of variance
α -syn	alpha-synuclein
BBB	blood-brain-barrier
BDNF	brain-derived neurotrophic factor
BG	basal ganglia
CNS	central nervous system
COMT	catechol-O-methyltransferase
D1	direct pathway
D2	indirect pathway
DA	dopamine
DAB	3,3' diaminobenzidine
DAT	dopamine transporter
DBS	deep brain stimulation
DDC	DOPA decarboxylase
DPBS	Dulbecco's PBS
Enk	enkephalin
FDA	Food and Drug Administration
GABA	γ -aminobutyric acid
GDNF	glial cell-line derived neurotrophic factor

GFAP	glial fibrillary acidic protein
GPe	globus pallidus pars externa
GPi	globus pallidus pars interna
IACUC	Institutional Animal Care and Use Committee
ILBD	Incidental Lewy Body disease
i.p.	intraperitoneal
LB	Lewy body
LCM	laser capture microdissection
LID	levodopa-induced dyskinesia
LRRK2	leucine-rich repeat kinase 2
LTP	long-term potentiation
MHC-II	major-histocompatibility complex-II
MOA	monoamine oxidase
MPTP	1-methyl-4-phenyl-1,2,3,6-tetrahydropyridine
MSN	medium spiny neurons
NGF	nerve growth factor
NMDA	N-methyl-d-aspartate
NTN	neurturin
p75	low affinity nerve growth factor receptor, LNGFR
PFA	paraformaldehyde
PFF	pre-formed fibril
PINK-1	PTEN-induced putative kinase 1
pSyn	α -syn phosphorylated at serine 129

pSyn*	pSyn-STAR; phosphorylated α -syn that is truncated, adamant and reactive
ROI	region of interest
SN	substantia nigra
SNARE	soluble NSF attachment protein receptor
SNP	single nucleotide polymorphism
SNpc	SN pars compacta
SNpr	SN pars reticulata
SP	substance P
STN	subthalamic nucleus
SubQ	sub-cutaneous
TBS	tris-buffered saline
TEM	transmission electron microscopy
TH	tyrosine hydroxylase
TrkB	tropomyosin-related kinase receptor B
Tx-100	Triton X-100
UPDRS	Unified Parkinson's Disease Rating Scale
VPS35	vacuolar protein sorting associated protein 35
VTA	ventral tegmental area

Chapter 1: Introduction

Parkinson's Disease

I. Demographics

The first cases of Parkinson's disease (PD) were described in 1817 by Dr. James Parkinson in his seminal piece "An essay on the shaking palsy" [1]. Today Parkinson's disease is the second most common neurodegenerative disorder, behind Alzheimer's disease [2], affecting over a million Americans and resulting in nearly \$25 billion per year in health care costs [3]. The "shaking palsy" phenotype that Parkinson first described is part of the four cardinal motor symptoms of PD: tremor, rigidity, bradykinesia, and postural instability. The average age of diagnosis for PD is 62.5 years, however 10% present with early onset, which is characterized as below the age of 50 years [3]. Age is the biggest risk factor for PD, with an estimated 1% prevalence for persons over the age of 65 [4, 5]. PD is also more common in males than in females across all ages [6].

II. Clinical Description of Parkinson's Disease

There is no cure for PD. Disease progression is highly variable, with some patients living decades, and others only a few years. However, across all ages of onset, the life expectancy of patients diagnosed with PD is 5-10 years less than the general population [7]. Reaching a conclusive diagnosis is difficult due to the diverse presentation of PD and the lack of a single, conclusive diagnostic.

Motor Symptoms

Each person living with Parkinson's disease presents slightly differently, however there

are commonalities. Clinical PD is characterized by the following criteria: presence of bradykinesia, and one or more of the other cardinal symptoms (tremor, rigidity, or postural instability) [8, 9]. Diagnosis is further confirmed by ruling out other forms of parkinsonism, responsiveness to dopaminergic medication, and progressive worsening of symptoms as measured by the Unified Parkinson's Disease Rating Scale (UPDRS) [10, 11]. Motor symptoms typically present unilaterally and expand bilaterally as the disease progresses [12, 13]; thus, asymmetry is also included as part of the diagnostic criteria [12]. Overall, the process of getting an accurate clinical diagnosis and beginning treatment can take months or even a year, and may require travel to find a movement disorders specialist. A conclusive diagnosis can only be achieved postmortem. However, as that is not very useful for patients living with Parkinson's disease symptoms, a clinical diagnosis is achieved as described above.

Non-Motor Symptoms

It is now appreciated that PD is a complex, multisystem disorder with non-motor symptoms accompanying the classic motor symptoms. There are many nonmotor symptoms, with the average PD patient reporting 11 nonmotor symptoms [14]; however they can generally be broken up into four categories: neuropsychiatric, cognitive, autonomic, and sleep dysfunction [15]. Depression and cognitive decline are each estimated to affect up to 80% of PD patients [16, 17], and depression is consistently identified as a determinant of poor quality of life in patients living with PD [18]. Cognitive decline is not only devastating to patients and their families, but also a financial burden on society; long-term care is estimated to account for 41% of medical costs and lost

productivity for patients/caregivers is estimated at \$9000 per patient, per year [2]. Despite this, there are few therapies targeting these non-motor symptoms, in part because the pathological mechanism behind them is less clear.

Parkinson's Disease Neuropathology

I. Neuroanatomy

Basal Ganglia

The basal ganglia (BG) are a group of structures associated with voluntary movement, procedural learning, and emotion, among other functions [19, 20]. The basal ganglia are highly interconnected subcortical nuclei comprised of the caudate and putamen (collectively the dorsal striatum), the globus pallidus pars interna (GPi) and pars externa (GPe), the subthalamic nucleus (STN), and the substantia nigra (SN) – further divided into the SN pars compacta (SNpc) and SN pars reticulata (SNpr) [21]. In PD, the basal ganglia circuit is affected, causing the motor symptoms described above [22].

The primary input to the basal ganglia is cortical, glutamatergic projections, and the primary output is provided by the GPi and SNpr [21]. Two functionally antagonistic pathways called the direct and indirect pathways mediate information flow within the basal ganglia [23]. The SNpc contains dopaminergic neurons that project to the dorsal striatum providing critical dopamine release [21]. Dopamine (DA) binds to the D1 and D2 receptors on medium spiny neurons within the striatum to either facilitate movement (D1, direct pathway) or inhibit it (D2, indirect pathway). The balance of the direct and indirect pathways are tightly regulated, facilitating controlled, voluntary movement [20].

In PD, loss of dopaminergic input from the SNpc to the striatum results in overactive indirect pathway signaling, and decreased direct pathway signaling, resulting in diminished voluntary movement [23].

The Direct Pathway

The direct pathway is named according to the fact that there is only one synapse between the first structure in basal ganglia processing (the putamen) and its output structures (the GPi and SNpr). Input to striatal medium spiny neurons (MSN) expressing D1 receptors comes from both cortical and SNpc neurons. Cortical input causes a release in γ -aminobutyric acid (GABA) and substance P (SP) at the GPi and the SNpr [21]. Similarly, DA release into the striatum from SNpc neurons activates the D1 receptor of MSN, activating SP release [21, 24]. GPi and SNpr output neurons are tonically active, transmitting GABA to inhibit the thalamus [21, 23, 25]. SP neurons are typically at rest, however when activated via corticostriatal or nigrostriatal input, D1 MSNs suppress GPi and SNpr output [21, 24]. This effectively disinhibits the thalamus and its target structures (e.g. cortex) [21, 24]. Overall, movement is facilitated through both cortical and SNpc activation of D1 receptors in striatal MSN [21, 24].

The Indirect Pathway

In contrast to the one synapse arrangement of the direct pathway, the indirect pathway has three synapses between the putamen and the GPi and SNpr: (1) Striatal neurons expressing D2 receptors release GABA and enkephalin (Enk) into the GPe. (2) The GPe sends inhibitory GABAergic input to the STN, causing (3) excitatory glutamate

release into the GPi and SN [21, 26]. In contrast to the direct pathway (with suppressed basal ganglia output), the indirect pathway has activated BG output, causing inhibition of the thalamus, cortex, and movement.

II. Nigrostriatal Degeneration

The pathological hallmarks of PD are degeneration of dopaminergic neurons in the SNpc and presence of alpha-synuclein (α -syn) aggregated into intracellular structures termed Lewy bodies. It is estimated that at the time of clinical diagnosis, there is already a 60% or more loss of striatal DA caused by a 50% loss of nigrostriatal dopamine neuron cell bodies [27, 28]. However, not all midbrain dopaminergic neurons are affected equally in PD. Ventral SNpc neurons, which project to the putamen, are the first and most affected, with a 95% loss [29, 30]. Dorsal SNpc neurons, which project to the caudate nucleus, are less susceptible to degeneration, with typically an 80% loss [29-32]. Interestingly, neighboring DA neurons of the ventral tegmental area (VTA) which project to the nucleus accumbens, hypothalamus, and cortex and are involved in the reward pathway, are largely spared in PD [31]. The cause of this selective vulnerability of dopaminergic populations is not completely understood, however evidence suggests it may in part be attributed to high metabolic demand and oxidative stress production, iron and neuromelanin content, and proximity to the dense microglial population of the SNpr [33-36]. Overall, neurodegeneration of nigrostriatal projections underlies the motor PD phenotype.

III. Lewy Pathology

To date, the only way to truly diagnose PD is by verifying degeneration of nigrostriatal neurons in the SNpc and presence of Lewy bodies via post-mortem autopsy. Lewy bodies (LBs) were first described by Dr. Friedrich Lewy in the dorsal motor nucleus of the vagus nerve [33, 37]. Almost a century later Dr. Maria Spillantini identified α -syn as a primary component of LBs [38]. The consequences of α -syn inclusions and Lewy pathology are discussed in Chapter 2.

Lewy bodies are found throughout the central nervous system in structures ranging from the olfactory bulb to the brainstem and spinal cord [34, 39, 40]. Some structures degenerate with Lewy pathology (SN, locus ceruleus), while other structures don't show overt neurodegeneration (amygdala, cerebral cortex, hypothalamus, posterior pituitary, dorsal raphe nucleus, dorsal vagal nucleus, cerebellum and spinal cord; [34]. Braak and colleagues have characterized LB pathology to six distinct stages of PD progression: Olfactory bulb and dorsal vagal nucleus (Stage 1), progressing into the pontine tegmentum (Stage 2), midbrain and neostriatum (Stage 3), basal procencephalon and mesocortex (Stage 4), and finally into the neocortex (Stages 5-6; [34, 41]. The Braak staging hypothesis has contributed two major developments in PD research: its driven the field to consider the possibility of pathologic α -syn spreading between cells in a prion-like fashion [42], but more importantly, it provided a neuropathological explanation for the progressive nature of PD symptoms. Braak staging is still the predominant method for evaluating PD pathology, however it is not without caveats. It excludes all cases without pathology in the dorsal motor nucleus of the vagus nerve, which is

problematic because it fails to classify up to 50% of PD cases that either don't have dorsal motor nucleus pathology or otherwise don't fit the predicted spread [43, 44]. Nonetheless Braak staging remains the framework under which postmortem staging for PD is conducted.

Etiology of Parkinson's Disease

Cases of PD are classified as either familial or sporadic. Roughly 5-10% of PD cases are caused by inherited monogenic mutations or multiplications of disease-related genes [45]. An additional ~10% of cases are still familial in origin, however with the underlying genetic cause unknown [45]. The remaining ~80% of cases are sporadic with unknown origin [45]. There are several factors discussed below that are thought to contribute to the etiology of sporadic PD, however none have been unequivocally shown to cause PD. Thus, the cause, or likely causes, of sporadic PD are still considered unknown.

I. Genetics

With the advancement of genetic laboratory techniques over the last few decades, our understanding of the role genetics plays in PD has increased tremendously. Many genes have been identified as risk factors for PD [46] – meaning they increase the likelihood of developing the disease – however, only the most common, monogenic mutations are discussed herein.

The gene SNCA codes for α -syn and was the first to be demonstrated as a definitive genetic contributor to PD when the A30P missense mutation was identified [47]. Since then, other missense mutations (A53T, E46K, G51D) and multiplications of SNCA have been identified as autosomal dominant causes of PD that typically result in early onset PD [48-52]. It is not fully understood why these mutations lead to PD, but there is some evidence that they may increase α -syn aggregation kinetics [53-55]. Other autosomal dominant genes associated with PD are leucine-rich repeat kinase 2 (LRRK2), and vacuolar protein sorting associated protein 35 (VPS35). While mutations in SNCA are quite rare, LRRK2 is the most commonly mutated gene in PD, and results in a toxic gain-of-function [56-58]. VPS35 is normally involved in retrograde transport of proteins from endosomes to the trans-golgi network, and mutations cause a toxic loss-of-function [59].

There are also autosomal recessive genes associated with PD: PRKN, PINK1, and DJ-1. PRKN encodes parkin, an E3 ubiquitin ligase, PINK1 encodes a mitochondrial serine/threonine kinase, and DJ-1 encodes deglycase, a cysteine protease [49-51, 56, 57, 60-68]. These mutations typically result in loss-of-function, leading to early onset PD.

II. Environmental Exposure

Several toxicants have been linked to PD, including metals (manganese, lead), pesticides (rotenone, paraquat, dieldrin) and carbon disulfide, which is used in the production of rubbers [69-74]. Not surprisingly, occupations that expose people to these

toxicants (farmers, steel industry workers, welders) are also linked to PD [75-77]. Many of these toxicants cause selective death of DAergic neurons, and provided the first in vitro and in vivo models for the study of PD.

III. Alpha-Synuclein

Because α -syn has been linked to both inherited and sporadic forms of PD, it remains an important factor in unraveling PD etiology. α -syn is a 140 amino acid, natively unfolded protein in the nervous system [78]. It is highly abundant, comprising 1% of all cytosolic proteins, and it is enriched in presynaptic terminals [79] where it is thought to play a critical role in synaptic transmission [80]. α -syn is described as an intrinsically disordered protein; allowing for dynamic changes in tertiary conformation depending on the environment [81]. This is thought to facilitate the diverse range in physiological functions of α -syn [80]. Of relevance to the present research, this also leaves α -syn vulnerable to aggregation. Indeed, α -syn can self-assemble, forming insoluble aggregates [53].

IV. Aging

Aging is the largest risk factor for developing PD [82-84]. While it is speculated that the process of aging doesn't cause PD per se, it is likely that age-related changes contribute to PD in a 'stochastic acceleration' manner [85]. As a function of normal aging, many cellular processes change; mitochondrial turnover and ubiquitin-proteasome-mediated degradation become less efficient in aged nigral DA neurons, perhaps priming them to be impacted by other genetic and/or environmental factors that

previously hadn't met the threshold for pathology [82-89].

V. Inflammation

Postmortem examination and biofluid sampling from living patients has consistently revealed an altered inflammatory environment in PD. Our immune systems are comprised of two complimentary arms: innate and adaptive. The innate arm is the first line of defense, and includes phagocytes and macrophages capable of engulfing bacteria, debris, or other pathogens, while the adaptive arm is comprised of T cells and B cells, and is responsible for remembering pathogens in the event of future insult [90]. Together these systems form a coordinated effort at protecting the 'self' from the 'non-self'. In the central nervous system (CNS) a glial cell termed microglia serve as the resident macrophages. Microglia reside throughout the CNS and are estimated to represent ~10% of the total number of cells [91, 92]. They survey the brain, sensitive to signals from neurons or other glial cells, ready to mount a response when needed [93, 94]. Microglia function as first responders, secreting cytokines and chemoattractants to recruit nearby glial cells in response to infection, cell death, or other acute stressors [95, 96]. Thus, chronic stressors, including PD, cause microglia to initiate a snowball effect of cytokine secretion and glial activation, which can be harmful to nearby neurons. Major-histocompatibility complex-II (MHC-II; HLA in humans) is a surface protein that presents antigens on microglia and other antigen presenting cells, helping the immune system produce antibodies against it [97]. MHC-II activity is largely undetectable in the healthy CNS, thus the observation of activated microglia in the SN and other brain regions in PD patients [98-100] suggested that some component of PD pathology

induces a deleterious inflammatory response. An interesting retrospective analysis showed chronic consumption of anti-inflammatory drugs was associated with decreased PD incidence [101, 102], further suggesting a role for inflammation in PD.

Current Treatment Strategies for Parkinson's Disease

To date, there are no disease-modifying treatments for PD. Disease-modifying is an ambiguous and somewhat controversial term; at its core it is intended to represent an intervention that halts or slows the progression of the disease, however the outcome measures used to evaluate this are less straightforward [103, 104]. For the sake of this dissertation, we will define disease-modifying as preventing, or slowing nigrostriatal degeneration [105], for which there are no known treatments for PD. Nonetheless, there are effective symptomatic treatments, particularly for PD motor symptoms. Moreover, we now appreciate that in order to slow nigrostriatal degeneration, neuroprotective therapies should commence within the first 4 years post diagnosis as >90% of nigrostriatal innervation is lost during this this time [27, 105].

I. Pharmacotherapies

Current pharmacotherapies are primarily aimed at enhancing diminished DA signaling [106]. DA is a catecholamine that does not cross the blood-brain-barrier (BBB), and is normally tightly regulated; therefore, it is not feasible to directly administer DA.

However, levodopa (L-dihydroxyphenylalanine, L-DOPA) is a precursor to DA, and readily crosses the BBB. It is the product of the rate-limiting step in DA synthesis (hydroxylation of tyrosine by TH), so levodopa effectively boosts DA levels in remaining

SNpc neurons, allowing temporary compensation of nigrostriatal signaling. Moreover, it has to be taken up by neurons and converted to DA in order to have an effect, allowing it to be regulated as normal DA would, minimizing side effects. Levodopa is administered orally and is absorbed in the small intestine [107]. In order to prevent conversion of levodopa to dopamine via DOPA decarboxylase (DDC) in the periphery (before it can reach the brain), carbidopa, a drug that inhibits peripheral DDC is co-administered [107]. Overall, levodopa in combination with DDC is the gold standard of care for the treatment of PD.

Other approaches to enhancing striatal DA signaling include the use of DA agonists (bromocriptine, pramipexole, ropinirole, apomorphine, and cabergoline) [108], or decreasing DA metabolism [107]. Catechol-O-methyltransferase (COMT) and monoamine oxidase (MOA) are enzymes that metabolize DA; inhibiting these enzymes results in DA persisting at the synapse longer, allowing it to have a greater effect [107].

All of these pharmacotherapies are quite effective at treating motor symptoms in early-stage PD, and result in what is known as “the honeymoon period” where patients live mostly symptom-free. However, as disease progresses two problems present: patients need to take higher doses, more frequently to have the same benefit, and the remaining DA neurons become less functional, causing mishandling of DA [109]. Consequently, prolonged use of levodopa causes levodopa-induced dyskinesias (LIDs) [110-112]. In an effort to delay levodopa use (and eventual LIDs), DA agonists are typically the first treatment used, particularly for younger patients who will have longer overall use. DA

agonists often result in fewer on-off periods (when medicine has not 'kicked in' yet), however, they act on all DA receptors which causes more side effects including insomnia, hallucinations, and decreased impulse control [113, 114].

II. Surgical Therapies

After dyskinesias have become intolerable (typically ~10 years into disease progression) [115, 116], surgical treatment is explored as a last resort [117]. Early lesioning approaches evolved into deep brain stimulation (DBS), which received United States Food and Drug Administration (FDA) approval for use in the GPi or STN for essential tremor in 2002 [118].

Deep Brain Stimulation

DBS is the most commonly used surgical treatment for PD, and is used to treat resting tremor with increasing frequency each year [119]. DBS acts as a pacemaker for the basal ganglia, helping to restore the imbalance in electrical signaling that results from nigrostriatal degeneration [120]. Brain surgery is inherently risky, thus DBS has traditionally been used as a treatment of last resort, only after pharmacotherapies are no longer effective [121].

Deep Brain Stimulation

Due to the risky, expensive, and experimental nature of DBS at the time of its initial consideration, FDA approval required patients be at least five years post diagnosis, and mild-moderate disability in order to qualify [122-125]. As a result, until very recently

patients receiving DBS surgery are on average 12-14 years into their diagnosis [126].

I. Clinical considerations

The questions of whether DBS is right for a patient, and whether it's the right time are not straightforward to answer. Studies have revealed that some groups of PD patients benefit more from DBS than others [127]. Moreover, there are factors outside of PD including financial situation, ability of their caregiver(s), and overall health that should be considered too.

There is no single criterion that determines whether a patient should receive DBS, however there are guideline inclusion and exclusion criteria. Patients are considered good candidates for DBS if they present with resting tremor and respond well to levodopa, but have short response periods [122, 124]. Accordingly, patients who have developed debilitating levodopa-induced dyskinesias are often recommended for DBS, as stimulation offsets some of the need for levodopa, allowing for lower dosage. In contrast, patients experiencing problems with gait, speech or postural instability are not recommended for DBS, as it has not been shown to improve those symptoms [128-130]. Finally, patients without dedicated caregivers are not good candidates for DBS [130].

II. STN DBS

The STN is the most common structure targeted with DBS, and results in drastically improved UPDRS motor scores (~50%) as well as improvements in non-motor

symptoms and overall quality of life [122, 131-139]. The benefit of improved motor performance is further extended by the ability to reduce levodopa usage [131, 140]. Despite the many benefits of STN DBS, it has been reported to worsen depression and impulse control [131, 141] and therefore is not recommended for patients presenting these symptoms prior to surgery.

III. GPi DBS

Historically fewer patients have received GPi DBS than STN DBS, however its use is on the rise, in part due to a recent finding that GPi is as effective as STN DBS in relieving motor symptoms [131]. Moreover, GPi DBS has not been associated with worsening non-motor symptoms, so patients experiencing depression or cognitive dysfunction are better candidates for GPi DBS than STN DBS [131, 142-144]. However, GPi DBS has not shown the same potential for decreasing levodopa therapy, so patients with severe dyskinesias might opt for STN DBS [131, 142-144].

IV. The Mechanism of STN DBS

The specific mechanism by which STN DBS provides symptomatic alleviation is currently unresolved. Several hypotheses have been proposed over time. (1) Isolation of STN from pathology; one study suggests that STN DBS may decouple the STN from upstream and downstream pathology, restoring normal firing patterns and function [145]. (2) Reduction of pathological beta oscillations that are increased in the parkinsonian brain; STN DBS replaces aberrant firing patterns with a new, beneficial firing pattern. This hypothesis is in line with the 'pace-maker' analogy. STN DBS has

both excitatory and inhibitory effects, stabilizing output from STN neurons [146, 147]. This is further supported by the observation that PD is associated with increased beta oscillations within the basal ganglia, and STN DBS decreases these via altered STN firing patterns [148-153].

Animal Models of Parkinson's Disease

In order to treat PD, we have to understand PD. Many animal models have been employed to study the mechanisms driving the pathophysiology in PD, and to test potential therapies. The advantages and disadvantages of the most commonly used rodent models of PD are described below.

I. Toxicants

Toxicant models selectively induce degeneration of dopaminergic neurons, resulting in the development of parkinsonian motor symptoms. Classic toxicant models include 6-hydroxydopamine (6-OHDA), 1-methyl-4-phenyl-1,2,3,6-tetrahydropyridine (MPTP), and pesticides: rotenone and paraquat (reviewed in [154]). These models result in motor impairments mirroring the motor symptoms observed in PD patients.

6-OHDA

6-OHDA is a metabolite of DA that is administered into the striatum via stereotaxic surgical injection. It was developed as “an animal model of akinesia with a very high mortality rate” in 1968, and has since become one of the most widely used models for PD [155, 156]. 6-OHDA is structurally similar to DA and thus is taken up by

dopaminergic neurons. Once it is intracellular, 6-OHDA induces oxidative damage and eventual cell death [157], modeling the nigrostriatal degeneration seen in PD. Intrastriatal injection of 6-OHDA results in near complete absence of tyrosine hydroxylase immunoreactive nigrostriatal terminals in the striatum within 1-2 weeks followed by the loss of the majority of nigral dopamine neurons within 4-6 weeks [158]. Thus, the degeneration of nigrostriatal neurons induced by 6-OHDA is relatively immediate and complete.

MPTP

In 1982 there was a misfortunate outbreak of Parkinsonism in young drug users in northern California [159, 160]. Dr. William Langston identified that a toxic impurity, MPTP, was unknowingly contaminating synthetic heroine that had been distributed around the area [161]. While this atypical example does not account for PD, it did introduce a way to study selective death of DAergic neurons [162-164]. MPTP crosses the BBB [165], and once in the brain, MPTP is converted into its toxic metabolite, MPP+, which is then selectively taken up by the dopamine transporter (DAT) [166]. MPP+ accumulates in DA neurons, inhibits ATP production, and produces superoxide radicals [166]. MPTP can be administered via oral gavage, stereotaxic injection, subcutaneous (SubQ) injection, or intraperitoneal (i.p.) administration, however SubQ and i.p. are most commonly used [167]. Depending on the protocol used, MPTP administration results in large variations in responses, however chronic administration reliably results in SNpc degeneration, striatal dopamine loss, and behavioral deficits [168]. Thus, the MPTP mouse model has resulted in a better understanding of the

consequences of nigrostriatal degeneration, and has provided an important platform in which to explore neuroprotective strategies [168].

Pesticides

Two other neurotoxicants that have been used to model PD are pesticides: rotenone and paraquat. Rotenone is used as an insecticide and piscicide, and is a mitochondrial complex I inhibitor that impairs mitochondrial function [169]. Paraquat is a herbicide, and its exposure also results in toxic reactive oxygen species [170]. These models are not as commonly used as 6-OHDA or MPTP, as they lack selective dopaminergic toxicity, offering greater potential for widespread toxicity in non-dopaminergic neurons [154]. However, rotenone and paraquat have both been used to induce selective loss of dopaminergic neurons in vitro and in vivo [171-174] and can help explain the link between toxicant exposure and PD [75, 76].

Overall, neurotoxicant models do result in nigrostriatal degeneration, however they have many limitations. They rely on oxidative stress as the mechanism of toxicity, which is only one of many likely contributors to PD. In general, the degeneration that occurs happens acutely, and often fails to model α -syn pathology.

II. Alpha-Synuclein

Neurotoxicant models have advanced our understanding of the consequences of nigrostriatal denervation, and have led to the development of the current treatment options. However, PD is still without a disease-modifying therapy. In an effort to

understand and mitigate the pathophysiological changes that occur in PD patients, non-toxicant models have been developed. The majority of PD cases are idiopathic, and thus their causes unknown. However, the strong genetic contribution to PD has led to the investigation of specific genes, and their role in pathology. Transgenic or viral vector approaches have been used for targeted overexpression of normal or mutated forms of some of the genes related to PD. These include but are not limited to leucine-rich repeat kinase 2 (LRRK-2), parkin, and PTEN-induced putative kinase 1 (PINK1), however this dissertation will focus on the involvement of α -syn in PD.

Alpha-Synuclein Overexpression

Mutations (A30P, A53T and E46K) in SNCA, the gene encoding α -syn, and increases in α -syn caused by SNCA multiplication are associated with development of PD and an earlier onset of disease symptoms [47, 49-51, 60, 61]. Moreover, the primary component of Lewy bodies is aggregated α -syn [38]; thus, transgenic and viral vector-mediated overexpression of wildtype or mutated α -syn were the first synuclein-based approaches to modeling PD. Transgenic overexpression of α -syn generally results in α -syn aggregate formation, but lacks nigrostriatal degeneration [175-178], whereas viral vector-mediated overexpression reliably achieves nigrostriatal degeneration, and therefore became the predominant approach [80, 179-181]. Viral vector-mediated overexpression of α -syn recapitulates some aspects of PD, including nigrostriatal degeneration and dysfunction [182, 183], Lewy body-like inclusions containing α -syn [180, 184, 185], and neuroinflammation [186-188]. However, unlike clinical PD, these models do not result in progressive nigrostriatal degeneration, formation of Lewy bodies

or α -syn inclusions, or parkinsonian motor symptoms unless α -syn is overexpressed beyond physiological levels [189].

Alpha-Synuclein Pre-Formed Fibril

α -syn overexpression and other synuclein-based models have addressed some of the limitations of toxicant models, namely α -syn pathology. However, they often rely on supraphysiological levels that are not analogous to human PD. In an effort to better model the pathology observed in PD, the α -syn preformed fibril (PFF) model was developed in cultured cells [190], then extended to mice [191], and rats [192]. There are three key features of the PFF model discussed below that address the limitations of the previously described models.

Aggregation

The strongest disease-relevant feature of the PFF model is widespread nigrostriatal synucleinopathy under physiological levels of α -syn. Fibrils generated from recombinant α -syn monomers are sonicated into fragments and injected into two sites in the dorsal striatum. These fragments are subsequently taken up at synaptic terminals, where they seed endogenous α -syn into insoluble, Lewy body-like inclusions [193-195]. Importantly, these experiments were conducted in wildtype cultures/animals, and resulted in the conversion and propagation of endogenous α -syn into inclusions [190-192]. These inclusions contain phosphorylated α -syn (pSyn), and start as Lewy neurite-like, and over time progress into Lewy body-like somatic inclusions [196, 197]. Notably, synucleinopathy in this model is not limited to the nigrostriatal system. pSynir inclusions

are also found bilaterally throughout the cortex [193]. Particularly relevant for the experiments herein, pSyn inclusion load peaks in the SNpc 1-2 months post injections [193].

Neuroinflammation

Another major advantage of the PFF model is the α -syn inclusion-triggered neuroinflammation, preceding nigrostriatal degeneration [198]. The nigrostriatal system in PD is associated with neuroinflammation [98-100, 199-203], therefore markers indicative of reactive microgliosis is a key component of modeling PD. While 6-OHDA and α -syn overexpression models can result in a neuroinflammatory response [186-188, 204-206], they lack the spatial and temporal separation needed for neuroinflammation to be studied apart from neurodegeneration [207]. PFF injection induces peak reactive microglial activation in the SNpc at 2 months, the time point corresponding to peak inclusions [198]. This relationship between microglial activation and α -syn inclusion burden has also been reported in human PD [98] further supporting the use of the α -syn PFF model.

Neurodegeneration

In PD, nigrostriatal degeneration occurs progressively over years. An advantage of the PFF model over others, is that it has prolonged neurodegeneration (6 months), with loss of TH phenotype preceding cell death (4 months). This allows for the largest window to examine pathology over multiple pathological stages (discussed further in Chapter 2), as well as the potential for therapy to intervene during specific stages. Moreover,

degeneration starts ipsilateral to PFF injections, and over time presents bilaterally. This is disease analogous to human PD which is typically bilateral with a dominant side [12, 13].

Is STN DBS Disease-Modifying?

One original rationale for how STN DBS might be disease modifying is via decreased excitotoxicity; STN DBS results in reduced excitatory glutamate release in post-synaptic targets. Evidence showing that STN DBS actually increases glutamate in target structures (SNpc and GPI) [208-211] refutes this hypothesis, however this is a misconception that some still hold. Nonetheless, there is evidence suggesting that patients receiving STN DBS fare better than those who do not [134, 212-214].

Specifically, some neurologists observed that STN DBS patients in which stimulation was turned off exhibited milder motor symptoms than what would be expected based upon their disease duration. This led to the hypothesis that STN DBS could potentially be disease-modifying. This question remains open, as the majority of STN DBS patients are on average 12-14 post diagnosis at the time of starting DBS [126], well beyond the period of preserving nigrostriatal terminal function [27, 105]. An early stage clinical trial conducted at Vanderbilt University began to address this question with promising preliminary results, however the cohort is too small and will need follow-up before any meaningful conclusions can be made [215, 216].

The disease modifying potential of STN DBS has also been investigated in the context of preclinical studies. STN DBS applied prior to, or after 6-OHDA insult results in

protection of DAergic neurons in the SNpc [158, 217-219]. These findings have been replicated in a non-human primate model using MPTP [220]. In contrast, STN DBS in rats with α -syn overexpression has yielded mixed results on neuroprotection [221, 222]. Whether STN DBS can attenuate the formation of α -syn aggregates is directly examined in the rat preformed fibril model in Chapter 3. Overall, the question of whether STN DBS is disease-modifying has yet to be explored in the correct clinical setting, and promising preclinical results may be model dependent. STN DBS-mediated neuroprotection observed in the 6-OHDA rat model was dependent on brain-derived neurotrophic factor (BDNF) [223]. This is consistent with a role for BDNF in stimulation-mediated effects in other contexts [224-226].

Brain-Derived Neurotrophic Factor

For decades, the potential for trophic factors to protect nigrostriatal neurons in PD has been explored with the specific factors glial cell-line derived neurotrophic factor (GDNF) and neurturin (NTN) advancing to clinical trials in PD subjects [227-232]. With major research efforts directed toward GDNF and NTN, other trophic factors have received little attention. BDNF is similar in structure to nerve growth factor (NGF) and therefore classified as a neurotrophin [233], however BDNF and NGF serve distinct functions. NGF is anti-apoptotic, necessary for the survival of developing sensory neurons [234, 235], whereas BDNF also promotes growth and survival, however in distinct, nonoverlapping cellular populations [236-238]. BDNF is found widespread throughout the CNS [239-242], including in relevant structures of the basal ganglia [243].

I. Synthesis, Release and Signaling

BDNF protein is initially synthesized as a precursor protein in endoplasmic reticulum. Following cleavage of the signal peptide into a 32-kDa proBDNF protein, it is either cleaved intracellularly into mature BDNF (mBDNF) or transported to the Golgi for sorting into either constitutive or regulated secretory vesicles for release (reviewed in [244]). Mature BDNF is the prominent isoform in the adult, whereas proBDNF is highly expressed at early postnatal stages [245]. proBDNF was initially thought to be an inactive, intracellular precursor for mature BDNF (mBDNF, or BDNF) in the adult, but it is now understood to be a secreted, biologically active molecule [245-249]. While proBDNF regulation and secretion are still relatively unclear processes, both proBDNF and BDNF are packaged into vesicles of the activity-regulated secretory pathway with secretion of proBDNF more prominent than BDNF [246].

BDNF biological activity is tightly regulated by its gene expression, axonal transport, and release. It is well known that BDNF is synthesized and released in an activity-dependent manner and as such, endogenous BDNF levels are extremely low [250]. BDNF release is dependent on stimulus pattern, with high-frequency bursts being the most effective [251]. The *bdnf* gene has nine promoters that produce 24 different transcripts, all of which are translated into a single, identical, mature dimeric protein [252]. This allows for tight, activity-dependent regulation whereby specific exon-containing transcripts are differentially regulated by specific neuronal activities including physical exercise, seizures, antidepressant treatment, and regular neuronal activation [253-259]. Neuronal activity also regulates the transport of BDNF mRNA into dendrites

allowing for locally translated BDNF to modulate synaptic transmission and synaptogenesis [260-262].

BDNF acts on postsynaptic neurons via two signaling pathways: the canonical and the non-canonical pathways. In the canonical pathway, BDNF binds to its high-affinity receptor tropomyosin-related kinase receptor B (TrkB). TrkB signaling activates PLC- γ , PI3K-Akt, and Erk, inducing a pro-survival cascade including neuronal survival, growth/arborization, and regulation of synaptic plasticity through mediating long-term potentiation (LTP) [263-265]. In contrast, all neurotrophins bind to p75 with low affinity (also known as low affinity nerve growth factor receptor, LNGFR) inducing apoptosis, and the balance of p75 and the Trk receptors ultimately determines cell survival or death (reviewed in [266]). Effects of canonical pathway signaling are relatively slow, on the order of hours, as they require alterations in transcription and translation of specific genes, ultimately resulting in the production of new proteins [263].

In the non-canonical pathway, the effects of BDNF are still mediated through TrkB, however they can occur but much faster as protein synthesis is not required. Instead, PI3K-Akt signaling results in an intermediate, Girdin, which is phosphorylated and results in the phosphorylation of the NMDA receptor 2B subunit (NR2B) [267, 268]. NR2B phosphorylation strengthens the response by NMDA receptor-mediated currents [267-269].

BDNF protein is found widespread throughout the CNS both pre- and postsynaptically.

It undergoes both retrograde and anterograde transport [270, 271], therefore the site of BDNF synthesis and function are not always the same. For example, BDNF protein is abundant in the striatum where it is critical for normal function, however there is relatively little BDNF mRNA in the striatum [240]. Instead, the overwhelming majority of BDNF is anterogradely transported from the cortex and to a lesser extent from the SNpc to the striatum [271, 272]. BDNF release is triggered in an activity-regulated, Ca^{2+} -dependent manner. This can occur by presynaptic influx of Ca^{2+} [273], postsynaptic influx of Ca^{2+} [274] or from release of intracellular Ca^{2+} stores [275].

II. BDNF in Parkinson's Disease

Of relevance to the present research, BDNF-TrkB signaling has effects on DA signaling and the survival and plasticity of nigrostriatal neurons. Examination of BDNF mRNA and protein levels in PD subjects has revealed alterations relative to aged matched controls. Postmortem examination suggests that BDNF mRNA and protein are downregulated in the SN of patients with PD [276-278]. This decrease in SN mRNA was correlated with both decreased soma size and neuron survival, suggesting that individual nigral neurons with low BDNF levels may be particularly vulnerable to degeneration [276]. Similarly, BDNF serum levels are lower in early-stage PD patients compared to controls, whereas in later stages BDNF serum levels correlate positively with duration and disease severity [279], possibly reflecting a compensatory mechanism. These limited findings from PD patients raise two essential questions, are decreases in BDNF a consequence or a contributor to the disease process, and is BDNF supplementation a possible therapeutic avenue?

The discovery that nigral DA neurons fare better with the addition of BDNF [280], led the PD field to consider BDNF as a potential therapy. Indeed, BDNF application is neuroprotective in toxicant models of PD [281-284]. BDNF release can be driven through electrical stimulation *in vitro* and *in vivo*. In neuronal cultures, high-frequency stimulation leads to increased BDNF release while low-frequency stimulation leads to increased proBDNF release [285]. Similarly, high-frequency STN DBS increases BDNF levels in the nigrostriatal system *in vivo* [223]. High-frequency STN DBS is therapeutic for PD and low-frequency STN DBS worsens PD symptoms [153, 286-288], offering a potential mechanism for this observed difference.

Other means of BDNF induction have also positively correlated with preclinical outcomes. In the α -syn A53T mutant mouse model, FDA-approved drug, Gilenya (FTY720/fingolimod) decreased α -syn aggregation in the enteric nervous system and alleviated gut motility symptoms in a BDNF-TrkB dependent manner [289]. A preclinical study investigating the therapeutic potential of Telmisartan, an angiotensin type 1 receptor antagonist, found a strong negative correlation between motor function and α -syn, and a strong positive correlation between motor function and BDNF [290]. Metformin (anti-hyperglycemic drug) lowers α -syn phosphorylation and upregulates BDNF in the MPTP mouse model of PD [291]. Some investigators have begun exploring exercise as a less invasive way to stimulate BDNF-TrkB, as exercise is known to increase BDNF. This approach has proven promising in several preclinical animal models of PD in which exercise induced BDNF and significantly reduced α -syn aggregation, with no change to soluble α -syn [292-295]. Temsirolimus (analog of

rapamycin) improved behavioral deficits in MPTP animal model of PD by ameliorating upregulation of α -syn, and restoring downregulated BDNF [296]. D-Ala²-GIP-glu-PAL, a long-acting glucose dependent insulinotropic polypeptide, reduced chronic inflammation, inhibited α -syn increase, and promoted BDNF in MPTP mouse model [297].

Goals of Current Study

STN DBS applied early in disease progression, prior to denervation of nigrostriatal neurons has yielded encouraging results for the treatment of Parkinson's disease [216, 298, 299]. In order to understand the disease-modifying potential of STN DBS we evaluated the impact it has on α -syn aggregation (Chapter 3), inclusion-associated gliosis (Chapter 4), and BDNF protein expression (Chapter 5) using our well-characterized rat PFF model of synucleinopathy. A general experimental overview is provided in Figure 1.1. Chapter 2 provides an overview of the pathogenesis associated with LBs and α -syn inclusions formed via PFF exposure, and the potential for BDNF signaling to intervene. Chapter 6 summarizes the key findings and identifies important gaps in knowledge to follow up on in future studies.

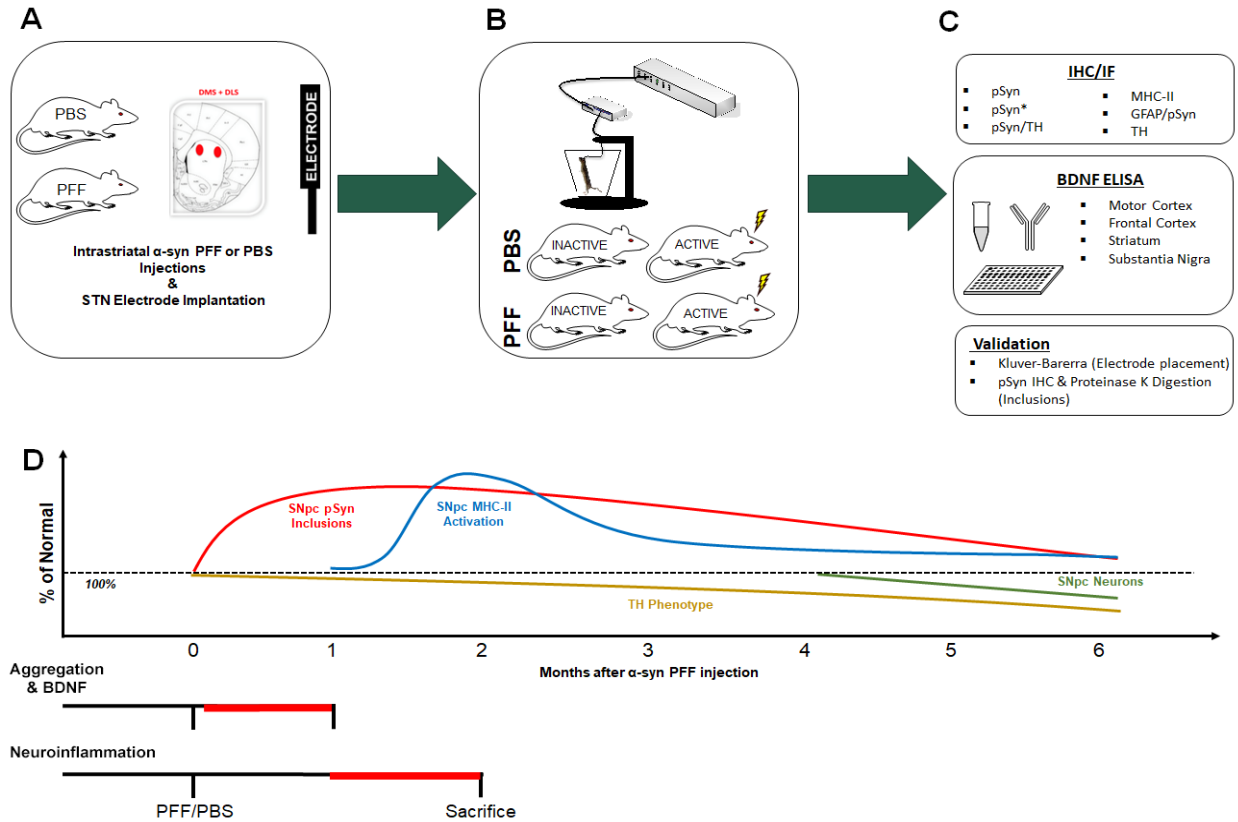


Figure 1.1: General experimental overview

Rats received two intrastriatal injections of α -syn PFFs or PBS and electrode implantation into the subthalamic nucleus (STN) during the same surgical session (**A**). Three days later, half of each group were randomly assigned to receive INACTIVE (stimulation never turned on) or ACTIVE stimulation (**B**). Outcome measures evaluate impact on aggregation (Chapter 3), neuroinflammation (Chapter 4), and BDNF protein expression (Chapter 5). Additionally, validation of electrode placement (Kluver-Barerra) and inclusion formation (Proteinase K digestion) was completed on all animals (**C**). End points and stimulation period (red bar) were determined according to the period of peak inclusion formation (1-2 months, red), and microglial activation (2 months, blue) prior to loss of TH phenotype (2-6 months, yellow) and degeneration of SNpc neurons (4-6 months, green; **D**).

**Chapter 2: Synucleinopathy-Associated Pathogenesis and the Potential for STN
DBS Induced Brain Derived Neurotrophic Factor**

Abstract

The lack of a disease-modifying treatments for Parkinson's disease (PD) is in part due to an incomplete understanding of the disease's etiology. Alpha-synuclein (α -syn) has become a point of focus in PD due to its connection to both familial and idiopathic cases – specifically its localization to Lewy bodies, a pathological hallmark of PD. Within this review, we will present a comprehensive overview of the data linking synuclein-associated Lewy pathology with intracellular dysfunction. We first present the alterations in neuronal proteins and transcriptome associated with Lewy bodies in postmortem human PD tissue. We next compare these findings to those associated with Lewy-body like inclusions initiated by in vitro exposure to α -syn preformed fibrils (PFFs) and highlight the profound and relatively unique reduction of brain derived neurotrophic factor (BDNF) in this model. Finally, we discuss the multitude of ways in which BDNF offers the potential to exert disease modifying effects on the basal ganglia. What remains unknown is the potential for BDNF to mitigate inclusion-associated dysfunction within the context of synucleinopathy. Collectively, this review reiterates the merit of using the PFF model as a tool to understand the physiological changes associated with LBs, while highlighting the neuroprotective potential of harnessing endogenous BDNF.

Introduction

Parkinson's disease (PD) affects over a million Americans and results in nearly \$25 billion per year in health care costs as well as immeasurable personal costs to patients and families (PDF, 2017). It is now appreciated that PD is a complex, multifaceted disorder that impacts both the central and peripheral nervous systems with patients experiencing symptoms ranging from motor dysfunction to constipation to dementia; all contributing to a significant detriment to the quality of life. However, the cardinal motor symptoms of tremor, rigidity, akinesia/bradykinesia, and postural instability first described by James Parkinson in 1817 are still requisite for diagnosis and are the primary target for therapeutic intervention [1, 300]. PD motor symptoms are caused by the loss of dopaminergic transmission in the striatum due to progressive loss of dopamine (DA) neurons in the substantia nigra pars compacta (SNpc) and their projections to the caudate and putamen. As a result, current pharmacotherapies attempt to augment nigrostriatal DA transmission. Unfortunately, these approaches are not disease-modifying, with pharmacotherapy ultimately losing therapeutic efficacy as disease progression continues. Thus, PD remains a tremendous burden to those afflicted as well as to society as a whole.

The lack of a disease-modifying treatments for PD is in part due to an incomplete understanding of the disease's etiology. PD belongs to a family of disorders termed synucleinopathies, all chiefly characterized pathologically by the deposition of the protein alpha-synuclein (α -syn) into neuronal inclusions termed Lewy bodies (LBs) that can be found throughout the body. Despite the identification of genetic forms of PD

(reviewed in [301]), the molecular etiology underlying disease origin and progression remain unknown. Nevertheless, abnormal α -syn proteostasis is a common factor between both sporadic and familial forms of PD (reviewed in [80]). Together with the loss of nigrostriatal DA neurons, accumulation of α -syn into LBs are the pathological hallmarks of PD. There are many ideas surrounding the mechanism by which aberrant α -syn proteostasis may contribute to PD (reviewed in [302]), however each are contested, and none have been proven outright. Further, whether LBs themselves directly cause toxicity or are merely a cellular marker associated with pathogenic processes has yet to be clarified. In either case, understanding the pathogenic mechanisms either associated with, or induced by LB formation is critical to the development of disease modifying treatments.

α -Synuclein

I. Normal α -Synuclein Function

α -syn is a small (14 kDa) protein encoded by the SNCA gene, that is abundantly expressed in the nervous system where it comprises up to 1% of all cytosolic protein [79]. Structurally, it can be broken down into three domains: the N-terminus, which is highly conserved within the synuclein family [303] and results in the alpha helix secondary structure of α -syn [304]; the hydrophobic core, known as the NAC [305], which causes α -syn to be prone to aggregation [306, 307]; and the C-terminal tail, which undergoes post-translational modifications that are thought to regulate its function [303, 308-310]. α -syn is a natively unfolded protein, with changing conformation depending on its environment [81]. This means it is unfolded and soluble under normal physiological

conditions, but changes conformation when interacting with its many binding partners. For example, α -syn has a strong affinity for high curvature lipid membranes (i.e. vesicles), and it changes conformation from two alpha helices [311] to one alpha helix upon interacting with them [304, 312, 313].

Functionally, α -syn is enriched in synaptic terminals where it is known to play critical roles in neurotransmission [78-80, 314-317]. It is thought to mediate trafficking, docking, and endocytosis of synaptic vesicles via interactions with soluble NSF attachment protein receptor (SNARE) complex proteins [315, 316, 318] and synaptic vesicles directly [78]. Of relevance to nigrostriatal neurons, α -syn is involved in dopamine synthesis [319-321], handling [322-327], and release [316, 328, 329], and is posited to serve as a negative regulator of synaptic transmission [80, 317, 330].

II. α -Synuclein Aggregation

Despite the myriad of identified normal functions of monomeric α -syn, it remains an 'intrinsically disordered' protein due to its dynamic nature with no clear tertiary structure, making it particularly vulnerable to aggregation [81, 331, 332]. α -syn interacts with itself to form tetramers [333-335] and β -pleated sheets [336]. While some posit the tetramers are the 'functional' conformation of α -syn [333-335], the β -pleated sheets, if not cleared, can form insoluble α -syn aggregates [53]. While these misfolded oligomers have not directly been proven toxic, they are associated with toxicity (reviewed in [337, 338]). For example, they are found in the brains of Parkinson's disease patients [339, 340], and when applied to cell cultures induce cell death [341-344]. Moreover, stable oligomers

have a higher seeding propensity than unstable oligomers [345], and mutations that result in oligomeric α -syn induce cell death [346, 347], whereas those that don't are not toxic [348].

Many conditions can promote this transition from soluble, functional α -syn into insoluble fibrils (reviewed in [80]), and once this process begins, it proceeds in a feed-forward manner in which fibrils seed and recruit soluble α -syn into more fibrils, a process that once escalated is largely irreversible [190, 349, 350]. Within PD and other synucleinopathies, α -syn transforms from a soluble, functional protein to a phosphorylated, aggregated, protein that becomes associated with pathogenic consequences [351-354], i.e., LBs.

Synucleinopathy-Associated Pathogenesis

I. Insights Derived from Postmortem PD Tissue

Three different technical approaches have been used that provide insight into what pathophysiological mechanisms are associated with LBs (Table 2.1). First, quantitative immunofluorescent techniques have been used to examine proteins within LB-containing vs. non LB-containing neurons. These studies have demonstrated that LB-containing neurons exhibit reduced ubiquitin proteasome system (UPS) and lysosomal markers [355], kinesin motor proteins, and pro-survival myocyte enhancer factor 2D [356, 357], and increased DNA strand breaks [358], and toll-like receptor 2 [359].

Whereas this immunofluorescence approach maintains the specificity of the comparison, LB vs. no LB, it remains limited by the number of different proteins that can

be analyzed at any one time.

In contrast to the immunofluorescence approach, several studies have used the approach of microarray profiling (Table 2.1) to compare whole nigral tissue from varying stages of PD to control brains, identifying a wide array of dysregulated genes involved in synaptic transmission, protein degradation, DA handling, ion transport, transcription, inflammation, vesicle trafficking, axon guidance and mitochondrial function [360-365]. The whole tissue microarray approach has the advantage of an unbiased survey of gene expression changes but at the cost of losing the specificity necessary to precisely pinpoint differences between neurons possessing LBs compared to those without due to the fact that LB and non-LB containing neurons (and other cell types) are present within the whole tissue punch. Further, depending on disease stage, the whole tissue approach can be confounded by the loss of nigral neurons themselves.

The approach of laser capture microdissection (LCM) combined with gene expression analysis has been used to compare dopaminergic nigral neurons in PD vs. control brains, allowing for single cell neuronal resolution to be combined with either focused or unbiased expression analysis (Table 2.1). To our knowledge, only a single LCM study (conducted fifteen years ago) has specifically compared expression differences between LB-containing and non-LB containing nigral neurons [366]. This focused study, conducted in a small sample size, suggested that LB-containing nigral neurons have increased expression of proapoptotic and proUPS genes and decreased expression of genes associated with cytoskeletal organization and molecular chaperones. The

remainder of LCM studies have examined transcript differences between nigral DA neurons in PD or Incidental Lewy Body disease (ILBD) cases and control nigral DA neurons with the presence of LBs not a determining selection factor. These studies show that nigral DA neurons from PD brains have alterations in genes associated with protein kinase activity, UPS functioning, mitochondrial function, dopamine metabolism and ion channels [367-371]. Less agreement has surfaced from LCM studies with regards to expression of α -syn itself, with earlier studies suggesting increased SNCA expression [372] in PD nigral neurons and a more recent analysis suggesting no change SNCA expression, or trophic factor signaling and dopamine metabolism genes [189].

In order to understand what pathogenic mechanisms are consistently associated with LBs, it is reasonable to look for consensus across methodological approaches with an emphasis on LB-specific analyses. Both immunofluorescence and LCM of LB-containing nigral neurons reveal alterations in proteolysis markers [355, 366] as well as alterations in transport/cytoskeleton organization [357, 366]. Some whole SN tissue analysis and LCM studies of nigral DA neurons also have detected proteolysis and transport/cytoskeletal dysfunction [360-362, 367, 368]. Mitochondrial dysfunction is quite frequently detected by both whole SN tissue analysis and LCM approaches [360-362, 368-370] however the association specifically with LBs has not directly been established. Despite these efforts using PD brain tissue, the pivotal pathogenic mechanisms associated with the formation of LBs has yet to be identified. The heterogeneity of PD combined with the difficulty of gleaning mechanistic insight using

analysis of static postmortem tissue further confound the potential for our understanding of LB associated pathogenesis. Fortunately, an alternative approach is providing new information of the dynamic cellular alterations associated with the formation of α -syn inclusions.

Table 2.1: Insights into synucleinopathy-associated pathogenesis derived from postmortem PD tissue

Quantitative Immunofluorescence			
Authors	Year	Comparator	Findings
Chu et al.	2009	LB vs non-LB neurons	Decreased ubiquitin proteasome system and lysosomal markers with LBs
Chu et al.	2011	LB vs non-LB neurons	Decreased myocyte enhancer factor 2D with LBs
Chu et al.	2012	LB vs non-LB neurons	Decreased kinesin motor proteins in neurons with LBs Increased expression of dynein in neurons with LBs
Dzamko et al.	2017	LB vs non-LB neurons	Increased toll-like receptor 2 in neurons with LBs
Schaser et al.	2019	LB vs non-LB neurons	Increased DNA double stranded breaks in neurons with LBs
Whole Tissue Microarray			
Authors	Year	Comparator	Findings
Grunblatt et al.,	2004	PD SN vs control SN	68 downregulated in PD involved in signal transduction, protein degradation, DA handling, ion transport, and energy pathways. 69 upregulated in PD involved in protein modification, metabolism, transcription, and inflammation.
Hauser et al.	2005	PD SN vs control SN	96 genes differentially expressed. Main pathways were chaperones, ubiquitination, vesicle trafficking, and mitochondrial function
Duke et al.	2006	PD SN vs control SN	Downregulation of pathways related to ubiquitin proteasome system and mitochondrial function.
Elstner et al.	2009	PD SN vs control SN	4 genes differentially expressed. Pathways were mitochondrial function, DA metabolism, axon guidance, and vesicle transport.
Botta-Orfila et al.	2012	PD LC vs control LC	Differential expression of genes related to synaptic transmission, neuron projection, and immune system related pathways
Dijkstra et al.	2015	PD SN vs ILBD SN vs control SN	Dysregulation of pathways related to axonal guidance, endocytosis and immune response (ILBD) as well as dysregulated mTOR and EIF2 signaling in both ILBD and PD.
Laser Capture Microdissection			
Authors	Year	Comparator	Findings
Lu et al.	2005	PD SN neurons with LBs vs PD SN neurons without LBs	Increased USP8 (pro UPS function) Increased ANP32B (proapoptotic) Decreased KLHL1 and BPAG1 (cytoskeleton organization), Decreased Stch (encodes HSP 70)
Cantuti-Castelvetri et al.	2007	PD SN neurons vs control SN neurons Both male and female	Females: Alterations in genes with protein kinase activity, genes involved in proteolysis and WNT signaling pathway. Males: Alterations in protein-binding proteins and copper-binding proteins.
Elstner et al.	2011	PD SN neurons vs control SN neurons	Downregulation of genes coding for mitochondrial and ubiquitin-proteasome system proteins
Grundemann et al.	2011	PD SN neurons vs control SN neurons	Increased SNCA expression
Lin et al.	2012	ILBD SN neurons vs PD SN neurons vs control SN neurons	Increased mitochondrial DNA mutations in early PD/ILBD group compared to late stage and controls
Grunewald et al.	2016	PD SN neurons vs control SN neurons	Reduced respiratory chain complex I and II
Su et al.	2017	PD SN neurons vs control SN neurons	Decreased SNCA expression, no changes in Nurr1, RET, PARK7, SLC18A2, BDNF, DDC, TH, MEF2D or PITX3
Duda et al.	2018	PD SN neurons vs control SN neurons	Dysregulation in genes encoding for ion channels, dopamine metabolism proteins, and PARK.

II. Insights from the α -Synuclein PFF Model

Since the earliest observation of LBs in the parkinsonian brain, the question of what role this intracellular structure plays in degeneration remains unanswered. LBs may trigger cytotoxic events, or alternatively be beneficial, or may simply represent an artifact that is inconsequential to either pathogenesis or neuroprotection. Transgenic animal models in which α -syn aggregates are formed rarely lead to overt degeneration [373-376], limiting their utility for understanding the relationship between α -syn aggregation and degeneration. However, a relatively recent model first described in wildtype mice in 2012 by Luk and colleagues [191] demonstrated the ability of intrastriatal injection of preformed α -syn fibrils (PFFs) to seed LB-like aggregates in the SN and multiple cortical regions. PFFs are taken up into neurons [196] and once inside initiate a conversion of normal α -syn into phosphorylated and misfolded α -syn, ultimately accumulating to form LB-like aggregates [190, 195, 196]. Importantly, a definitive link between fibril seeded pathological α -syn aggregation and eventual neuronal death has been established in this model [377].

Although multiple studies have examined the degenerative phenotype induced by PFF injections to mice and rats [191-193, 198, 378], studies using PFFs in primary neuronal cultures prove particularly useful in revealing the intracellular events observed in tandem with the formation and maturation of PFF triggered LB-like inclusions. Although no conclusive evidence exists that α -syn inclusions themselves are toxic, neurons in which phosphorylated α -syn inclusions form following α -syn PFF exposure exhibit multiple structural, protein and transcriptomic changes that are associated with

pathophysiological processes and, in the case of longer *in vitro* intervals, cell death (Table 2.2). Specifically, PFF initiated α -syn inclusions result in decreased expression of synaptic proteins [196, 197, 379], impairments in axonal transport [195], and mitochondrial impairment [379-381]. Structurally and functionally, α -syn inclusion bearing neurons display impaired excitability and decreased spine density [196, 382, 383]. Notably, these results from the *in vitro* PFF model reveal heavy overlap with results from Lewy body containing neurons or tissue from PD brains, particularly with regard to transport/cytoskeleton disorganization and mitochondrial dysfunction. The most comprehensive study to date in cultured neurons with PFF-seeded α -syn inclusions was conducted by Mahul-Mellier and colleagues [197] who examined longitudinal transcriptomic alterations in neurons as α -syn inclusions matured. In addition to observing decreased expression of synaptic genes, cytoskeletal organization genes and mitochondrial genes, this study also revealed decreased expression of a gene that had previously received little attention with regard to α -syn inclusion-associated alterations: brain derived neurotrophic factor (BDNF). Specifically, out of the 11767 total mouse genes that were examined only 0.05% were significantly decreased across all time points with one of these being *bdnf*. In inclusion bearing neurons *bdnf* decreased 1.2 fold at day 7, 2.32 fold at day 14 and 2.5 fold at day 21. Further, of all the genes significantly decreased at day 21, the magnitude of *bdnf* decrease was greater than 98% of all the others. In other words, only 9 other genes (out of 11767 total, 562 were downregulated) exhibited a greater magnitude of reduction than *bdnf* at day 21.

Table 2.2: Insights into synucleinopathy-associated pathogenesis derived from in vitro PFF studies

In Vitro Experiments			
Authors	Year	Comparator	Findings
Volpicelli-Daley et al.	2011	Hippocampal neurons with and without α -syn aggregates	Decreased expression of multiple synaptic proteins. Impairments in neuronal excitability and connectivity.
Volpicelli-Daley et al.	2014	Hippocampal neurons with and without α -syn aggregates	Impairment of axonal transport of RAB7 and TrkB-containing endosomes and autophagosomes. Accumulation of pERK5.
Tapias et al.	2017	Mesencephalic DA neurons with and without α -syn aggregates	Decreased expression of synaptic proteins. Alterations in axonal transport-related proteins. Impaired mitochondria. Increased oxidative stress.
Froula et al.	2018	Hippocampal neurons with and without α -syn aggregates	Decreased mushroom spine density. Increased excitatory postsynaptic currents. Increased presynaptic docked vesicles. Decreased frequency and amplitude of spontaneous calcium transients.
Grassi et al.	2018	Hippocampal neurons with and without α -syn aggregates	pSyn* induces mitochondrial toxicity and fission, energetic stress and mitophagy.
Wu et al.	2019	Hippocampal neurons with and without α -syn aggregates	Decreased excitatory post-synaptic current frequency. Altered dendritic spines.
Wang et al.	2019	Cortical neurons with and without α -syn aggregates	Deficits in mitochondrial respiration
Mahul-Mellier et al.	2020	Hippocampal neurons with and without α -syn aggregates	<p>Transcriptomic changes over time:</p> <p><u>D7</u>: 75 total genes (27 upregulated, 48 downregulated) encoding for proteins located within synapses, axons, or secretory and exocytic vesicles. Genes encoding for proteins involved in neurogenesis and the organization, growth, and the extension of the axons and dendrites</p> <p><u>D14</u>: 329 total genes (106 upregulated, 223 downregulated) linked to the synaptic, neuritic, and vesicular cellular compartments. Genes associated with neurogenesis, calcium homeostasis, synaptic homeostasis, cytoskeleton organization, response to stress, and neuronal cell death process.</p> <p><u>D21</u>: 1017 total genes (455 upregulated, 562 downregulated) with enrichment in genes encoding for proteins related to the ion channel complex, plasma membrane protein complex, cell–cell junctions, synaptic functions, response to oxidative stress and mitochondria.</p> <p><u>D14 vs. D21</u>: Differential expression of genes associated with mitochondrial and synaptic functions.</p>

Brain-Derived Neurotrophic Factor (BDNF)

For decades the potential for trophic factors to protect nigrostriatal neurons in PD has been explored leading to the factors glial cell-line derived neurotrophic factor (GDNF) and neurturin (NTN) advancing to clinical trials in PD subjects [227-232]. With major research efforts directed toward GDNF and NTN, the potential of other trophic factors has largely remained unexplored. BDNF is a member of the neurotrophin family and is abundantly expressed in the central nervous system from development through adulthood playing critical roles in neuronal survival, migration, axonal and dendritic outgrowth, synaptogenesis, synaptic transmission, and synaptic plasticity [250, 384-388]. BDNF also promotes neuroprotection after injury by inhibiting pro-apoptotic molecules [389].

Examination of BDNF mRNA and protein levels in PD subjects has revealed alterations relative to aged matched controls. Postmortem examination suggests that BDNF mRNA and protein are downregulated in the SN of patients with PD [276-278]. This decrease in SN mRNA correlates with both decreased soma size individual and neuron survival, suggesting that individual nigral neurons with low BDNF levels may be particularly vulnerable to degeneration [276].

BDNF biological activity is tightly regulated by its gene expression, axonal transport, and release. It is well known that BDNF is synthesized and released in an activity-dependent manner and as such, endogenous BDNF levels are extremely low [250]. BDNF release is dependent on stimulus pattern, with high-frequency bursts being the

most effective [251]. The *bdnf* gene has nine promoters that produce 24 different transcripts, all of which are translated into a single, identical, mature dimeric protein [252]. This allows for tight, activity-dependent regulation whereby specific exon-containing transcripts are differentially regulated by specific neuronal activities including physical exercise, seizures, antidepressant treatment, and regular neuronal activation [253-259]. Neuronal activity also regulates the transport of BDNF mRNA into dendrites allowing for locally translated BDNF to modulate synaptic transmission and synaptogenesis [260-262].

BDNF protein is initially synthesized as a precursor protein (proBDNF) in endoplasmic reticulum. Following cleavage of the signal peptide into a 32-kDa proBDNF protein, it is either cleaved intracellularly into mature BDNF (mBDNF) or transported to the Golgi for sorting into either constitutive or regulated secretory vesicles for release (reviewed in [244]). Mature BDNF is the prominent isoform in the adult, whereas proBDNF is highly expressed at early postnatal stages [245]. proBDNF was initially thought to be an inactive, intracellular precursor for mBDNF in the adult, but it is now understood to be a secreted, biologically active molecule [245-249]. While proBDNF regulation and secretion are still relatively unclear processes, both proBDNF and mBDNF are packaged into vesicles of the activity-regulated secretory pathway with secretion of proBDNF more prominent than mBDNF [246].

BDNF protein is found widespread throughout the CNS both pre- and postsynaptically. It undergoes both retrograde and anterograde transport [270, 271], therefore the site of

BDNF synthesis and function are not always the same. For example, BDNF protein is abundant in the striatum where it is critical for normal function, however there is relatively little BDNF mRNA in the striatum [240]. Instead, the overwhelming majority of BDNF is anterogradely transported from the cortex and to a lesser extent from the SNpc to the striatum [271, 272]. BDNF release is triggered in an activity-regulated, Ca^{2+} -dependent manner. This can occur by presynaptic influx of Ca^{2+} [273], postsynaptic influx of Ca^{2+} [274] or from release of intracellular Ca^{2+} stores [275].

BDNF binds and activates two known surface receptors: mBDNF binds to tropomyosin related kinase receptor B (TrkB) whereas proBDNF binds to pan neurotrophin receptor (p75NTR; p75) [390]. TrkB is part of the tyrosine kinase family of receptors, along with TrkA and TrkC. BDNF binds to TrkB with high affinity inducing a pro-survival cascade. In contrast, all neurotrophins bind to p75 with low affinity (also known as low affinity nerve growth factor receptor, LNGFR) inducing apoptosis, and the balance of p75 and the Trk receptors ultimately determines cell survival or death (reviewed in [266]). The majority of BDNF signaling is attributed to mBDNF binding and activating TrkB. However, evidence suggests that proBDNF binds p75, and pro- and mBDNF elicit opposing synaptic effects through activation of their respective receptors [245-248, 391]. Moreover, mBDNF also binds a truncated TrkB receptor lacking the tyrosine kinase domain involved in downstream signaling [392, 393]. Thus, when bound to p75 or truncated TrkB BDNF is functionally inhibited from activating the canonical BDNF-TrkB signaling pathway, acting as a dominant negative regulatory mechanism [394].

BDNF-trkB signaling can activate two distinct postsynaptic signaling pathways: the canonical and the noncanonical pathways. In the canonical pathway, three signaling cascades have been identified: (1) the mitogen-activated protein kinase/extracellular signal related-kinase (MAPK/ERK) cascade, (2) the phosphatidylinositol 3-kinase/AKT (PI3K/AKT) cascade, and (3) the phospholipase C gamma (PLC γ) cascade [395, 396]. MAPK/ERK and PI3K/AKT cascades mediate translation and trafficking of proteins [264], whereas PLC γ mediates transcription via intracellular Ca²⁺ regulation and cyclic adenosine monophosphate and protein kinase activation [395]. Collectively, these cascades affect neuronal survival, growth/ arborization, and synaptic plasticity [264]. In the noncanonical pathway, intracellular PI3K-Akt signaling results in phosphorylation of the NMDA receptor 2B subunit, [267-269], resulting in potentiated responses. Noncanonical signaling has also been suggested to have effects on presynaptic dopamine release and reuptake [397]. These immediate phosphorylation events in the noncanonical pathway occur at a much faster rate than the translational and transcriptional events in the canonical pathway. Thus, BDNF can exert a multitude of effects on the basal ganglia over various time spans.

Can BDNF Provide Neuroprotection from Synucleinopathy?

α -syn inclusions are associated with a profound decrease in BDNF mRNA in neurons [197]. Targeted α -syn overexpression in the nigrostriatal system has consistently been shown to negatively regulate BDNF and TrkB expression, as well as downstream BDNF-TrkB signaling [398-401]. Similarly, α -syn overexpression in rats leads to decreased BDNF protein expression in the SN [399]. *In vitro*, α -syn overexpression

results in decreased BDNF mRNA and protein expression, both in the media and in the cell lysate [399]. Conversely, silencing of α -syn results in an upregulation of BDNF mRNA [400]. Retrograde transport of BDNF is impaired in neurons that overexpress α -syn [398]. Neurons with PFF-seeded α -syn inclusions have reduced retrograde transport of TrkB [195] and overexpression of α -syn has also been shown to inhibit BDNF-TrkB signaling *in vitro* [402]. Collectively, these studies suggest that pathological α -syn decreases levels of BDNF, interferes with retrograde BDNF transport, and decreases TrkB levels and TrkB signaling. It is therefore possible that increased BDNF expression could counteract or mitigate the pathological consequences of synucleinopathy.

Neurons with LBs exhibit alterations in proteolysis markers, transport/cytoskeleton organization and mitochondrial dysfunction [355, 360-362, 366-368, 370]. These effects are recapitulated in neurons seeded with α -syn inclusions via PFF exposure, with additional findings of decreased expression of synaptic proteins and reductions in spine density [196, 197, 354, 379-383]. BDNF has been linked to positive effects on many of these same cellular processes. Specifically, BDNF increases mitochondrial oxidative efficiency and combats mitochondrial dysfunction [389, 403], enhances synaptic transmission [404], and promotes synaptic plasticity [405] including increasing dendritic spine density [406]. BDNF application to mesencephalic dopamine neurons *in vitro* protects from neurotoxicants [281, 407]. BDNF also protects nigral dopamine neurons from neurotoxicant insult in both rodent and non-human primate models [282-284]. In

summary, BDNF-TrkB signaling has the potential to exert a multitude of disease modifying effects on the basal ganglia and other nuclei.

What remains unknown is whether BDNF can exert neuroprotective effects within the context of synucleinopathy. One way to increase endogenous production and release of BDNF is through high frequency stimulation [274, 285]. We have previously demonstrated that subthalamic nucleus deep brain stimulation (STN DBS) specifically induces BDNF mRNA and protein throughout the basal ganglia [223, 243, 408-410]. Moreover, TrkB blockade prevented the neuroprotection normally associated with stimulation [411]. In Chapter 5 I describe the effect of PFF-seeded inclusions on BDNF levels in rat SN, striatum and cortex with and without STN DBS. Although neuroprotection of the nigrostriatal system was not examined in these short-term experiments, my results shed light on how the in vivo BDNF landscape is altered by synucleinopathy and whether STN DBS can harness endogenous BDNF for neuroprotective potential.

**Chapter 3: Impact of STN DBS on Endogenous α -Syn Aggregation Triggered by
Intrastriatal Fibril Injection**

Abstract

Whether deep brain stimulation (DBS) of the subthalamic nucleus (STN) is disease-modifying for Parkinson's disease (PD) remains unclear. A hallmark of PD pathology is the progressive accumulation of α -synuclein (α -syn) inclusions (Lewy bodies). To date, only a single report has examined whether Lewy body pathology is impacted in PD subjects by DBS (PMID: 27911008). While no effect was observed, this study was limited by the 14-year disease duration prior to DBS, long after the establishment of Lewy body pathology. No preclinical study has examined whether STN DBS can prevent the initial formation of α -syn aggregates. The distinct α -syn aggregation phase in the α -syn preformed fibrils (PFF) model can be leveraged to examine the impact of STN DBS on accumulation of Lewy body-like pathology. Young and aged adult male rats received intrastriatal injections of α -syn PFFs and were implanted with electrodes in the STN during the same surgical session. Three days later, animals were randomly assigned to either receive stimulation (ACTIVE) or not (INACTIVE) for a period of 30 days. Stereological assessment of substantia nigra pars compacta (SNpc) neurons possessing phosphorylated α -syn (pSyn) and truncated phosphorylated α -syn (pSyn*) inclusions served as the primary outcome measures. The size and intensity of nigral DA neurons, and the size and intensity of individual aggregates were also characterized. STN DBS did not impact the number of nigral neurons possessing pSyn or pSyn* immunoreactive inclusions in young rats, and also did not impact the size or intensity of pSyn immunoreactive aggregates. The formation of pSyn inclusions within nigral neurons was associated with altered TH expression and reduced soma size, neither of which was impacted by STN DBS. Similarly, a modest decrease in SNpc tyrosine

hydroxylase immunoreactive (THir) neurons in the PFF-injected hemisphere was observed that was not impacted by STN DBS. Whereas STN DBS did not alter the number of pSyn or pSyn* nigral neurons in aged rats, fewer inclusion bearing neurons were observed compared to young rats. Collectively, our findings suggest that STN DBS does not impact the formation of inclusions triggered by α -syn PFF injection.

Introduction

I. Parkinson's Disease

Parkinson's disease (PD) is the second most common neurodegenerative disorder, affecting over a million Americans and resulting in nearly \$25 billion per year in health care costs (PDF, 2017). Age is the primary risk factor for PD, affecting 1% of individuals over the age of 65 years [85]. PD motor symptoms (tremor, rigidity, akinesia/bradykinesia, and postural instability) are caused by the progressive loss of dopamine (DA) neurons in the substantia nigra pars compacta (SNpc) and their projections to the striatum. As a result, current pharmacotherapies (e.g. levodopa) attempt to augment nigrostriatal DA transmission. However, as disease progression continues, pharmacotherapy often loses symptomatic efficacy and induces dyskinesias. Beyond pharmacotherapy, the surgical approach of deep brain stimulation (DBS) of the subthalamic nucleus (STN) is presently used with increasing frequency as a way to manage many PD motor symptoms. Since its introduction in 1995 and Food & Drug Administration (FDA) approval in 2002, more than 100,000 patients have received DBS [118]. STN DBS improves the quality of life of PD patients (motor disability, activities of daily living and levodopa-induced motor complications), sometimes to a greater extent than optimized pharmacotherapy [131, 137, 140].

II. STN DBS and Neuroprotection – Clinical Studies

Beyond its symptomatic efficacy, the question of whether STN DBS can be disease-modifying is still uncertain. To date, the clinical studies examining this issue have predominantly been retrospective studies of late-stage PD subjects who received DBS

an average of 12.6 years after diagnosis [412, 413]. Results from these studies clearly indicate that when applied to late stage PD, STN DBS is not neuroprotective. However, as is the case when examining any potentially disease-modifying therapy, intervention in early-stage PD patients will be required to answer this question. It is well established that the overwhelming majority of SNpc DA neurons and virtually all DAergic innervation in the striatum has already succumbed to degeneration at later stages of the disease [27, 105]. The practice of using STN DBS as a treatment of last resort (mean of 14 years after PD diagnosis [126]) has prevented our ability to evaluate its disease-modifying potential.

III. STN DBS and Neuroprotection – Preclinical Studies

Evidence from preclinical studies in rats and monkeys have consistently demonstrated that unilateral or bilateral STN DBS pretreatment can prevent the degeneration of SNpc DA neurons produced by DA-depleting neurotoxicants [217, 218, 220]. In contrast to results in neurotoxicant models, STN DBS applied in alpha-synuclein (α -syn) overexpression models has yielded mixed results with regards to neuroprotection [221, 222], and therefore whether STN DBS can protect the nigrostriatal system in the context of synucleinopathy remains an open question.

IV. Synucleinopathy Seeded by Injection of α -Syn Pre-Formed Fibrils (α -Syn PFFs)

Another limitation of previous STN DBS neuroprotection studies is that the majority of investigations have used neurotoxicant models that have yielded limited predictive

validity in clinical trials [412-414], warranting the use of non-toxicant based PD models. The use of STN DBS in α -syn overexpression models in two recent reports was an attempt to more closely approximate PD pathophysiology; however, neuroprotection results were mixed [221, 222]. Most recently an appreciation has developed that α -syn overexpression models may more closely recapitulate the rare duplication/triplication mutations in *SNCA* in which α -syn levels are elevated [415]. In contrast, α -syn mRNA and protein are not increased in human sporadic PD [416, 417] making the overexpression of α -syn less analogous to the sporadic disease state. Further, supraphysiological α -syn overexpression may introduce a pathogenic mechanism(s) not relevant to sporadic PD [222].

In the present study we leverage the α -syn preformed fibril (PFF) rat model of synucleinopathy to examine the effects of STN DBS on α -syn inclusion formation. Young and aged adult male rats received intrastriatal injections of α -syn PFFs and were implanted with DBS electrodes, then were randomly assigned to receive continuous STN DBS, or no stimulation, during month 1 after PFF injection; the period of peak α -syn accumulation. α -syn PFF injection resulted in accumulation of pSyn inclusions in the substantia nigra pars compacta (SNpc) and several cortical areas. Rats seeded with pSyn inclusions possessed fewer tyrosine hydroxylase immunoreactive (THir) SNpc neurons ($\approx 18\%$ decrease) reflecting loss of TH phenotype. STN DBS did not alter any of these pSyn inclusion-associated effects, and also did not impact the size or intensity of individual pSyn inclusions within the SNpc.

Methods

I. Experimental Overview

Sixty male Fischer 344 (Charles River, Wilmington, MA) rats were used for this study. In Experiment 1, young adult (3 months old) rats were used (n = 30), and in Experiment 2 aged (20 months old) rats were used (n = 30). All animals were unilaterally injected with preformed α -syn fibrils (PFF) into 2 sites in the striatum. During the same surgical session, all animals were implanted with an electrode targeting the subthalamic nucleus. In each experiment, three days after surgery 15 animals were randomly assigned to receive stimulation (ACTIVE) or no stimulation (INACTIVE) for 30 days. An overview of the experimental design is presented in Figure 3.1.

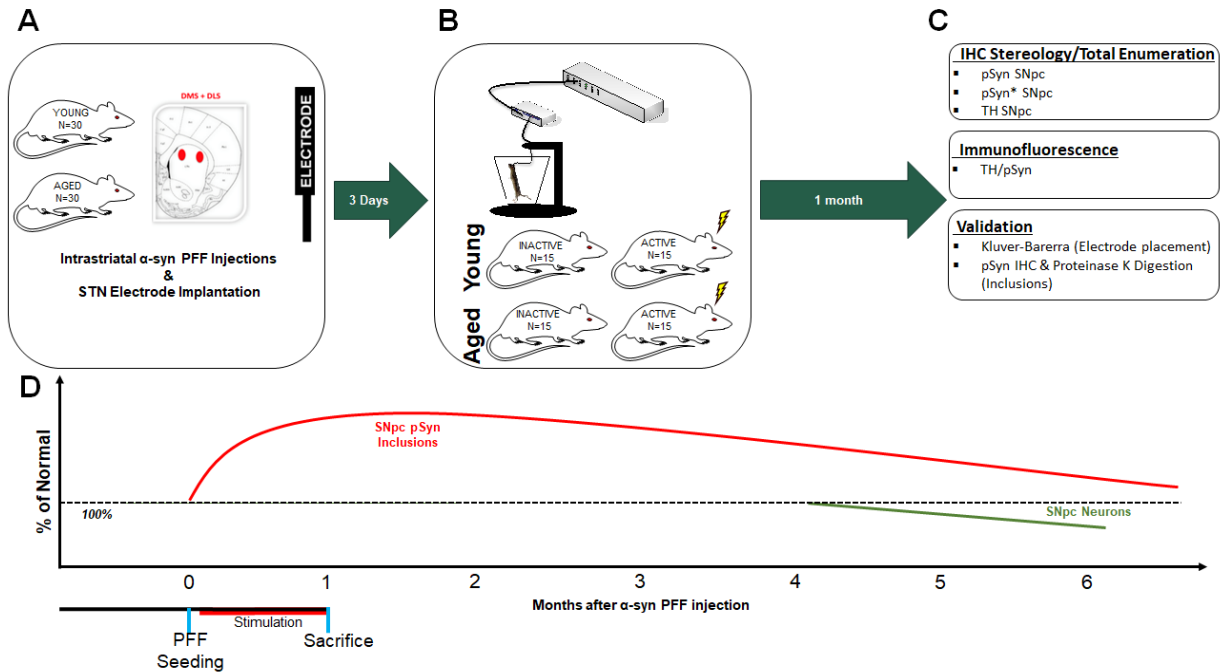


Figure 3.1: Experimental overview

Young (3 months old; $n = 30$) and aged (20 months old; $n = 30$) rats received two intrastriatal injections of α -syn PFFs and electrode implantation into the subthalamic nucleus (STN) during the same surgical session (**A**). Three days later, half of each group were randomly assigned to receive INACTIVE (stimulation never turned on; $n = 15$) or ACTIVE ($n = 15$) stimulation for one month, at which point all animals were sacrificed (**B**). Outcome measures include stereology (TH) or total enumeration (pSyn, pSyn*), dual-label immunofluorescence inclusion characterization (TH/pSyn), and validation of electrode placement (Kluver-Barerra) and inclusion formation (Proteinase K digestion; **C**). Time points were determined according to the period of peak inclusion formation (1-2 months, red), prior to degeneration of SNpc neurons (4-6 months, green; **D**).

II. Animals

All animals were given food and water *ad libitum* and housed in 12h light-dark cycle conditions in the Grand Rapids Research Center, which is fully Association for Assessment and Accreditation of Laboratory Animal Care (AALAC) approved. All procedures were conducted in accordance with guidelines set by the Institutional Animal Care and Use Committee (IACUC) of Michigan State University.

III. Preparation and Quality Control of α -Syn PFFs

Recombinant, full-length mouse α -syn PFFs were prepared and verified via in vitro fibril assembly as previously described [194-196, 418]. Prior to sonication, α -syn fibrils were assessed to verify lack of contamination (LAL Assay (~ 1 endotoxin units/mg), high molecular weight (sedimentation assay), beta sheet conformation (thioflavin T), and structure (electron microscopy). Prior to injection, PFFs were thawed, diluted in sterile Dulbecco's PBS (DPBS, 2 μ g/ μ l), and sonicated at room temperature using an ultrasonicating homogenizer (300VT; Biologics, Inc., Manassas, VA) with the pulser set at 20% and power output at 30% for 60 pulses at 1 s each [194]. Following sonication, a sample of the PFFs was analyzed using transmission electron microscopy (TEM). Formvar/carbon-coated copper grids (EMS DIASUM, FCF300-Cu) were washed twice with ddH₂O and floated for 1 min on a 10- μ l drop of sonicated α -syn fibrils diluted 1:20 with DPBS. Grids were stained for 1 min on a drop of 2% uranyl acetate aqueous solution; excess uranyl acetate was wicked away with filter paper and allowed to dry before imaging. Grids were imaged on a JEOL JEM-1400 transmission electron microscope. The length of ~500 fibrils per sample was measured to determine average

fibril size. The mean length of sonicated mouse α -syn PFFs was estimated to be 40.9 ± 0.55 nm, well within the optimal fibril length previously reported to result in seeding of endogenous phosphorylated α -syn inclusions in vitro and in vivo [419] (Fig. 3.2).

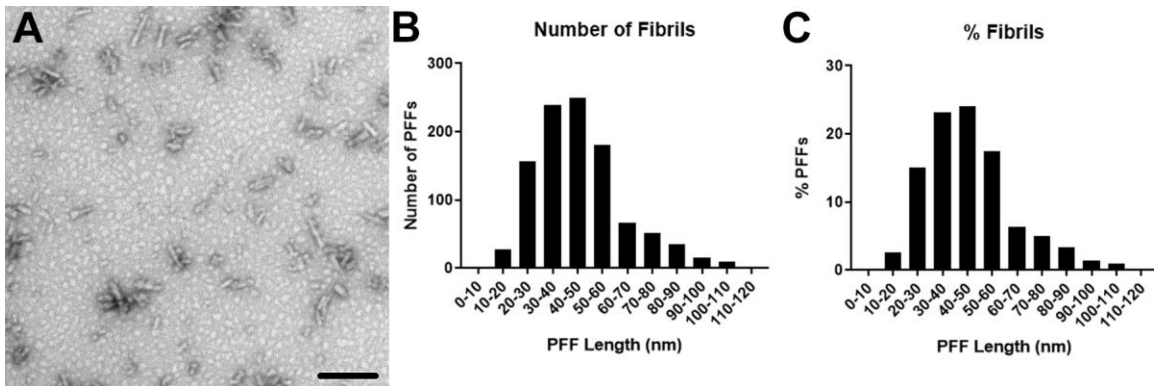


Figure 3.2: Distribution of sonicated α -syn PFF size prior to intrastriatal injection

Fibrils were sonicated into small fragments (A). Scale bar is 100 μ m. The number (B) and percentage (C) of PFFs at each size is quantified revealing that the majority of sonicated fibrils were smaller than 60 nm.

IV. Pre-Formed Fibril Injections

Intrastriatal α -syn PFF injections were conducted as described previously [193]. Rats were anesthetized before surgery with Equithesin (0.3 ml/100 g body weight i.p.; chloral hydrate 42.5 mg/ml sodium pentobarbital 9.72 mg/ml). Each rat received two unilateral, intrastriatal injections (AP +1.0 mm, ML +2.0 mm, DV -4.0 mm and AP +0.1 mm, ML+4.2 mm, DV -5.0 mm, AP and ML relative to bregma and DV relative to dura, injection rate 0.5 μ l/min,) of sonicated α -syn PFFs (total 16 μ g in 2.0 μ l per site). Sonicated PFFs were kept at room temperature during the duration of the surgical procedures. Injections were administered made using a pulled glass needle attached to

a 10- μ l Hamilton syringe [194]. After each injection, the needle was left in place for 1 min, retracted 0.5 mm, left in place for an additional 2 min, and then slowly withdrawn. Drill holes were filled with bone wax to prevent entry of dental cement during electrode placement.

V. Electrode Implantation

Immediately following PFF injections, rats were unilaterally implanted (ipsilateral to α -syn PFF injections) with a bipolar, concentric microelectrode (inner electrode projection 1.0 mm, inner insulated electrode diameter 0.15 mm, outer electrode gauge 26, Plastics One, Roanoke, VA) targeted to the dorsal border of the STN (AP 3.4 mm, ML 2.5 mm, relative to bregma and DV 7.7 mm, relative to dura). The dorsal STN border placement site was selected to minimize damage to the nucleus, as has been described previously [158]. Burr holes were drilled in the skull; the electrode was fixed in place using bone screws, Metabond (Parkell, Brentwood, NY), and dental acrylic. Animals were treated postoperatively with 1.2 mg/kg continuous-release buprenorphine and monitored daily post-surgery.

VI. Deep Brain Stimulation

Continuous stimulation platform. Three days following surgery half of the rats were assigned to receive either continuous stimulation for 1 month (ACTIVE) or no stimulation for the same period (INACTIVE). Rats received STN stimulation that was continuously delivered in a freely moving setup as previously described [158]. Stimulation was generated by an Accupulser Signal Generator (World Precision

Instruments) via a battery-powered Constant Current Bipolar Stimulus Isolator (World Precision Instruments). Stimulation parameters consisted of a frequency of 130 Hz, a pulse width of 60 μ s and an intensity of \sim 50 μ A. At the onset of stimulation, intensity settings were increased until orofacial or contralateral forepaw dyskinesias were observed to confirm stimulation delivery. Immediately following a positive dyskinetic response, the intensity was set below the lower limit of dyskinesias (20-50 μ A), such that no rat was functionally impaired by stimulation as previously described [158].

VII. Euthanasia

Rats were euthanized 1 month post-surgery. Rats were deeply anesthetized (60 mg/kg, pentobarbital, i.p.) and perfused intracardially with heparinized normal saline at 37°C followed by ice-cold normal saline. Care was taken to minimize the tissue damage resulting from removing the skull with the electrode still intact. All brains were placed in ice-cold normal saline for 1 min and then hemisected on the coronal plane at the optic chiasm. The caudal half was post-fixed in 4% paraformaldehyde (PFA) for 1 week and transferred to 30% sucrose in 0.1 M phosphate buffer until sinking. The rostral half was immediately flash-frozen in 3-methyl butane on dry ice and stored at -80° C until microdissected (see Chapter 5).

IIIX. Tissue Processing

Brains were frozen and sectioned on a sliding microtome at 40 μ m. Free-floating sections (1:6 series) were transferred to 0.1 M tris-buffered saline (TBS). Following the washes, endogenous peroxidases were quenched in 3% H₂O₂ for 1 h and rinsed in

TBS. Sections were blocked in 10% normal goat serum/0.5% Triton X-100 in TBS (NGS, Gibco; Tx-100 Fischer Scientific) for 1 h. Following the blocking, sections were immunolabeled with primary antibodies: pan rabbit-anti α -syn (Abcam, Cambridge, MA; AB15530, 1:1000), mouse anti-phosphorylated α -syn at serine 129 (pSyn, 81A; Abcam, Cambridge, MA; AB184674; 1:10,000), rabbit anti-phosphorylated α -syn truncated adamant and reactive (pSynSTAR, pSyn*; GeneTex, Irvine, CA; GTX50222; 1:2000), or rabbit anti-tyrosine hydroxylase (TH; Millipore, Temecula, CA; MAB152, 1:4000) overnight in 1% NGS/0.5% Tx-100/TBS at 4 °C. Following the washes, sections were incubated in biotinylated secondary antibodies (1:500) against mouse (Millipore, Temecula, CA; AP124B) or rabbit IgG (Millipore, Temecula, CA; AP132B) followed by washes in TBS and 2 h incubation with Vector ABC standard detection kit (Vector Laboratories, Burlingame, CA; PK-6100). Immunolabeling for pSyn, pSyn*, and TH was visualized by development in 0.5 mg/ml 3,3' diaminobenzidine (DAB; Sigma-Aldrich St. Louis, MO; D5637-10G) and 0.03% H₂O₂. Slides were dehydrated in an ascending ethanol series and then xylenes before coverslipping with Cytoseal (Richard-Allan Scientific, Waltham, MA). pSyn-labeled sections were also counterstained with cresyl violet for quantification of intraneuronal pSyn inclusions in the SNpc.

IX. Kluver–Barrera Histology

Saline-perfused/PFA-postfixed brains (caudal half after hemisection) were frozen on dry ice and sectioned at 40 μ m thickness using a sliding microtome in six series. Every sixth section of the STN was stained using Kluver–Barrera histochemistry (Kluver and Barrera, 1953) to evaluate for appropriate targeting of the electrode to the STN. Only

rats with correctly positioned electrodes were included in the data analysis (see, e.g., Fig. 3.3). Electrode location was considered to be appropriate if the tip of the electrode was observed within 250 μm of the border of the STN within any of the sections based on previous estimations of current spread conducted using similar stimulation parameters [158].

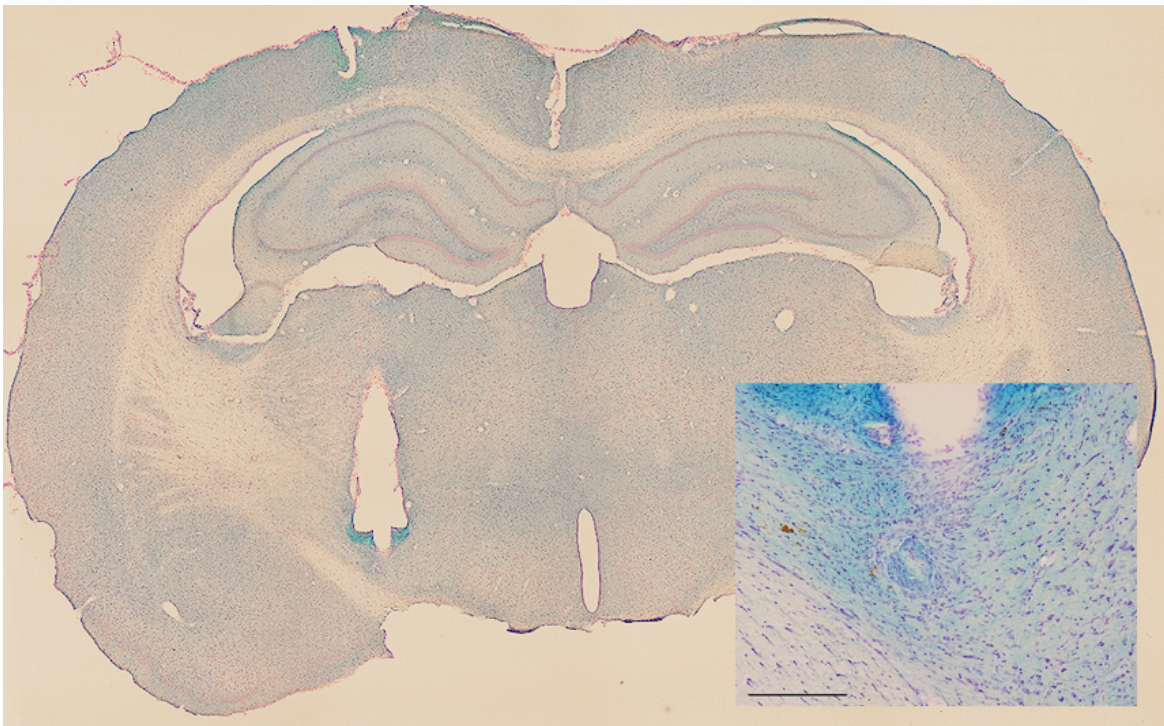


Figure 3.3: Electrode placement validation

All rats included in the study were verified to have correct electrode placement.

Inclusion criterion required any part of the electrode to be within 250 μm of any part of the STN (as shown in inset, scale bar = 200 μm).

X. Proteinase K Digestion

To determine whether pSyn immunoreactive inclusions were non-soluble (Lewy body-like) as previously described [420, 421], a subset of nigral sections were treated with or without 10 ug/mL proteinase K (Invitrogen, Carlsbad, CA; #25530015) then stained for pan rabbit-anti α -syn (Abcam, Cambridge, MA; AB15530, 1:1000) as described above. Soluble α -syn is digested by Proteinase K, while non-soluble inclusions are not (Fig. 3.4).

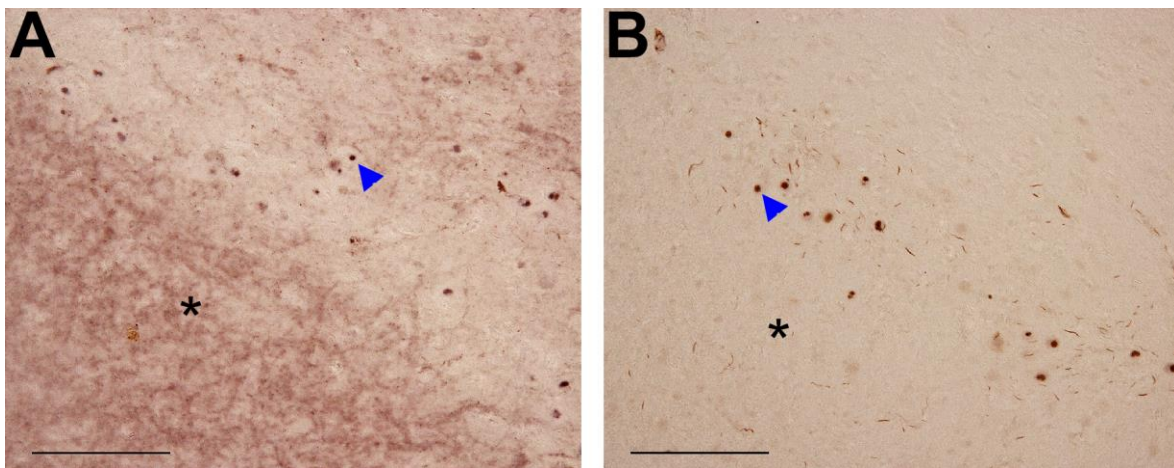


Figure 3.4: Nigral α -syn inclusions are Proteinase K-resistant

Adjacent nigral sections were treated without (**A**) or with (**B**) Proteinase K and stained for α -syn. Soluble α -syn in the substantia nigra pars reticulata (asterisk) is present without Proteinase K, but is absent following treatment. Inclusions (arrow) remain after Proteinase K treatment.

XI. Unbiased Stereology of THir Neurons in the SNpc

The number of THir neurons in the SNpc ipsilateral and contralateral to α -syn PFF injection was estimated using unbiased stereology with the optical fractionator principle. Using a Nikon Eclipse 80i microscope, Retiga 4000R camera (QImaging) and Microbrightfield StereoInvestigator software (Microbrightfield Bioscience, Williston, VT), THir neuron quantification was completed by drawing a contour around the SNpc borders using the 4X objective on every sixth (9 –11 sections per brain) and counting THir neurons according to stereological principles at 60X magnification. Briefly, counting frames (50 μ m x 50 μ m) were systematically and randomly distributed over a grid (183 μ m x 112 μ m) overlaid on the SNpc. A coefficient of error < 0.10 was accepted. THir data are reported as total estimates of THir neurons in each hemisphere.

XII. Total Enumeration of pSyn and pSyn* Immunoreactive Nigral Neurons

Due to heterogeneity in the distribution of both pSyn and pSyn* immunoreactive profiles within the SNpc, total enumeration rather than sampled counting frames was used for quantification. Neurons with intraneuronal inclusions were defined as profiles of dark, densely stained immunoreactivity within cresyl violet-positive neurons. Contours were drawn around the SNpc using the 4x objective on every sixth section through the entire SNpc (9 – 11 sections). pSyn and pSyn* inclusions were then systematically counted within each contour using the 20x objective. Numbers represent the raw total number of inclusions per animal multiplied by 6 to extrapolate the population estimate.

XIII. TH and pSyn Double Label Immunofluorescence

Sections of rat tissue were blocked in 10% normal goat serum for 1 hour and subsequently transferred to the primary antisera (TH: Millipore Ab152, rabbit anti-TH, 1:4000; and pSyn: Abcam AB184674, mouse anti-pSyn, 1:10,000) to incubate overnight at 4°C. Following primary incubation, tissue was incubated in the dark in secondary antisera against rabbit IgG (Invitrogen A11034, Alexa Fluor 488 goat anti-rabbit IgG, 1:500) and mouse IgG2a (Invitrogen A21135, Alexa Fluor 594 goat anti-mouse IgG2a, 1:500) for 1 hour at room temperature. Sections were mounted on subbed slides and coverslipped with Vectashield Hardset Mounting Medium (Vector Laboratories H1400, Burlingame, CA).

XIV. Fluorescent Quantification

Images were taken on a Nikon 90i fluorescence microscope with a Nikon DS-Ri1 camera under identical exposure parameters. The eight median pSyn-seeded animals were included from each group: PFF injected, ACTIVE (5536 ± 180) or PFF injected, INACTIVE (5781 ± 223) with the 3 sections containing the most pSyn immunoreactive nigral neurons selected for analysis. Images were taken with the 20X objective so that the entire ipsilateral nigra was included with no overlap between images (7-16 frames per section). Outcome measure values from each animal were averaged and treated as sample replicates to form a single mean for each animal. Figures were produced in Photoshop 7.0 (San Jose, CA). Brightness, saturation, and sharpness were adjusted only as necessary to best replicate the immunostaining as viewed directly under the microscope.

Soma Analyses

Individual THir SNpc neurons were manually outlined using the NIS Elements Software Draw Bezier ROI tool (NIS Elements, Nikon Instruments, New York, NY). Only cells in the focal plane were analyzed. Within the outlined regions of interest (ROIs), pSyn intensity (mean intensity of ROI), TH intensity (mean intensity of ROI), TH density (mean density of ROI), and ROI area were evaluated. Intensity measures the average TH intensity of each pixel in the ROI, whereas density measures how homogenous the intensity values are (lower values signify a more heterogenous distribution of TH immunofluorescence within the neuron).

Aggregation Analyses

All pSyn-ir aggregates were automatically outlined, and manually verified using the NIS Elements Software Auto Detect ROI tool (Nis Elements, Nikon Instruments, New York, NY). Only aggregates in the focal plane were analyzed. Aggregates were considered individual aggregates if there was a clear separation of space between neighboring inclusions (clumps that could not be delineated were treated as a single aggregate). Within outlined ROIs, pSyn intensity (mean pSyn intensity), and ROI area were evaluated.

XV. Statistical Analyses

Using previous PFF model data, new data for power calculations was simulated to represent the STN DBS intervention group from a Poisson distribution and then fit to a generalized linear model to determine if differences could be detected. Results

determined that only 5 rats per group would be required to detect a minimum of a 25% difference in pSyn aggregates due to DBS with over 90% power. Additional rats were then added per group based on our past experience with both the PFF and DBS models to account for injection failure rates, electrode failure over the month-long stimulation interval and improper electrode placement. Statistical outliers were assessed using the Absolute Deviation from the Median method using the “very conservative” criterion [422]. All statistical tests of the results were completed using GraphPad Prism software (version 8, GraphPad, La Jolla, CA). All studies utilized two-way analysis of variance (ANOVA), or independent samples t-tests to assess differences between groups. The THir and soma fluorescence quantification results were analyzed with two-way ANOVA with two treatment factors, stimulation and inclusions. The pSynir, pSyn*ir, and aggregation fluorescent quantification results were analyzed with two-tailed, independent samples t-tests. The Tukey *post hoc* analyses were used on all ANOVA tests to determine significance between individual groups using the harmonic mean of the group sizes to account for unequal sample sizes. Statistical significance was set at p 0.05.

Results

I. The number and Size of PFF-Induced α -Syn Inclusions in the SNpc is not Impacted by STN DBS

Numerous inclusions immunoreactive for pSyn and pSyn* were observed within neurons in the SNpc ipsilateral to α -syn PFF injection one month after surgery.

Quantification revealed 5580 ± 297.2 pSyn^{ir} neurons in the ipsilateral SNpc of rats that received electrodes that were never activated (INACTIVE) compared to 5351 ± 249.1 pSyn^{ir} neurons in the ipsilateral SNpc of rats that received STN DBS (ACTIVE, Fig. 3.5 A-C). There was no difference in the number of inclusion-bearing neurons in PFF-treated rats due to STN DBS ($p > 0.05$). Autophagic degradation of pSyn results in a species of pSyn that is truncated at both terminals and termed pSyn* (pSyn-STAR; phosphorylated α -syn that is truncated, adamant and reactive), and has been proposed to be the toxic species of pSyn [380]. To determine whether STN DBS impacted the formation of pSyn* the number of pSyn* immunoreactive nigral neurons were also quantified. We observed no difference in the number of pSyn*^{ir} nigral neurons in rats that received STN DBS (ACTIVE = 4931 ± 292.5) compared to those that did not (INACTIVE = 5028 ± 304.5 ; Fig. 3.5 D-F, $p > 0.05$). Lastly, beyond quantifying the number of SNpc neurons with α -syn inclusions, we assessed the size and immunofluorescence intensity of individual pSyn immunoreactive aggregates themselves to evaluate whether either parameter is impacted by STN DBS. (Fig. 3.5 G-J). Neither the size nor pSyn intensity of pSyn aggregates were affected by stimulation ($p > 0.05$). Collectively, these results suggest that STN DBS during the first month

following α -syn PFF injection does not impact the formation or degradation of α -syn inclusions.

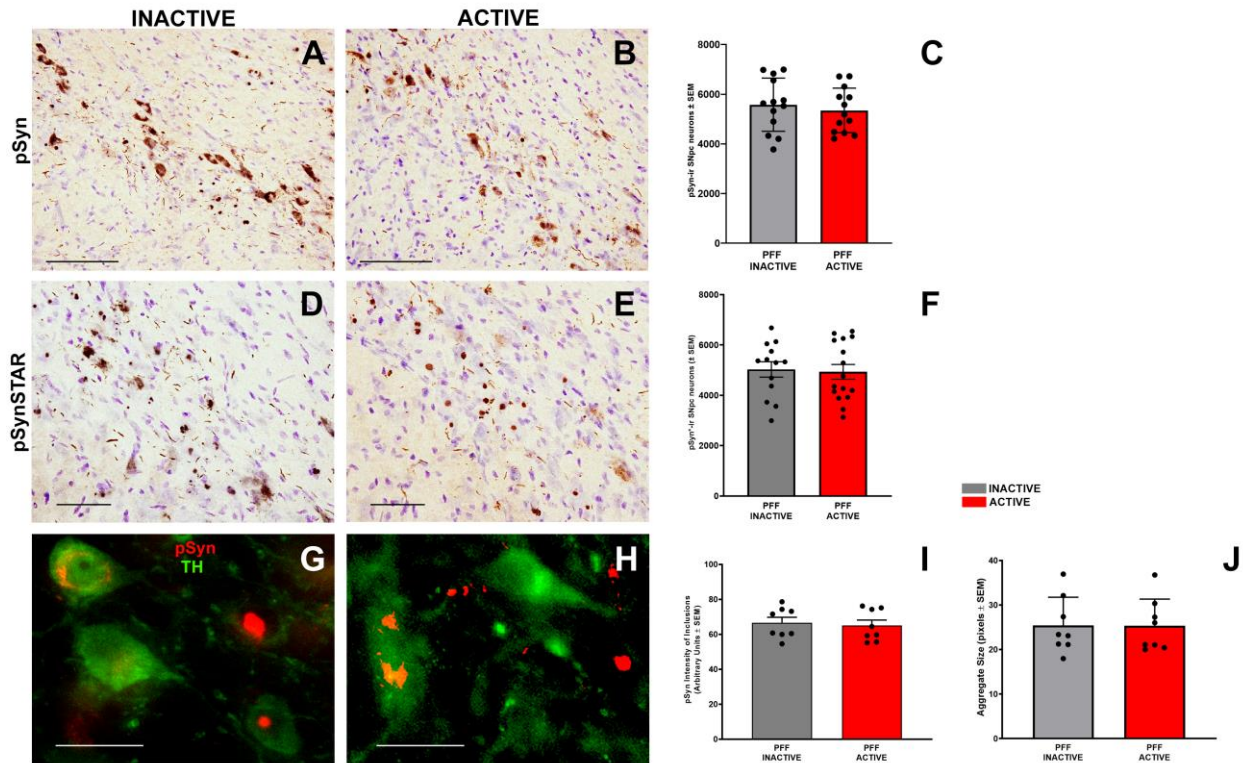


Figure 3.5: α -syn aggregates in the substantia nigra pars compacta (SNpc) of young rats are not impacted by STN DBS

The number of pSyn^{ir} (A-C) and pSynSTAR^{ir} (D-F) SNpc neurons was not impacted by STN DBS. Scale bars = 100 μ m. The pSyn immunofluorescence intensity (G, I) and size (H, J) of pSyn^{ir} inclusions were similar in INACTIVE STN DBS (G) and ACTIVE STN DBS (H). Their neurons (green) and pSyn inclusions (red) Scale bars = 25 μ m.

II. STN DBS does not Impact Nigral TH Neuron Phenotype in the Rat α -Syn PFF Model.

Previous studies using identical intrastriatal α -syn PFF injection parameters reveal significant decreases in ipsilateral SNpc THir neurons at 4 and 6, but not 2 months after injection [193]. In the present study we observed a modest, yet significant decrease (~18%) in THir neurons in the SNpc ipsilateral to PFF injection at one month ($p < 0.05$, Fig. 3.6). However, when comparing THir neurons in the ipsilateral inclusion-bearing hemispheres of rats that received STN DBS (ACTIVE; 11842 ± 931.2) vs. THir neurons in rats that received no stimulation (INACTIVE; 15004 ± 959.9) we observed no significant differences ($p > 0.05$; Fig. 3.6E). These results suggest that STN DBS does not impact the modest ipsilateral decrease of THir SNpc neurons induced by α -syn PFF injection.

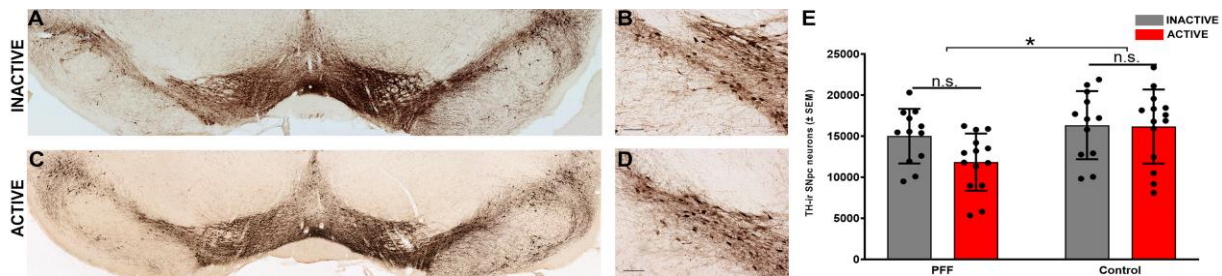


Figure 3.6: STN DBS does not impact modest PFF-inclusion associated loss in TH-ir nigral neurons

Nigral THir neurons in rats without (INACTIVE: **A-B**) and with (ACTIVE: **C-D**) STN DBS. Scale bars in B and D = 100 μ m. **E**. Quantification of THir neurons in the SNpc.

III. STN DBS does not Alter pSyn-Associated Effects on Nigral THir Neurons

We first evaluated the impact of pSyn inclusions on average TH immunofluorescence intensity, TH immunofluorescence density (homogeneity of TH distribution) and soma size of THir neurons at the level of individual neurons in the SNpc (Fig. 3.7). Not surprisingly, THir SNpc neurons with inclusions exhibited a 9X increased in pSyn intensity ($p < 0.0001$) compared to neighboring THir neurons without inclusions (Fig. 3.7A). Further, THir SNpc neurons with pSyn inclusions displayed roughly 25% decreased soma size (Fig. 3.7B, $p < 0.0001$), 13% increased TH intensity (Fig 3.7C, $p < 0.05$), and 8% decreased TH density (Fig. 3.7D, $p < 0.05$). We next examined whether STN DBS stimulation status impacted inclusion-associated alterations within nigral THir neurons. STN DBS had no effect on pSyn intensity, TH soma size, TH intensity or TH density (Fig. 3.7 H-K, $p > 0.05$) of THir nigral neurons bearing pSyn inclusions. These results suggest that the formation of pSyn inclusions within nigral DA neurons alters TH expression and compromises neuronal size but that these inclusion-associated effects are not impacted by STN DBS.

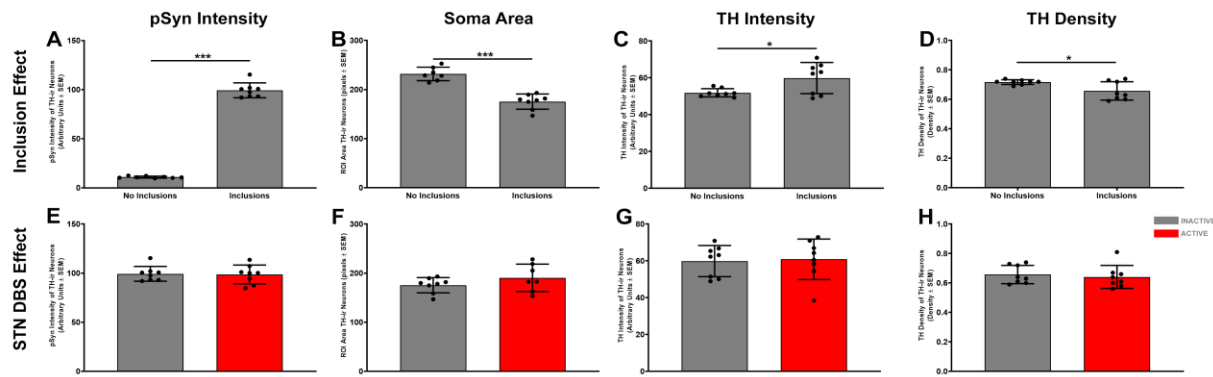


Figure 3.7: STN DBS does not alter pSyn-associated effects on SNpc in rats treated with PFFs

The effect inclusions have on mean pSyn intensity, soma area, mean TH intensity, and mean density of individual neurons within a PFF-treated rat are quantified **(A-D)**. pSyn intensity increased from 10.97 ± 0.34 arbitrary units in neurons without inclusions to 99.34 ± 2.67 in neurons containing inclusions **(A)**. Soma area decreased from 231.83 ± 5.20 pixels without inclusions to 175.45 ± 5.49 with inclusions **(B)**. TH intensity increased from 51.89 ± 0.79 arbitrary units in neurons without inclusions to 59.89 ± 2.30 in neurons with inclusions **(C)**. TH density decreased from 0.72 ± 0.01 arbitrary units in neurons without inclusions to 0.66 ± 0.02 in neurons containing inclusions **(D)**. STN DBS had no effect on pSyn intensity (ACTIVE = 98.68 ± 3.38 ; **E**), soma area (ACTIVE = 190.52 ± 10.58 ; **F**), TH intensity (ACTIVE = 60.90 ± 3.89 ; **G**), or TH density (ACTIVE = 0.64 ± 0.03 ; **H**).

IV. STN DBS does not Impact α -Syn Inclusion Formation or Inclusion-Associated TH Phenotype in Aged Rats.

Age is the biggest risk factor for PD [85], making examination of the effects of STN DBS in the aged brain environment PD-relevant. Therefore, we evaluated the impact of STN DBS on the number of SNpc neurons with pSyn^{ir} or pSyn^{*ir} inclusions and TH^{ir} neurons in a separate cohort of aged rats that received intrastriatal injections of α -syn PFFs. Numerous inclusions immunoreactive for pSyn and pSyn^{*} were observed within neurons in the ipsilateral SNpc in aged rats one month after surgery. Quantification revealed 4095 ± 467.8 pSyn^{ir} neurons in the ipsilateral SNpc of rats that received electrodes that were never activated (INACTIVE) compared to 4764 ± 284.7 pSyn^{ir} neurons in the ipsilateral SNpc of rats that received STN DBS (ACTIVE; Fig. 3.8 A-C). Quantification of the number of ipsilateral pSyn^{*ir} SNpc neurons revealed 3625 ± 527.2 (INACTIVE) and 4226 ± 254.1 (ACTIVE; Fig. 3.8 D-F). Interestingly, aged rats exhibited fewer pSyn^{ir} neurons in the ipsilateral SNpc compared to young rats injected under identical PFF injection parameters ($p < 0.01$; Fig. 3.8G). No differences were observed in the number of nigral pSyn^{ir} or pSyn^{*ir} neurons in rats that received STN DBS compared to those that did not ($p > 0.05$; Fig. 3.8C, F). As with young rats, a (~17%) reduction in TH^{ir} neurons in the SNpc ipsilateral to PFF injection at one month was observed ($p < 0.05$, Fig. 3.8H). However, when comparing TH^{ir} neurons in the ipsilateral inclusion-bearing hemisphere of rats that received STN DBS (15018 ± 587.6) vs. rats that received no stimulation (12424 ± 1272.1) we observed no significant differences ($p > 0.05$). These results suggest that STN DBS does not impact the early decrease of TH^{ir} SNpc neurons induced by α -syn PFF injection.

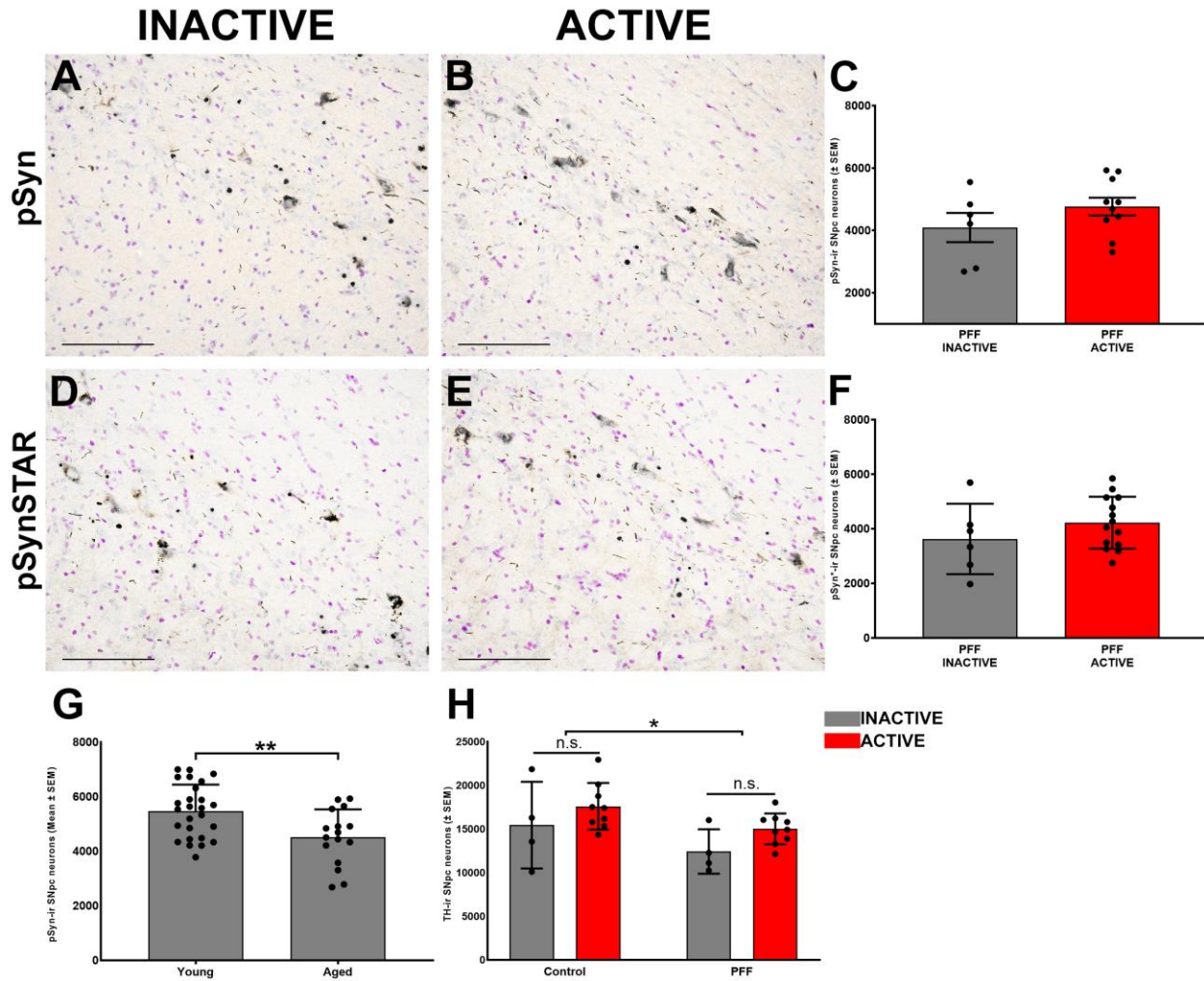


Figure 3.8: STN DBS does not impact α -syn inclusion formation or inclusion-associated TH phenotype in aged rats

The number of pSynir (A-C) and pSyn*ir (D-F) SNpc neurons are not changed by STN DBS. However, the number of pSynir is decreased in aged animals when compared to young (G). Because there were no stimulation-induced differences, ACTIVE and INACTIVE groups were compared for this analysis. Unbiased stereological assessment of THir neurons revealed a significant ipsilateral decrease that was not impacted by ACTIVE STN DBS (H). Scale bars = 100 μ m.

Discussion

STN DBS has traditionally been a treatment of last resort, however, this practice may be shifting. In 2013 a randomized clinical trial in mid-stage PD patients (7.5 year disease duration) reported that STN DBS provided superior therapeutic outcomes compared to standard medical therapy [423]. Further, results from a clinical trial examining the safety and efficacy of STN DBS in early-stage PD (less than four years of medication and without motor fluctuations or dyskinesias) were recently published [215]. Both STN DBS and optimized drug therapy groups received significant therapeutic benefit with no differences between treatment groups observed [215], demonstrating that subjects with early-stage PD will elect to receive DBS, and that the DBS treatment that they receive is efficacious and well tolerated. Moreover, follow-up on this study revealed that STN DBS in early PD is in fact disease modifying for tremor [424]. This shift in clinical STN DBS practices warrants a clearer understanding of the disease-modifying potential of STN DBS in preclinical PD.

Lewy pathology is associated with nigral neuronal degradation and therefore reducing α -syn aggregation is an active area of preclinical PD investigation. We chose to use the rat α -syn pre-formed fibril (PFF) model for this study due to the early α -syn aggregation phase, preceding any neurodegeneration [193]. In this model, intrastriatal PFFs induce aggregation of endogenous nigral α -syn [190, 195, 196]. Importantly, fibrils are taken up by neurons as early as hours after exposure, with fibrils that remain in the extracellular space cleared in vivo within a few days [425, 426]. In the present stimulation paradigm, STN DBS was not activated until day 3, after uptake of PFFs would be expected to

occur. Therefore, our present experimental design allows us to address the question of whether STN DBS modifies the aggregation process with any potential effects of DBS on internalization of fibrils unlikely to confound our results.

High frequency stimulation has been shown in cultured neurons to cause α -syn dispersion away from the presynaptic terminal, where α -syn is normally concentrated [317]. In this study, we tested the hypothesis that DBS during the period of peak α -syn aggregation may interfere with or slow the formation of inclusions. We found that STN DBS did not impact inclusion formation when examined at the one month timepoint when assessed for number of nigral dopamine neurons with inclusions, or the size and intensity properties of individual aggregates. It is possible that, had we examined α -syn inclusions earlier, we may have observed an impact of STN DBS that we cannot appreciate at the one month timepoint, however by definition any STN DBS mediated effect on inclusion formation would be modest and transient.

I. α -Syn Aggregation in the Young SNpc

To thoroughly understand the impact STN DBS might have on α -syn inclusion formation, we took several complimentary approaches. **(1) Total number of phosphorylated α -syn-immunoreactive (pSynir) nigral neurons.** When α -syn is phosphorylated at serine 129 it has a conformational change, making it more prone to aggregation [353]. Indeed, Lewy bodies and Lewy body-like inclusions stain heavily for pSyn, and it is thought of as the pathological species of α -syn [353, 377, 427, 428]. This is supported by the findings that less than 5% of α -syn in human brains is

phosphorylated, and naïve rats have no detectable pSyn [193, 429]. **(2) Total number of truncated phosphorylated α -synir (pSyn*) nigral neurons.** A recent study identified a species of pSyn that is truncated from both terminals, that is associated with mitochondrial-induced toxicity [380]. The species is a product of incomplete lysosomal degradation, and was proposed to be the true pathological species of α -syn. We used antibodies mutually exclusive to pSyn and pSyn*. **(3) Characteristics of inclusion-bearing nigral neurons and neighboring inclusion-free neurons.** Not all nigral neurons of a PFF-seeded rat are pSynir. Therefore, in addition to global nigral assessments, we evaluated individual dopamine neurons (identified by tyrosine hydroxylase, TH, immunoreactivity). Using this method we assessed THir intensity, pSynir intensity, and soma size. While there were no differences in any of these outcome measures as a result of ACTIVE STN DBS, there were differences in inclusion-bearing neurons compared to neurons without detectable pSyn. THir was higher with the presence of inclusions. This finding is in agreement with our earlier studies revealing an early transient increase in striatal TH immunofluorescence following α -syn PFF injection [193]. This may represent an early compensatory mechanism that ultimately fails. Interestingly, the soma size of inclusion-bearing nigral neurons was smaller than neighboring unaffected neurons, suggesting that those cells were already displaying an unhealthy phenotype. This finding supports the notion that temporary upregulation of TH is the cell's attempt at offsetting the pathology observed with inclusions. **(4) Characteristics of individual inclusions.** The selection criteria for 'inclusion-bearing' is binary; either levels of pSyn immunoreactivity achieve a threshold that allows the observer to detect inclusions, or it isn't. In an effort to probe for more

subtle differences in inclusion characteristics, we evaluated inclusion size and pSyn immunofluorescence intensity. ACTIVE stimulation did not impact any of the inclusion-related metrics we assessed. There are genetic, molecular, biochemical, and cellular changes occurring throughout the fibrilization process [197], and we only evaluated the impact of STN DBS on somatic inclusions. Thus, we could be missing more subtle changes in the early fibrilization process. Collectively, these data suggest that STN DBS does not impact the formation or characteristics of nigral somatic α -syn inclusions.

II. α -Syn Aggregation in the Aged SNpc

We also observed that STN DBS did not impact α -syn inclusion formation in the SNpc of aged rats. However, we did observe that the number of pSyn and pSyn* inclusions in aged rats were fewer (~17%) compared to young rats receiving the same quantity of α -syn PFFs. While we did not examine the mechanism of this reduction in α -syn inclusion formation in aged rats there are a few possibilities. This could perhaps be a result of decreased striatal innervation with age in rats [88], or a decrease in the receptors responsible for uptake of PFFs in aging which could cause less initial uptake of PFFs [430]. Alternatively, some studies have reported mislocalized α -syn in aged rats [84], which could also potentially interfere with aggregation. Lastly, it is possible that the difference we observe in the magnitude of α -syn inclusions between young and aged rats reflects a transient difference, perhaps the formation of pSyn inclusions is slower in aged rats. Further investigation will need to investigate the mechanism of decreased α -syn inclusion formation in aged rats following PFF injection.

In the present experimental paradigm we did not examine the impact of STN DBS on α -syn inclusion associated degeneration of nigral dopamine neurons. We have previously documented that the PFF parameters we used do not result in overt degeneration of nigral dopamine neurons in the ipsilateral hemisphere until 6 months following degeneration, although loss of TH immunoreactivity precedes this degeneration [193]. In the present study we observed decreased soma area and homogeneity of TH distribution in nigral neurons that possess inclusions, perhaps signaling a very early stage of toxicity. STN DBS did not impact these assessments. Whereas STN DBS does not appear to impact PFF-seeded α -syn inclusion formation it is possible that stimulation applied after the one month time point may impact 1) α -syn inclusion triggered neuroinflammation, 2) production and/or trafficking of brain-derived neurotrophic factor or 3) degeneration of the nigrostriatal system. In my next two chapters I will examine these first two possibilities whereas future studies in my lab will address the neuroprotective potential of STN DBS in the PFF rat model through applying stimulation starting at 1 month and continuing to month 6.

**Chapter 4: Impact of Subthalamic Nucleus Deep Brain Stimulation on
Synucleinopathy-Triggered Neuroinflammation in the Substantia Nigra**

Abstract

Subthalamic nucleus deep brain stimulation (STN DBS) to treat the cardinal motor symptoms of Parkinson's disease (PD) is a vetted, safe, and efficacious neurosurgical therapy for the treatment of motor symptoms; however the question of whether early STN DBS can modify the progression of PD has yet to be examined in an appropriately designed clinical trial. Neuroinflammation has been implicated as a potential contributor to the degenerative process in PD. In the present experiment we leveraged the α -synuclein preformed fibril (α -syn PFF) model of synucleinopathy to examine the effects of STN DBS on gliosis in the substantia nigra, specifically by quantification of major histocompatibility complex-II immunoreactive (MHC-II^{ir}) microglia, assessment of glial fibrillary acidic protein (GFAP) immunofluorescence intensity, and morphometric analysis of GFAP immunoreactive astrocytes. Previously we demonstrated in the rat α -syn PFF model that MHC-II^{ir} microglia peak at 2 months immediately adjacent to phosphorylated α -syn (pSyn) inclusions. To assess whether STN DBS impacts pSyn inclusion-associated neuroinflammation, male Fischer 344 rats (n = 35) received unilateral intrastriatal injections of α -syn PFFs or control PBS injections and were simultaneously implanted with electrodes in the STN. One month following surgery, rats were assigned to receive either continuous stimulation or no stimulation for an additional 1 month interval. Quantification of tyrosine hydroxylase immunoreactive (TH^{ir}) neurons, pSyn^{ir} neurons, MHC-II^{ir} microglia, GFAP immunofluorescence intensity, and morphometric analysis of GFAP^{ir} astrocytic processes was performed. Two months following PFF injection we observed abundant pSyn inclusions in the ipsilateral substantia nigra pars compacta (SNpc) that were associated with a 33% loss

of THir neurons. Similarly, in PFF treated rats we observed more MHC-IIir microglia, increased GFAP immunofluorescence intensity, and increased process length and branching complexity of astrocytes compared to control rats. However, STN stimulation had no impact on any of these outcome measures. These findings suggest that PFF-induced pSyn inclusions in the SNpc trigger microglial and astrocytic activation, and that these specific neuroinflammatory responses are not modulated by stimulation of the STN.

Introduction

Immune responses have been heavily implicated in the pathophysiology of PD (reviewed in [431]). Early post-mortem investigations identified increased microglia in the brains of PD patients [99, 100]. Initially, this was thought to be a consequence of the preceding neurodegeneration. However, more recent findings have contributed to the current understanding of the immune response in PD, “which is proposed to occur early...and is likely to influence disease progression” [431]. Indeed, the “inflammation hypothesis” in PD has gained momentum as clinical and preclinical evidence supports the role of aberrant immune activity in contributing to disease progression.

Analyses of postmortem PD tissue have consistently revealed an increase in the number of microglia expressing major histocompatibility complex class II (MHC-II; HLA-DR in humans) [98, 99, 365]. Single nucleotide polymorphisms (SNPs) have been identified for several inflammation-related genes as being associated with PD [432-434], further supporting the idea that the immune system plays a role in PD pathogenesis.

Insight into the role of gliosis in disease progression has been explored using animal models of PD as well. Interestingly, α -syn pathology is associated with microglia activation, independent of neuronal loss [187, 435, 436], and microgliosis is observed in other brain regions that lack overt cell death [99, 203, 437, 438]. In addition to microglia, astrocytes have also been implicated in the neuroinflammatory response to neurodegeneration [439-441]. The rat α -syn preformed fibril (PFF) model of PD provides a platform to investigate the relationship between α -syn aggregations, gliosis and

neurodegeneration, as there is a protracted temporal separation between peak α -syn aggregation (1-2 months) and neurodegeneration (>4 months) in the SNpc [193, 198]. Further, *in vivo* preclinical studies suggest a potential link between STN DBS and an impact on neuroinflammation. Collectively these findings support the use of the α -syn PFF model platform to examine the impact of STN DBS on α -syn inclusion-triggered gliosis.

I. Present Study

In this study we leveraged our understanding of the time course and magnitude of accumulation of α -syn inclusions and microglial activation induced by intrastriatal α -syn PFF injection to determine whether the neuroinflammation associated with pSyn inclusions in the SNpc is impacted by STN DBS. The impact of STN DBS on microglial activation was examined by quantifying MHC-IIir microglia in the SNpc. To understand whether PFF-triggered α -syn inclusions and/or STN DBS impacts astrogliosis, we also analyzed GFAP immunofluorescence intensity and astrocytic morphometric parameters. These analyses were done during the peak of α -syn inclusion accumulation, two months following PFF injection, and immediately following a month of continuous STN stimulation (ACTIVE) or in rats with inactive STN electrodes (INACTIVE). As we previously observed, α -syn inclusion accumulation in the SNpc is associated with increased immediately adjacent microglial activation. We extend these observations to report α -syn inclusion-associated astrocytic activation as well. However, STN stimulation did not impact PFF-induced α -syn inclusion accumulation in the SN nor did it impact the microglial and astroglial activation associated with nigral α -syn inclusions.

Methods

I. Experimental Overview

Previously we observed increased microglial activation in SN at two months, but not one month, following PFF injection [198]. Therefore, the present experiment was designed to evaluate the impact of STN DBS during the interval immediately preceding the peak of α -syn inclusion associated microglial activation. A cohort of thirty-five rats was unilaterally injected into the striatum with preformed α -syn fibrils (PFF; $n = 19$) or PBS as a control ($n = 16$) into the striatum. During the same surgical session, all rats were also implanted with an electrode into the STN. 30 days following surgery, half of the rats from each group were randomly assigned to receive continuous STN stimulation (ACTIVE) or no stimulation (INACTIVE) for 30 days.

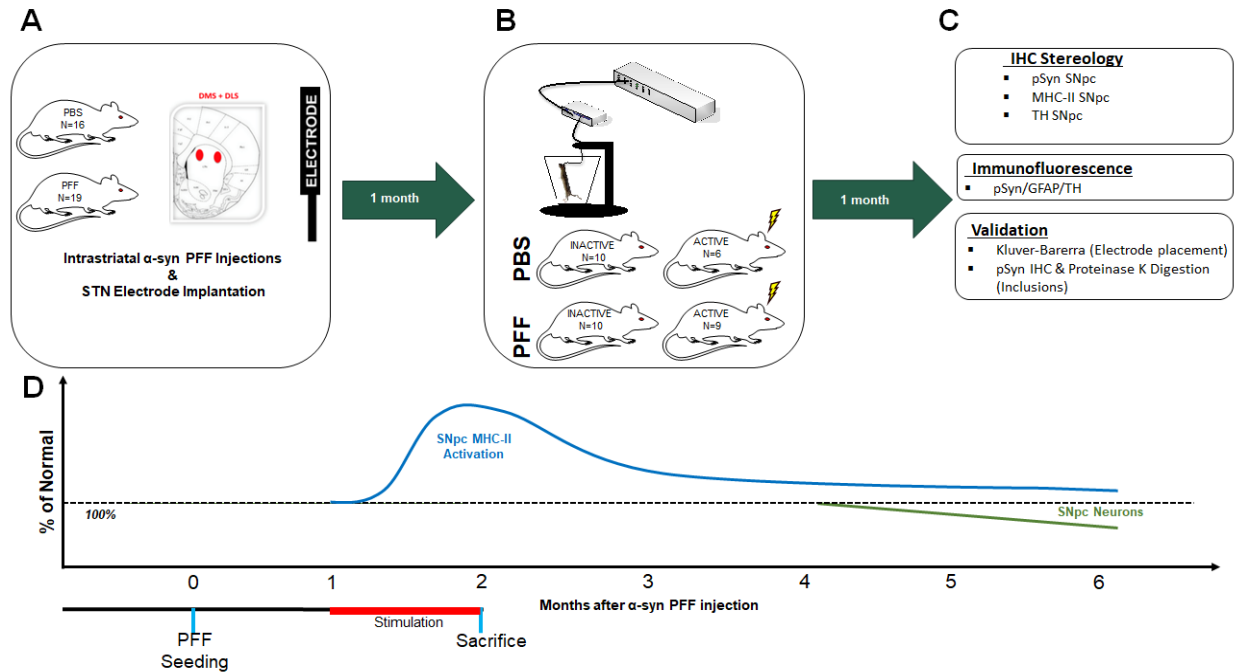


Figure 4.1: Experimental overview

Young (3 months old) rats received two intrastratial injections of PBS ($n = 16$) or α -syn PFFs ($n = 19$) and electrode implantation into the subthalamic nucleus (STN) during the same surgical session (**A**). One month later, half of each group were randomly assigned to receive INACTIVE (stimulation never turned on; $n = 10$) or ACTIVE ($n = 6-9$) stimulation for one month, at which point all animals were sacrificed (**B**). Outcome measures include stereology (TH) or total enumeration (pSyn, MHC-II), triple-label immunofluorescence neuroinflammation characterization (pSyn/GFAP/TH), and validation of electrode placement (Kluver-Barerra) and inclusion formation (Proteinase K digestion; **C**). Time points were determined according to the period of peak microglial activation (2 months, blue), prior to degeneration of SNpc neurons (4-6 months, green; **D**).

II. Animals

All animals were given food and water *ad libitum* and housed in 12h light-dark cycle conditions in the Grand Rapids Research Center, which is fully Association for Assessment and Accreditation of Laboratory Animal Care (AAALAC) approved. All procedures were conducted in accordance with guidelines set by the Institutional Animal Care and Use Committee (IACUC) of Michigan State University.

III. Preparation and Quality Control of α -Syn PFFs

Recombinant, full-length mouse α -syn PFFs were prepared and verified via in vitro fibril assembly as previously described [194-196, 418]. Prior to sonication, α -syn fibrils were assessed to verify lack of contamination (LAL Assay (~ 1 endotoxin units/mg), high molecular weight (sedimentation assay), beta sheet conformation (thioflavin T), and structure (electron microscopy). Prior to injection, PFFs were thawed, diluted in sterile Dulbecco's PBS (DPBS, 2 μ g/ μ l), and sonicated at room temperature using an ultrasonicating homogenizer (300VT; Biologics, Inc., Manassas, VA) with the pulser set at 20% and power output at 30% for 60 pulses at 1 s each [194]. Following sonication, a sample of the PFFs was analyzed using transmission electron microscopy (TEM). Formvar/carbon-coated copper grids (EMS DIASUM, FCF300-Cu) were washed twice with ddH₂O and floated for 1 min on a 10- μ l drop of sonicated α -syn fibrils diluted 1:20 with DPBS. Grids were stained for 1 min on a drop of 2% uranyl acetate aqueous solution; excess uranyl acetate was wicked away with filter paper and allowed to dry before imaging. Grids were imaged on a JEOL JEM-1400 transmission electron microscope. The length of over 500 fibrils per sample was measured to determine

average fibril size. The mean length of sonicated mouse α -syn PFFs was estimated to be 40.90 ± 0.55 nm, well within the optimal fibril length previously reported to result in seeding of endogenous phosphorylated α -syn inclusions *in vitro* and *in vivo* [419] (See Fig. 3.2).

IV. Pre-Formed α -Syn Fibril Injections

Intrastriatal α -syn PFF injections were conducted as described previously [193]. Rats were anesthetized before surgery with Equithesin (0.3 ml/100 g body weight i.p.; chloral hydrate 42.5 mg/ml sodium pentobarbital 9.72 mg/ml). Each rat received two unilateral, intrastriatal injections (AP +1.0 mm, ML +2.0 mm, DV -4.0 mm relative to dura and AP +0.1 mm, ML +4.2 mm, DV -5.0 mm) of α -syn PFF (4 μ g/ μ l, 2.0 μ l per site, injection rate 0.5 μ l/min). Sonicated PFFs were kept at room temperature during the duration of the surgical procedures. Injections were made using a pulled glass capillary pipette attached to a 10- μ l Hamilton syringe [194]. After each injection, the needle was left in place for 1 min, retracted 0.5 mm, left in place for an additional 2 min, and then slowly withdrawn. Drill holes were filled with bone wax to prevent entry of dental acrylic during electrode placement.

V. Electrode Implantation

Immediately following PFF injections, rats were unilaterally implanted (ipsilateral to α -syn PFF injections) with a bipolar, concentric microelectrode (inner electrode projection 1.0 mm, inner insulated electrode diameter 0.15 mm, outer electrode gauge 26, Plastics One, Roanoke, VA) targeted to the dorsal border of the STN (AP 3.4 mm, ML 2.5 mm,

relative to bregma and DV 7.7 mm, relative to dura). The dorsal STN border placement site was selected to provide stimulation of the STN while minimizing damage to the nucleus, as has been described previously [158]. Burr holes were drilled in the skull; the electrode was fixed in place using bone screws, Metabond (Parkell, Brentwood, NY), and dental acrylic. Animals were treated postoperatively with 1.2 mg/kg continuous-release buprenorphine and monitored daily post-surgery.

VI. Deep Brain Stimulation

Thirty days following surgery half of the rats in each treatment group received STN stimulation that was continuously delivered for a period of one month delivered via a freely moving setup as previously described [158]. Stimulation was generated by an Accupulser Signal Generator (World Precision Instruments) via a battery-powered Constant Current Bipolar Stimulus Isolator (World Precision Instruments). Stimulation parameters consisted of a frequency of 130 Hz, a pulse width of 60 μ s and an intensity of \sim 50 μ A. At the onset of stimulation, intensity settings were increased until orofacial or contralateral forepaw dyskinesias were observed to confirm stimulation delivery. Immediately following a positive dyskinetic response, the intensity was set below the lower limit of dyskinesias (20-50 μ A), such that no rat was functionally impaired by stimulation as previously described [158].

VII. Euthanasia

Rats were euthanized two months post-surgery, one month following initiation of stimulation. Rats were deeply anesthetized (60 mg/kg, pentobarbital, i.p.) and perfused

intracardially with heparinized normal saline at 37°C followed by 4% paraformaldehyde (PFA; Electron Microscopy Sciences, Hatfield, PA). Care was taken to minimize the tissue damage resulting from removing the skull with the electrode still intact. Brains were post-fixed in 4% PFA for 3 days and transferred to 30% sucrose in 0.1 M phosphate buffer until sinking.

IIIX. Tissue Processing

Brains were frozen and sectioned on a sliding microtome at 40 µm. Free-floating sections (1:6 series) were transferred to 0.1 M tris-buffered saline (TBS). Following the washes, endogenous peroxidases were quenched in 3% H₂O₂ for 1 h and rinsed in TBS. Sections were blocked in 10% normal goat serum/0.5% Triton X-100 in TBS (NGS, Gibco; Tx-100 Fischer Scientific) for 1 h. Following blocking, sections were immunolabeled with primary antibodies: pan rabbit-anti α-syn (Abcam, Cambridge, MA; AB15530, 1:1000), mouse anti-phosphorylated α-syn at serine 129 (pSyn, 81A; Abcam, Cambridge, MA; AB184674; 1:10,000), rabbit anti-tyrosine hydroxylase (TH; Millipore, Temecula, CA; MAB152, 1:4000), mouse anti-major histocompatibility complex-II for antigen-presenting microglia (MHC Class II RT1B clone OX-6, Bio-Rad, Hercules, CA; MCA46G, 1:5000), or mouse anti-glial fibrillary acidic protein (GFAP; Millipore, Temecula, CA; AP124B) overnight in 1% NGS/0.5% Tx-100/TBS at 4 °C. Following the washes, sections were incubated in biotinylated secondary antibodies (1:500) against mouse (Millipore, Temecula, CA; AP124B) or rabbit IgG (Millipore, Temecula, CA; AP132B) followed by washes in TBS and 2-h incubation with Vector ABC standard detection kit (Vector Laboratories, Burlingame, CA; PK-6100). Labeling for pSyn and TH

was visualized by development in 0.5 mg/ml 3,3' diaminobenzidine (DAB; Sigma-Aldrich St. Louis, MO; D5637-10G) and 0.03% H₂O₂. MHC-II was developed and visualized according to the manufacturer's instructions using the Vector ImmPACT DAB Peroxidase kit (Vector Labs, Burlingame, CA; SK-4605). Slides were dehydrated in ascending ethanol series and then xylenes before coverslipping with Cytoseal (Richard-Allan Scientific, Waltham, MA). pSyn-labeled sections were also counterstained with cresyl violet for quantification of intraneuronal pSyn inclusions in the SNpc.

IX. Kluver–Barrera Histology

Every sixth 40 µm section of the STN was stained using Kluver–Barrera histochemistry (Kluver and Barrera, 1953) to evaluate for appropriate targeting of the electrode to the STN. Only rats with correctly positioned electrodes were included in the data analysis (see, e.g., Fig. 3.3). Electrode location was considered to be appropriate if the tip of the electrode was observed within 250 µm of the border of the STN within any of the sections based on previous estimations of current spread conducted using similar stimulation parameters [158].

X. Proteinase K Digestion

To verify that inclusions were non-soluble (Lewy body-like) as previously described [420, 421], a subset of nigral sections were treated with or without 10 µg/mL proteinase K (Invitrogen, Carlsbad, CA; #25530015) then stained for pan rabbit-anti α-syn (Abcam, Cambridge, MA; AB15530, 1:1000) as described above. Soluble α-syn is digested by Proteinase K, while non-soluble inclusions are not (Fig. 3.4).

XI. Unbiased Stereology of Tyrosine Hydroxylase Immunoreactive (THir) Neurons in the Substantia Nigra pars compacta (SNpc)

The number of THir neurons in the SNpc ipsilateral and contralateral to α -syn PFF injection was estimated using unbiased stereology with the optical fractionator principle. Using a Nikon Eclipse 80i microscope, Retiga 4000R camera (QImaging) and Microbrightfield Stereoinvestigator software (Microbrightfield Bioscience, Williston, VT), THir neuron quantification was completed by drawing a contour around the SNpc borders using the 4X objective on every sixth (9 – 11 sections per brain) and counting THir neurons according to stereological principles at 60X magnification. Briefly, counting frames (50 μ m x 50 μ m) were systematically and randomly distributed over a grid (183 μ m x 112 μ m) overlaid on the SNpc. A coefficient of error < 0.10 was accepted. THir data are reported as total estimates of THir neurons in each hemisphere.

XII. Total Enumeration of pSyn and MHC-II Immunoreactive Cells

Due to heterogeneity in the distribution of both pSyn and MHC-II immunoreactive profiles within the SNpc, total enumeration rather than counting frames was used for quantification. Neurons with intraneuronal inclusions were defined as profiles of dark, densely stained immunoreactivity within cresyl violet-positive neurons. Contours were drawn around the SNpc using the 4x objective on every sixth section through the entire SNpc (9 – 11 sections). pSyn inclusion-containing neurons and MHC-IIir microglia were systematically counted within each contour using the 20X objective. Numbers represent the raw total number of pSyn inclusion-containing SNpc neurons or MHC-IIir microglia per animal multiplied by 6 to extrapolate the population estimate.

XIII. GFAP and pSyn Double Label Immunofluorescence

Sections of nigral rat tissue were blocked in 10% normal goat serum for 1 hour and subsequently transferred to the primary antisera (GFAP: Millipore AP124B, mouse IgG1 anti-GFAP 1:2000; and pSyn: Abcam AB184674, mouse IgG2a anti-pSyn, 1:10,000) to incubate overnight at 4°C. Following primary incubation, tissue was incubated in the dark in secondary antisera against mouse IgG1 (Invitrogen A21121, Alexa Fluor 488 goat anti-mouse IgG1, 1:500) and mouse IgG2a (Invitrogen A21135, Alexa Fluor 594 goat anti-mouse IgG2a, 1:500) for 1 hour at room temperature. Sections were mounted on subbed slides and coverslipped with Vectashield Hardset Mounting Medium (Vector Laboratories H1400, Burlingame, CA).

XIV. Immunofluorescence Quantification

Images were taken on a Nikon 90i fluorescence microscope with a Nikon DS-Ri1 camera. Figures were produced in Photoshop 7.0 (San Jose, CA). Brightness, saturation, and sharpness were adjusted only as necessary to best replicate the immunostaining as viewed directly under the microscope. Three sections highly seeded with pSyn inclusions (or sections from PBS-injected controls corresponding to the same anterior-posterior coronal coordinates) were analyzed from each rat. Stitched images were taken with the 10X objective spanning the entire nigra was. Outcome measure values from each animal were averaged and treated as sample replicates to form a single mean for each animal.

GFAP Immunofluorescence Intensity

The SNpc was manually outlined based on THir, using the NIS Elements Software Draw Bezier ROI tool (NIS Elements, Nikon Instruments, New York, NY). Within the outlined region of interest (ROIs), GFAP intensity (mean immunofluorescence intensity of ROI), and pSyn immunofluorescence intensity (mean intensity of ROI) were measured and recorded in each appropriate channel.

Sholl Analysis

Three high magnification (40X) z-stack images were taken from heavily seeded sections of nigra for each animal using NIS Elements software (NIS Elements, Nikon Instruments, New York, NY). Within each image, an astrocyte was selected and morphological assessments were conducted as previously described [442]. Briefly, z-stacks were loaded into FIJI-ImageJ (Public Domain) and processes were reconstructed. Post-reconstruction morphological analyses included process length and number. Values represent the mean of the three replicates for each rat (total n = 30, 6-8 rats per treatment group). A 2-dimensional rendered image was produced for each sample.

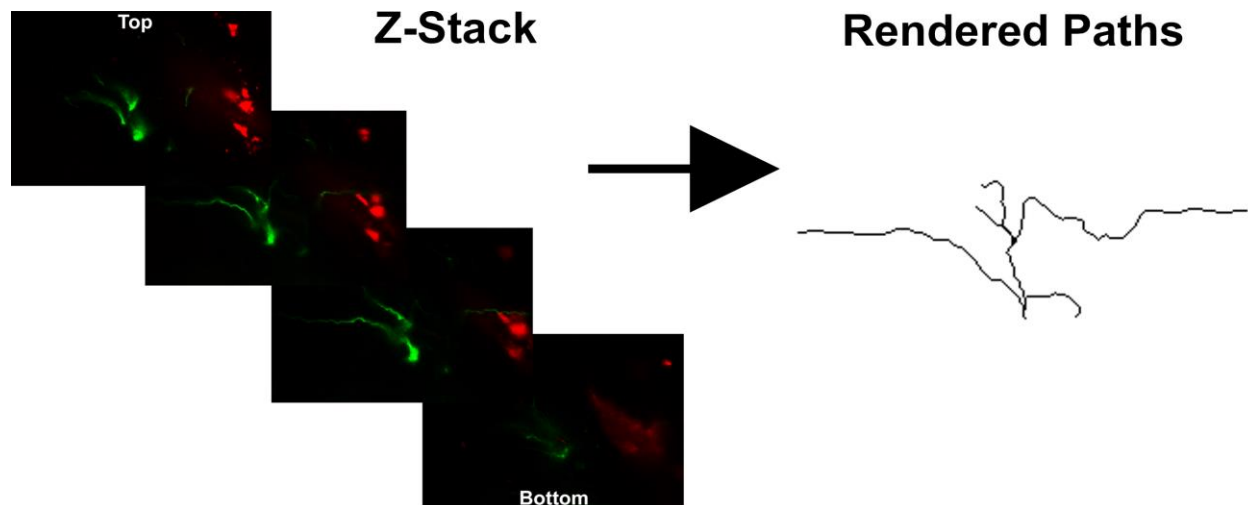


Figure 4.2: Production of astrocytic rendered paths

Z-stack images of dual-label immunofluorescence for GFAPir astrocytes (green) and pSynir inclusions (red) were outlined and compressed to create a 2D rendered path.

Astrocytes were selected based on (1) isolation from other astrocytes, (2) clear central point with complete processes, and (3) close proximity to inclusions.

XV. Statistical Analyses

Using previous PFF model data, new data for power calculations was simulated to represent the STN DBS intervention group from a Poisson distribution and then fit to a generalized linear model to determine if differences could be detected. Results determined that only 5 rats per group would be required to detect a minimum of a 25% difference in pSyn aggregates due to DBS with over 90% power. Additional rats were then added per group based on our past experience with both the PFF and DBS models to account for injection failure rates, electrode failure and improper electrode placement. Statistical outliers were assessed using the Absolute Deviation from the Median method using the “very conservative” criterion [422]. All statistical tests were completed using

GraphPad Prism software (version 8, GraphPad, La Jolla, CA) or R (version 3.6.3; www.r-project.org). All studies utilized two-way ANOVA, independent samples t-tests, linear regression, or linear mixed effects model to assess differences between groups. The THir and MHC-IIir quantification results were analyzed with two-way ANOVA with two treatment factors, stimulation and inclusions. The pSynir quantification results were analyzed with two-tailed, independent samples t-test. The Tukey *post hoc* analyses were used on all ANOVA tests to determine significance between individual groups using the harmonic mean of the group sizes to account for unequal sample sizes. Linear regression modeling was used to model the relationship between sum pSyn intensity (predictor) and sum GFAP intensity (outcome) while including an interaction term between stimulation group and sum pSyn intensity. In a separate analysis, linear mixed effects modeling was used to model the relationship between pSynir neurons (predictor) and GRAP intensity (outcome). This model also included an interaction term between pSynir and stimulation group, as well as a random intercept for animal ID to account for intra-individual variability in repeated pSynir data. Due to non-normality, pSynir data was log-transformed prior to modeling. Statistical significance was set at $p = 0.05$.

Results

I. The Number of PFF-Induced α -Syn Inclusions in the SNpc is not Impacted by STN DBS

Numerous pSynir inclusions were observed within neurons in SNpc ipsilateral to the α -syn PFF injection two months after surgery. Quantification revealed 6318 ± 343.8 pSynir neurons in the ipsilateral SNpc of rats that received electrodes and were never activated (INACTIVE) compared to 6096 ± 375.0 pSynir neurons in the ipsilateral SNpc of rats that received STN DBS (ACTIVE, Fig. 4.3 A-C). There was no difference in the number of inclusion-bearing neurons in PFF-treated rats due to STN DBS ($p > 0.05$).

Collectively, these results suggest that STN DBS during the second month following α -syn PFF injection does not impact the number of SNpc neurons that form α -syn inclusions. This also suggests that STN DBS does not induce the degradation of α -syn inclusions following formation.

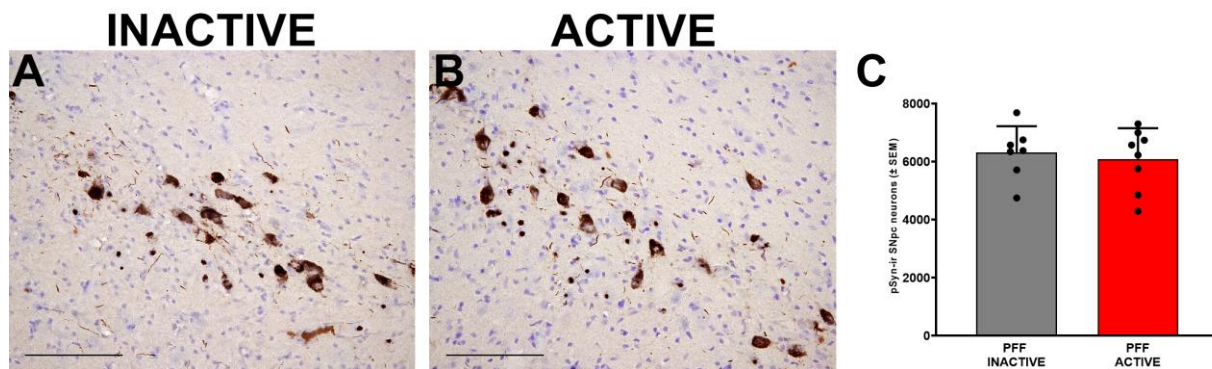


Figure 4.3: STN DBS does not change the number of pSyn immunoreactive nigral neurons

Rats with INACTIVE electrodes (**A**) or ACTIVE stimulation (**B**) had similar numbers of pSynir nigral neurons (**C**). Scale bars = 100 μ m.

II. STN DBS does not Impact Early α -Syn PFF Associated Reductions in Nigral TH Immunoreactive Neurons.

Previous studies using identical intrastriatal α -syn PFF injection parameters reveal significant decreases in ipsilateral SNpc THir neurons at 4 and 6, but not 2 months after injection [193, 198]. However, in the present study we observed a significant decrease (~33%) in THir neurons in the SNpc ipsilateral to PFF injection at two months ($p < 0.05$, Fig. 4.4). Nonetheless, when comparing THir neurons in the ipsilateral inclusion-bearing hemispheres of rats that received STN DBS (11878 ± 602.4) versus rats that received no stimulation (12099 ± 972.2), we observed no significant differences (Fig. 4.4I). These results suggest that STN DBS during the second month after PFF injection does not impact the ipsilateral decrease of THir SNpc neurons.

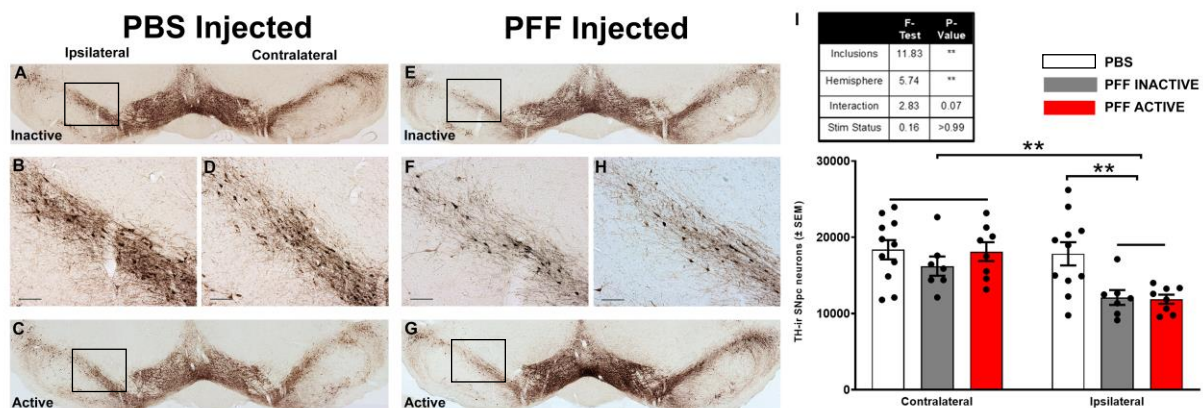


Figure 4.4: Stereological assessment revealed no stimulation effect on the ipsilateral loss of TH phenotype in PFF treated rats 2 months after injection

Whole nigra stitched images (**A, C, E, G**) and high magnification ipsilateral boxed insets (**B, D, F, H**, respectively) of THir neurons. INACTIVE (**A-B**) and ACTIVE (**C-D**) PBS-treated rats were statistically similar and combined. Contralateral THir counts were not different across groups. Ipsilateral THir counts were decreased in both INACTIVE (**E-F**) and ACTIVE (**G-H**) PFF-treated rats compared to their contralateral side or PBS-treated controls (**I**). Scale bars = 100 μ m.

III. STN DBS does not Impact the Number of MHC-IIir Microglia in the SN Associated with α -Syn Inclusions.

Formation of pSyn inclusions in the SNpc is associated with increased MHC-IIir microglia two months following intrastriatal PFF injection [198]. In the present experiment, we observed a similar pSyn-associated increase in MHC-IIir microglia at two months in the SN in rats injected with α -syn PFFs (693.1 ± 31.1) compared to control rats that received intrastriatal PBS injections (197.1 ± 36.1 ; Fig. 4.5). Stimulation

of the STN during month two did not impact the number of MHC-IIir microglia in the SN after PFF treatment ($p > 0.05$).

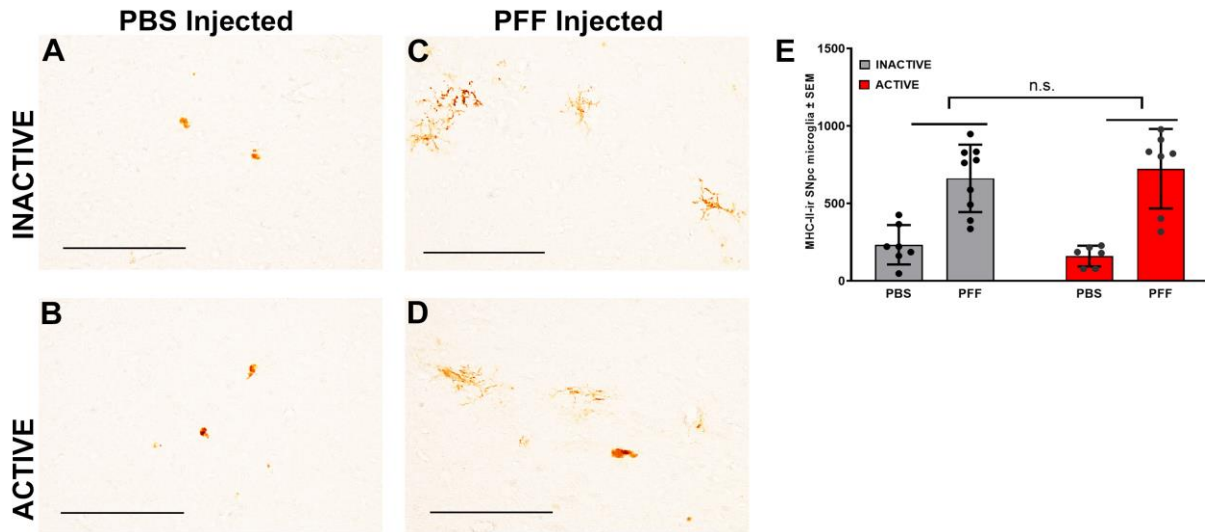


Figure 4.5: α -syn inclusion-associated microgliosis in the SN is not impacted by STN DBS

α -syn inclusions induced by PFF injection are associated with significantly more MHC-II immunoreactive (MHC-IIir) microglia in the SN (**C, D, E**) at the two month time point compared to rats that received control intrastriatal PBS injections (**A, B, E**) in which inclusions do not form. STN DBS (**D**) did not impact the number of MHC-IIir microglia (**C** versus **D, E**). Scale bars = 100 μ m.

IV. Increased GFAP Expression in the SN Associated with pSyn Inclusions is not Impacted by STN DBS.

Rats seeded to form pSyn inclusions in the SNpc displayed a ~36% increase in GFAP immunofluorescence intensity at two months compared to PBS control rats at the same

time point, (Fig. 4.6C; $p < 0.0001$). STN stimulation did not impact GFAP immunofluorescence in either PBS or PFF injected rats ($p > 0.05$). Importantly, consistent with our previous finding that ~ 33% of nigral neurons contain inclusions at this time point [193], we observed a ~33% increase in nigral pSyn intensity (Fig. 4.6D). Finally, to determine the impact inclusions have on the observed increase in GFAP expression, we used linear regression to model the relationship between the sum pSyn intensity and the sum GFAP intensity in PFF-treated rats, showing that there was a significant ($\beta = 1.21$, $p < 0.001$) positive association (Fig. 4.6E). Similarly, the mean GFAP intensity showed a significant positive association ($\beta = 224.04$, $p < 0.001$) with the number of pSynir neurons in the corresponding sections (Fig. 4.6F). In both of these comparisons, there was no significant interaction between pSyn intensity or pSynir neurons and stimulation group ($p > 0.05$). Collectively these data suggest that the inclusion load determines the amount of GFAP in the nigra, and that stimulation does not modify this relationship.

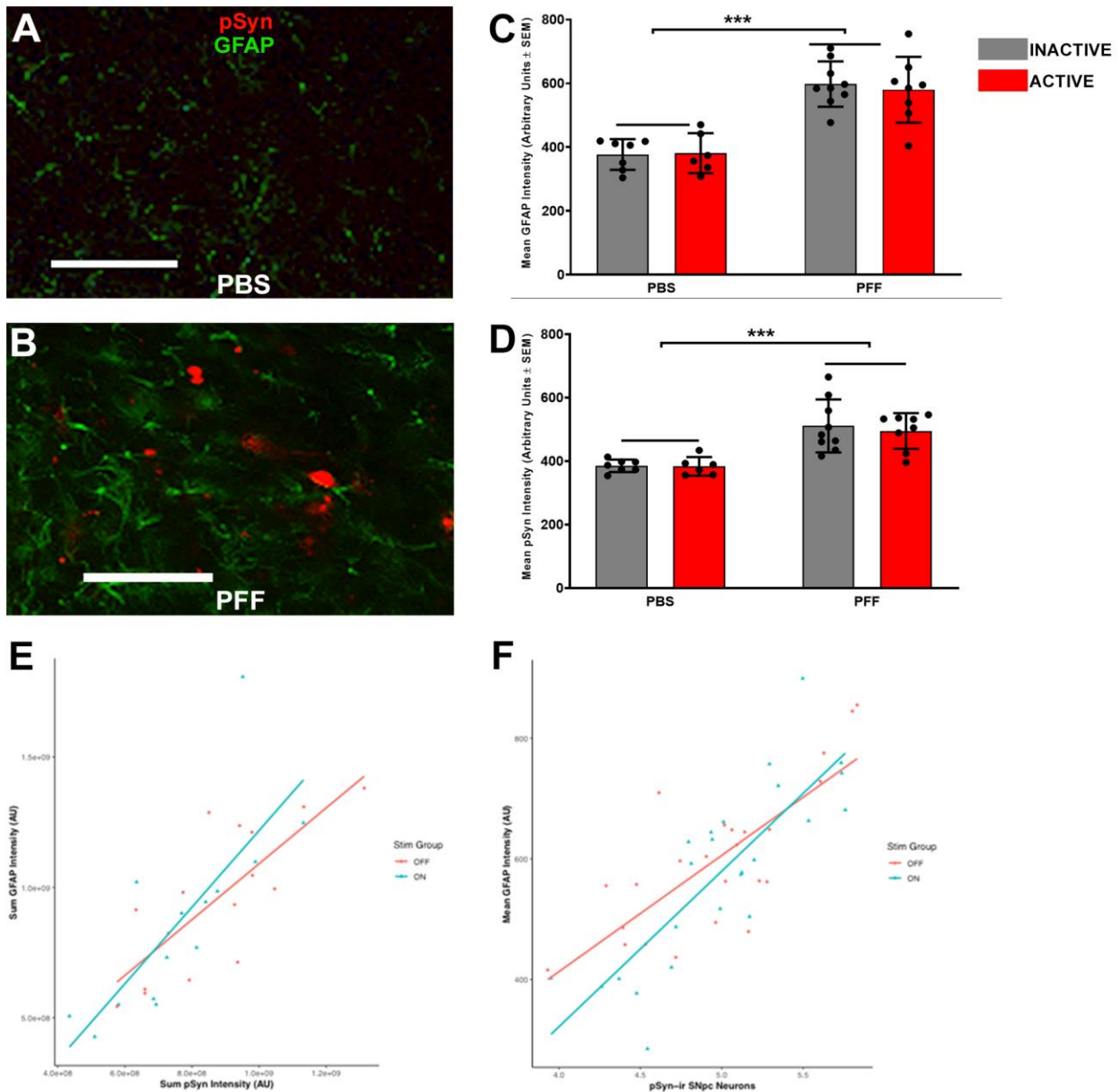


Figure 4.6: STN DBS does not impact inclusion-induced increase in GFAP in the SNpc

pSyn (red) and GFAP (green) fluorescent intensity were measured in the SNpc of PBS injected (**A**) and PFF injected (**B**) rats. Mean GFAP intensity in PFF-treated rats is higher (INACTIVE = 597.7 \pm 23.7, ACTIVE = 580.0 \pm 36.5) than in PBS-treated controls (INACTIVE = 376.7 \pm 18.2, ACTIVE = 381.0 \pm 25.6; **C**). Mean pSyn intensity is also higher in rats injected with PFFs (INACTIVE = 510.9 \pm 27.8, ACTIVE = 495.1 \pm 19.9)

Figure 4.6 cont'd

compared to controls (INACTIVE = 385.1 ± 7.4 , ACTIVE = 383.5 ± 11.9 ; **D**). There is a significant positive association between total intensity of GFAP in arbitrary units and total intensity of pSyn (**E**); this significant positive relationship was also present when comparing mean intensity of GFAP with the number of pSynir neurons in the adjacent sections (**F**). Scale bars = 50 μm .

V. Astrocytic Complexity in the SN is Increased in the Presence of α -Syn

Inclusions and is Unaffected by STN DBS.

We further characterized the length and complexity of GFAPir astrocytic processes in the presence of pSyn inclusions and the impact of STN DBS by evaluating their arborization using Sholl Analysis (Fig. 4.7). Astrocytes in the SN of rats that received PFFs, and thus formed pSyn inclusions in NS pc neurons exhibited ~36% longer total astrocyte process length compared to those astrocytes in rats treated with PBS ($p < 0.001$, Fig 4.7 A-C). Similarly, the number of astrocytic branches was ~31% greater in inclusion-bearing rats compared to controls ($p < 0.001$; Fig. 4.7A, B, D). STN DBS did not impact astrocytic process length or complexity in either PBS or PFF treated rats (Fig 4.7C and D, $p > 0.05$). Collectively, these studies show that the accumulation of pSyn inclusions is associated with increased microglial and astroglial reactivity, and that stimulation of the STN does not alter these neuroinflammatory parameters.

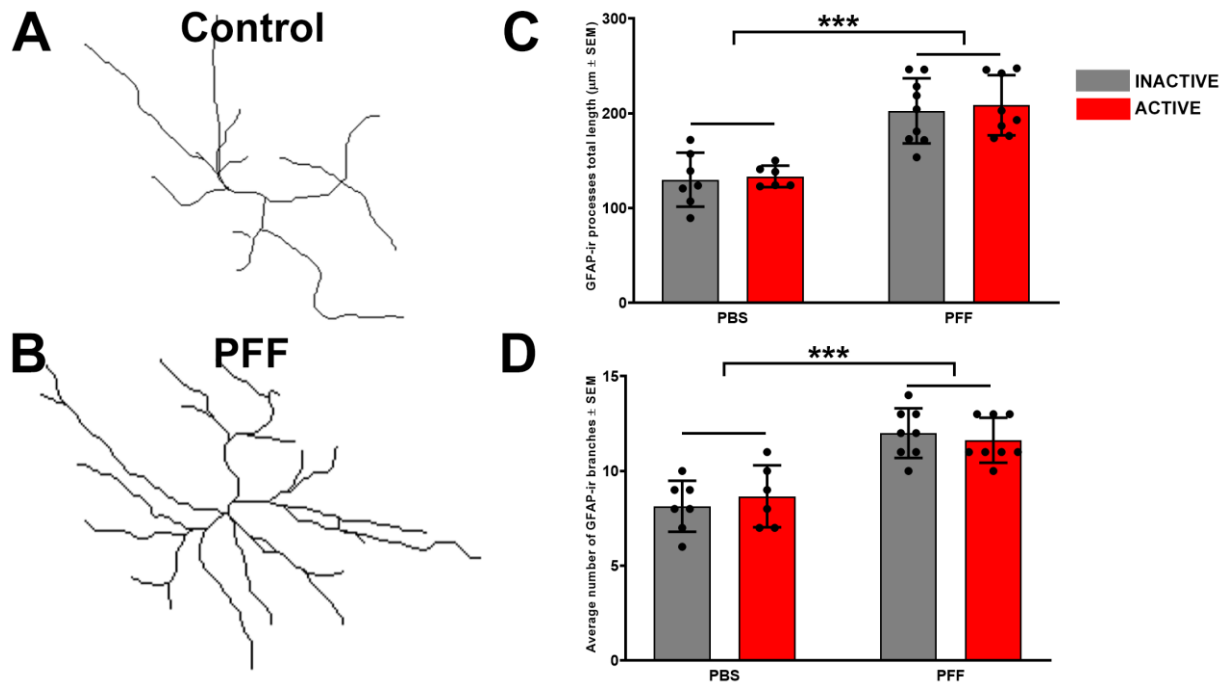


Figure 4.7: Sholl analysis reveals that increased astrocytic process length and branching in α -syn inclusion-bearing rats that is not impacted by STN DBS

GFAP^{ir} astrocytes from PBS injected (**A**) and PFF injected (**B**) rat nigras were outlined to produce 2D rendered paths. Total length of all paths (**C**) and number of branches (**D**) were quantified as an indicator of astrocyte complexity.

Discussion

STN DBS failed to mitigate microgliosis or astrocytosis in this study. We confirmed the previously reported association of pSyn inclusion accumulation with peak microglial reactivity [198] and extended our results to reveal significantly elevated astroglial reactivity in the SN of rats with pSyn inclusions. However, one month of continuous STN DBS did not attenuate either of these inclusion-associated neuroinflammatory responses. Similar to our results in Chapter 3 in which STN DBS was applied during Month 0-1, we observed that STN DBS applied during Month 1-2 did not change either the number of pSynir neurons (Fig. 4.3) or THir neurons in the SNpc (Fig. 4.4). In addition, STN DBS did not impact the number of MHC-IIir microglia in the SNpc (Fig. 4.5) or GFAP immunoreactivity either in PFF or PBS treated rats (Fig. 4.6-4.7). Collectively, these data support the notion that gliosis activation is likely a response to α -syn inclusions forming in the SNpc neurons. However, we did not observe any impact of STN DBS on these specific neuroinflammatory markers.

I. Neuroinflammation is Implicated in Clinical PD

Analyses of postmortem PD tissue have consistently revealed an increase in the number of microglia expressing major histocompatibility complex class II (MHC-II; HLA-DR in humans) [98, 99, 365]. MHC-II is a cell surface receptor found on antigen-presenting cells, and it is necessary for initiating peripheral immune responses from CD4⁺ T cells [443]. Positron emission tomography (PET) imaging studies suggest early and sustained activation of microglia in patients ranging from early- to advance-stage PD when compared to age-matched controls [438]. Not only has increased MHC-II

expression been observed, it positively correlates with α -syn burden [98]. Moreover, a single nucleotide polymorphism (SNP) in the gene encoding for MHC-II has been associated with increased risk of PD [432]. Thus, MHC-II is thought to most closely associate with a pro-inflammatory phenotype in microglia, thereby contributing to pathology in PD.

II. Microglia as a Contributor to Synucleinopathy

The mechanism(s) by which microglia contribute to PD are still under investigation. Initial efforts sought to discern whether microglial activation in fact does contribute to pathology, or is simply a result of neurodegeneration. Interestingly, in PD patients, α -syn pathology is associated with microglia activation, independent of neuronal loss [187, 435, 436], and microgliosis is observed in other brain regions that lack overt cell death [99, 203, 437, 438]. Microglia activation correlates with patient's motor deficit (assessed using the UPRDS) [438] and decline in DAergic terminals [444]. Therefore, there is likely a relationship between synucleinopathy, microglia activation, and neuronal dysfunction that precedes neurodegeneration.

Insight into the role of gliosis in disease progression has been explored using animal models of PD as well, albeit providing less certainty. This is in part because until recently we lacked the appropriate model to address this question; one demonstrating α -syn pathology and progressive nigral neurodegeneration. Transgenic models expressing human wildtype or mutant α -syn generally include widespread α -syn pathology, but lack nigrostriatal degeneration [102, 178, 373, 445]. In contrast, viral

vector-mediated overexpression of α -syn in the nigrostriatal system results in a neuroinflammatory response associated with α -syn aggregates and neurodegeneration [184, 187, 188, 445-451], however relies on supraphysiological α -syn levels, for which the contribution to neuroinflammation is unclear. In human PD total levels of α -syn are modestly increased, if at all, with idiopathic PD associated with an increase in phosphorylated α -syn [189, 429, 452]. Moreover, neurodegeneration occurs rapidly in these models, making it difficult to delineate contributors to degeneration from consequences of degeneration.

The rat α -syn preformed fibril (PFF) model of PD provides a platform to investigate the relationship between α -syn aggregation, gliosis, and neurodegeneration, as there is a protracted temporal separation between peak α -syn aggregation (1-2 months) and neurodegeneration (>4 months) [193, 198]. Moreover, there is spatial separation between the PFF injection site (striatum) and the SNpc, reducing the confound of surgical-related neuroinflammation. Previously we have revealed in the rat α -syn PFF model that reactive microglia in the SNpc peak at 2 months, corresponding to the time point in which the greatest number of pSyn inclusions are observed [198]. Moreover, MHC-IIir microglia significantly correlated with pSyn inclusion load [198]. Together these findings are consistent with what has been reported in PD patients [98], suggesting that the microglial activation associated with α -syn inclusion formation in the PFF model recapitulates a key pathogenic cascade observed in PD. Collectively these findings support the use of the α -syn PFF model to examine the potential of modulating α -syn-triggered gliosis via STN DBS.

III. Gliosis Beyond Microglia

Astrocytes are another glial cell in the CNS, and are thought to be the most abundant cell type in the brain [453, 454]. They serve a variety of functions in the CNS including metabolic support, trophic support, synapse formation and function, water transport, and blood circulation, as well as contributing to the blood-brain-barrier (BBB); thus they are essential for maintaining neuronal health [455-459]. Much like microglia, upon injury, astrocytes undergo changes in their expression profile, transforming into reactive astrocytes [460-462]. Reactive astrocytes can be further classified as displaying an A1 pro-inflammatory phenotype, or A2 anti-inflammatory phenotype [460]. It has recently been appreciated that A1 astrocytes are induced by activated microglia [460], raising the question of whether they play a role in PD progression. Indeed, A1 astrocytes have been found in PD tissue, as well as tissue from other neurodegenerative diseases (Alzheimer's, Huntington's, and amyloid lateral sclerosis), and it's been proposed that axotomized neurons trigger A1 activation and subsequent death of neurons and oligodendrocytes [460]. Further, in the mouse PFF model, blockade of microglial-triggered A1 astrocyte activation provided nigrostriatal neuroprotection [463]. Collectively these studies provide merit to evaluating the response astrocytes have to α -syn pathology in the nigrostriatal system.

Glial fibrillary acidic protein (GFAP) is an intermediate filament protein responsible for the cytoskeleton structure of astrocytes, and involved in cell-cell communication and BBB function, among other functions [464-466]. Because of its structural role, GFAP serves as a pan marker of both A1 and A2 astrocytes, which have thickened and

elongated processes [465]. In the present study we used GFAP as a marker of activated astrocytes and found a ~33% increase in total GFAP intensity, as well as processes length and branching. This suggests that (1) astrocytes are responding to inclusions with increased activation, and (2) that the increase in GFAP is likely due to increased branching rather than increased number of astrocytes.

IV. Can DBS Impact Neuroinflammation?

In Chapter 3 we showed that STN DBS had no impact on α -syn inclusion formation or TH phenotype when applied during the period of peak aggregation (0-1 months post intrastriatal PFF injection). In this set of experiments we evaluated whether ACTIVE STN DBS applied after inclusion formation, during the period of peak MHC-II activation impacts the neuroinflammatory response to inclusions. *In vitro* and *in vivo* preclinical studies suggest a potential link between STN DBS and an impact on neuroinflammation. Stimulation is associated with a decrease in activated microglia in the tissue immediately surrounding the electrode compared to sham controls [467]. Similarly, DBS is associated with a glial scar around the electrode site [468]. DBS of the thalamus in a preclinical status epilepticus model is associated with a significant decrease in proinflammatory cytokines [469]. We have demonstrated that STN DBS drives an increase in brain-derived neurotrophic factor (BDNF) in the nigrostriatal system [223] and a recent report suggests a link between BDNF-TrkB signaling and anti-inflammatory responses in microglia [470]. Specifically, astrocyte-derived BDNF appears to be involved in the anti-inflammatory actions of agents like minocycline, harnessing TrkB signaling pathways to attenuate neuroinflammation. These studies

suggest, in theory, that STN DBS has the potential to moderate neuroinflammation triggered by α -syn-triggered gliosis.

V. Summary

Evaluation of MHC-IIir microglia and GFAP immunoreactivity are blunt instruments for assessment of the neuroinflammatory response to pSyn inclusions. Microglia and astrocytes exhibit complex phenotypes in response to specific environments [466, 471, 472]. Further information regarding the specific phenotype of microglia and astrocytes in response to pathological α -syn inclusions will be required to evaluate whether STN DBS has an impact. Should STN DBS prove to alter α -syn inclusion triggered neuroinflammatory cascades in future studies this would suggest the possibility that stimulation could attenuate eventual degeneration. Alternatively, STN DBS may provide neuroprotection from pSyn inclusion-induced degeneration via alternate mechanisms. In our previous work we have observed that STN DBS drives increases in BDNF mRNA and protein within the nigrostriatal system and the M1 cortex [223, 411]. This increase in BDNF, and BDNF/TrkB signaling in nigral dopamine neurons has been specifically linked to neuroprotection from the neurotoxicant 6-OHDA [411]. However, the ability of STN DBS to drive BDNF increases within the context of synucleinopathy has yet to be examined. In Chapter 5 we examine the impact of α -syn inclusions within the corticostriatal and nigrostriatal systems on BDNF, and the impact when STN DBS is overlaid upon the synucleinopathy induced in the PFF model.

Chapter 5: Deep brain stimulation of the subthalamic nucleus increases brain-derived neurotrophic factor (BDNF) in the context of nigrostriatal synucleinopathy in the rat preformed fibril model

Abstract

The question of whether STN DBS can be disease-modifying in Parkinson's disease (PD) remains unanswered. Preclinical studies link STN DBS-mediated neuroprotection of nigrostriatal dopamine neurons to BDNF signaling. However, the impact of STN DBS on BDNF levels has yet to be examined in the context of synucleinopathy. The rat α -syn preformed fibril (PFF) synucleinopathy model provides a relevant preclinical platform to examine the impact of STN DBS on multiple potentially disease-modifying factors. In this study we examine the effects of STN DBS on BDNF in the PFF model. Adult male rats received intrastriatal injections of PFFs or PBS and were implanted with DBS electrodes and assigned to receive continuous STN DBS (ACTIVE), or no stimulation (INACTIVE) for one month post PFF injection; the interval of time with widespread accumulation of pSyn inclusions in the substantia nigra pars compacta (SNpc) and cortical areas. Postmortem outcome measures included quantification of total BDNF protein levels in the frontal cortex, M1 cortex, SNpc, and striatum. Additionally, relationships between cortical- and nigrostriatal levels of BDNF were evaluated. The formation of pSyn inclusions did not alter total levels of BDNF in any of the individually evaluated structures. We observed a positive association between cortical/nigral BDNF levels and striatal BDNF levels that was disrupted when inclusions were present. Despite this, rats receiving PFF injection and STN DBS exhibited significantly increased BDNF protein in the striatum, which partially restored the normal corticostriatal BDNF relationship. Our results demonstrate that pSyn inclusions may alter BDNF transport to the striatum. However, STN DBS retains the ability to increase BDNF within the context of synucleinopathy. Future studies will examine whether DBS-induced increases in

BDNF can prevent the nigrostriatal degeneration associated with longer post PFF injection intervals.

Introduction

I. Mechanism of STN DBS-Mediated Neuroprotection – BDNF

Previous examination of the impact of STN DBS on levels of BDNF show that STN DBS significantly increases BDNF expression in the SNpc, the striatum and the M1 cortex [223]. Specifically, in 6-OHDA lesioned rats, STN DBS resulted in a doubling of BDNF mRNA and protein in the SNpc [223]. In unlesioned rats STN DBS produced a three-fold increase in BDNF in the striatum and a 50% increase in the M1 cortex [223]. Other laboratories have since confirmed an increase in BDNF in association with stimulation of other targets [224-226]. Evaluation of downstream BDNF- tropomyosin-related kinase type 2 (TrkB) signaling reveals a functional, pro-survival consequence of this BDNF increase in nigrostriatal dopamine neurons that is blocked when TrkB signaling is prevented via an antagonist or α -syn overexpression [222, 411]. These results suggest that BDNF-TrkB signaling is essential for STN DBS to protect nigral neurons.

II. α -Syn Pathology Beyond the Nigrostriatal System

α -syn pathology has been characterized in the substantia nigra in humans and animal models many times over. However, extranigral pathology is consistently seen in clinical cases of PD as well as in the PFF model. In the PFF model the frontal cortex contains numerous neurons with pSyn (α -syn phosphorylated at serine 129) immunoreactive inclusions that form within 1-2 months following PFF injection [193]. Similarly, we have observed an inclusion-associated increase in microglial activation in the cortex [198]. While neither of these responses have been quantified or characterized to the extent

that the SNpc has been, it suggests that PFF-induced inclusion formation in the cortex is not unique from that in the nigra.

III. BDNF Transport

BDNF in the striatum is derived largely by anterograde transport from cortical afferents, and to a lesser degree by nigral afferents [473]. The adult rat striatum has no detectable BDNF mRNA, nonetheless contains BDNF protein at levels similar to other BDNF mRNA-rich brain regions [474]. Thus, BDNF transcript and protein levels do not necessarily correlate and anterograde transport from cortical and nigral regions is critical for normal striatal function and health [473, 475, 476].

BDNF is unique from other neurotrophic factors in that it's transported both anterogradely and retrogradely along axons, and it can travel from neuron to neuron via transcytosis [477-483]. However, the majority of BDNF transport is anterograde, facilitated by kinesin-1 and phosphorylated huntingtin [484-486]. Both injury and electrical activity have been shown to increase the production, anterograde transport, and release of BDNF [487-492].

IV. Neuroprotective potential of BDNF

Results from our lab suggest a neuroprotective mechanism of STN DBS via increased BDNF-trkB signaling [223, 411]. Electrical stimulation drives BDNF release in neuronal cultures [274, 285] and glutamatergic signaling at N-methyl-d-aspartate (NMDA) receptors increases BDNF mRNA expression [493], providing two possible mechanisms

by which STN DBS could increase BDNF in the striatum [494]. Previous STN DBS research showed BDNF-dependent neuroprotection of nigral dopamine neurons from 6-OHDA insult [411], mirroring the pro-survival effect of BDNF application to dopamine neurons observed in other models [282-284, 495]. Moreover, reduced BDNF levels in the brains of PD patients further supports the notion that elevated BDNF could be neuroprotective [276, 496].

There are many possible mechanisms by which BDNF could be neuroprotective in PD beyond preservation of nigrostriatal projections as well [494]. We now appreciate that prior to neurodegeneration, there is dysfunction at the terminals of nigral neurons, and mitigating this dysfunction is a promising disease-modifying approach to PD [497-500]. BDNF signaling increases dopamine release, tyrosine hydroxylase synthesis, dopamine turnover, and dopamine neuron activity, all of which are decreased in PD [80, 501-507]. This is supported by evidence that STN DBS alters dopaminergic neurotransmission [508], perhaps via increased BDNF signaling. Beyond nigrostriatal dopaminergic neurons, BDNF is critical in maintaining gamma aminobutyric acid-ergic (GABAergic) and glutamatergic synapses by facilitating long-term potentiation and plasticity [492, 509, 510]. In the striatum, BDNF helps maintain postsynaptic spine density [511], which is decreased in postmortem PD brains [512]. Collectively, these data present a strong argument for BDNF having the ability to mitigate cellular dysfunction in PD, prior to neurodegeneration.

V. Present Study

In the present study we investigate the impact of α -syn inclusions on levels of BDNF as well as nigrostriatal and corticostriatal BDNF relationships. We then evaluate the ability of STN DBS to drive BDNF production in the striatum and M1 cortex in the context of synucleinopathy.

Methods

I. Experimental Overview

Adult (3 months old) male Fischer 344 (Charles River, Wilmington, MA) rats were used for this study. This study is comprised of three experiments. Experiment 3 includes the young animals evaluated in Chapter 3.

Experiment 1

Twenty rats were unilaterally injected with preformed α -syn fibrils (PFF; n = 10) or PBS (n = 10) into 2 sites in the striatum. Animals were sacrificed 30 days post injections. Primary outcome measures include quantification of BDNF protein (via ELISA) in the ipsilateral frontal cortex, bilateral striatum, and bilateral substantia nigra. Successful seeding of PFF treated rats was validated via the presence of pSynir inclusions in the contralateral frontal cortex (data not shown).

Experiment 2

Ten rats were unilaterally injected with PBS into 2 sites in the striatum. During the same surgical session, all animals were implanted with an electrode into the STN. Three days after surgery, animals were randomly assigned to receive stimulation (ACTIVE; n = 5) or no stimulation (INACTIVE, n = 5) for a period of 5 days. Outcome measures include ipsilateral quantification of BDNF protein (via ELISA) in the M1 cortex and striatum. ACTIVE stimulation was validated via a behavioral response to stimulation and correct electrode placement.

Experiment 3

Forty rats were unilaterally injected with preformed α -syn fibrils (PFF; n = 30) or PBS (n = 10) into 2 sites in the striatum. During the same surgical session, all animals were implanted with an electrode into the subthalamic nucleus. Three days after surgery, PFF-injected animals were randomly assigned to receive stimulation (ACTIVE) or no stimulation (INACTIVE) for 30 days. All PBS-injected animals were assigned to INACTIVE. Outcome measures include bilateral quantification of BDNF protein (via ELISA) in the M1 cortex and striatum. PFF treated animals were validated via the presence of proteinase K-resistant, pSyn immunoreactive inclusions in the SNpc (quantified, Chapter 3). ACTIVE stimulation was validated via a behavioral response to stimulation and correct electrode placement. An overview of the experimental design is presented in Figure 5.1.

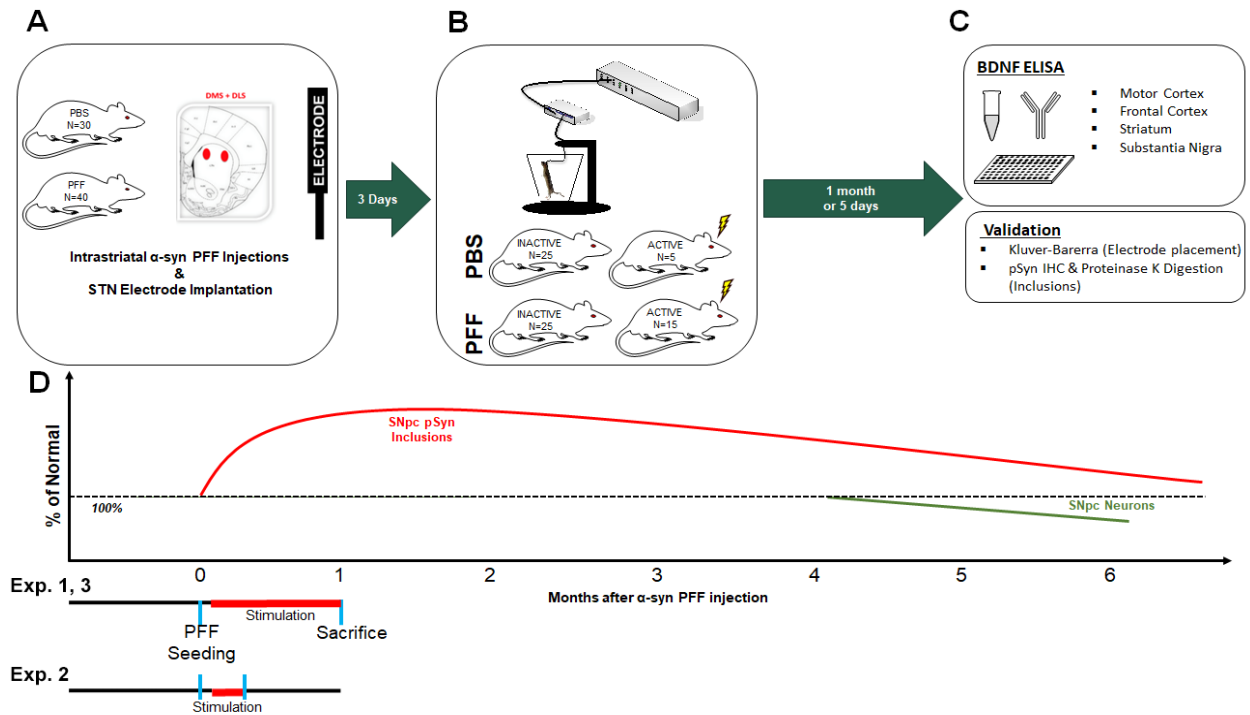


Figure 5.1: Experimental overview

Young (3 months old) rats received two intrastratial injections of PBS (n = 30) or α -syn PFFs (n = 40) and electrode implantation into the subthalamic nucleus (STN) during the same surgical session (**A**). Three days later, rats were randomly assigned to receive INACTIVE (stimulation never turned on; n = 50) or ACTIVE (n = 20) continuous stimulation, as described above. At the conclusion of the experiment (Exp. 1,3 = one month; Exp. 2 = 5 days) all animals were sacrificed (**B**). Outcome measures include ELISA probing for BDNF, and validation of electrode placement (Kluver-Barerra) and inclusion formation (pSyn IHC and Proteinase K digestion; **C**). Time points were determined according to the period of peak inclusion formation (1-2 months, red), prior to degeneration of SNpc neurons (4-6 months, green; **D**).

II. Animals

All animals were given food and water *ad libitum* and housed in 12h light-dark cycle conditions in the Grand Rapids Research Center, which is fully Association for Assessment and Accreditation of Laboratory Animal Care (AAALAC) approved. All procedures were conducted in accordance with guidelines set by the Institutional Animal Care and Use Committee (IACUC) of Michigan State University.

III. Preparation and Quality Control of α -Syn PFFs

Recombinant, full-length mouse α -syn PFFs were prepared and verified via in vitro fibril assembly as previously described [195, 196, 418]. Prior to sonication, α -syn fibrils were assessed to verify lack of contamination (LAL Assay (~ 1 endotoxin units/mg), high molecular weight (sedimentation assay), beta sheet conformation (thioflavin T), and structure (electron microscopy). Prior to injection, PFFs were thawed, diluted in sterile Dulbecco's PBS (DPBS, 2 μ g/ μ l), and sonicated at room temperature using an ultrasonicating homogenizer (300VT; Biologics, Inc., Manassas, VA) with the pulser set at 20% and power output at 30% for 60 pulses at 1 s each [194]. Following sonication, a sample of the PFFs was analyzed using transmission electron microscopy (TEM). Formvar/carbon-coated copper grids (EMS DIASUM, FCF300-Cu) were washed twice with ddH₂O and floated for 1 min on a 10- μ l drop of sonicated α -syn fibrils diluted 1:20 with DPBS. Grids were stained for 1 min on a drop of 2% uranyl acetate aqueous solution; excess uranyl acetate was wicked away with filter paper and allowed to dry before imaging. Grids were imaged on a JEOL JEM-1400 transmission electron microscope. The length of ~500 fibrils per sample was measured to determine average

fibril size. The mean length of sonicated mouse α -syn PFFs was estimated to be 40.9 ± 0.55 nm, well within the optimal fibril length previously reported to result in seeding of endogenous phosphorylated α -syn inclusions *in vitro* and *in vivo* [419] (Fig. 3.2).

IV. Pre-Formed Fibril Injections

Intrastriatal α -syn PFF injections were conducted as described previously [193]. Rats were anesthetized before surgery with Equithesin (0.3 ml/100 g body weight i.p.; chloral hydrate 42.5 mg/ml sodium pentobarbital 9.72 mg/ml). Each rat received two unilateral, intrastriatal injections (AP +1.0 mm, ML +2.0 mm, DV -4.0 mm and AP +0.1 mm, ML+4.2 mm, DV -5.0 mm, AP and ML relative to bregma and DV relative to dura, injection rate 0.5 μ l/min,) of sonicated α -syn PFFs (total 16 μ g in 2.0 μ l per site). Sonicated PFFs were kept at room temperature during the duration of the surgical procedures. Injections were administered made using a pulled glass needle attached to a 10- μ l Hamilton syringe [194]. After each injection, the needle was left in place for 1 min, retracted 0.5 mm, left in place for an additional 2 min, and then slowly withdrawn.

V. Electrode Implantation

Immediately following PFF injections, rats were unilaterally implanted (ipsilateral to α -syn PFF injections) with a bipolar, concentric microelectrode (inner electrode projection 1.0 mm, inner insulated electrode diameter 0.15 mm, outer electrode gauge 26, Plastics One, Roanoke, VA) targeted to the dorsal border of the STN (AP 3.4 mm, ML 2.5 mm, relative to bregma and DV 7.7 mm, relative to dura). The dorsal STN border placement site was selected to minimize damage to the nucleus, as has been described previously

[513]. Burr holes were drilled in the skull; the electrode was fixed in place using bone screws, Metabond (Parkell, Brentwood, NY), and dental acrylic. Drill holes were filled with bone wax to prevent entry of dental cement during electrode placement. Animals were monitored daily post-surgery.

VI. Deep Brain Stimulation

Continuous stimulation platform. Three days following surgery half of the rats were assigned to receive either continuous stimulation (ACTIVE) for 1 month (Exp. 1, 3) or 5 days (Exp. 2), or no stimulation for the same period (INACTIVE). Rats received STN stimulation that was continuously delivered in a freely moving setup as previously described [513]. Stimulation was generated by an Accupulser Signal Generator (World Precision Instruments) via a battery-powered Constant Current Bipolar Stimulus Isolator (World Precision Instruments). Stimulation parameters consisted of a frequency of 130 Hz, a pulse width of 60 μ s and an intensity of \sim 50 μ A. At the onset of stimulation, intensity settings were increased until orofacial or contralateral forepaw dyskinesias were observed to confirm stimulation delivery. Immediately following a positive dyskinetic response, the intensity was set below the lower limit of dyskinesias (20-50 μ A), such that no rat was functionally impaired by stimulation as previously described [513].

VII. Euthanasia

Rats were euthanized at the conclusion of the study. Rats were deeply anesthetized (60 mg/kg, pentobarbital, i.p.) and perfused intracardially with heparinized normal saline at

37°C followed by ice-cold normal saline. Care was taken to minimize the tissue damage resulting from removing the skull with the electrode still intact.

Experiment 1: Brains were placed in ice-cold normal saline for 1 min. The contralateral frontal cortex was microdissected and post-fixed in 4% paraformaldehyde (PFA) for 1 week and transferred to 30% sucrose in 0.1 M phosphate buffer until sinking. The remainder of the brain was immediately flash-frozen in 3-methyl butane on dry ice and stored at 80°C until microdissected.

Experiment 2: Brains were immediately flash-frozen in 3-methyl butane on dry ice and stored at 80°C until microdissected.

Experiment 3: Brains were placed in ice-cold normal saline for 1 min and then hemisected on the coronal plane at the optic chiasm. The caudal half was post-fixed in 4% paraformaldehyde (PFA) for 1 week and transferred to 30% sucrose in 0.1 M phosphate buffer until sinking (used for Chapter 3). The rostral half was immediately flash-frozen in 3-methyl butane on dry ice and stored at 80°C until microdissected.

IIIX. Tissue Processing

The contralateral frontal cortex (Experiment 1) and rostral half of the brain, including the STN and SNpc (Experiment 3) were processed as follows. Brains were frozen and sectioned on a sliding microtome at 40 µm. Free-floating sections (1:6 series) were transferred to 0.1 M tris-buffered saline (TBS). Following the washes, endogenous

peroxidases were quenched in 3% H₂O₂ for 1 h and rinsed in TBS. Sections were blocked in 10% normal goat serum/0.5% Triton X-100 in TBS (NGS, Gibco; Tx-100 Fischer Scientific) for 1 h. Following the blocking, sections were immunolabeled with primary antibodies: pan rabbit-anti α -syn (Abcam, Cambridge, MA; AB15530, 1:1000), or mouse anti-phosphorylated α -syn at serine 129 (pSyn, 81A; Abcam, Cambridge, MA; AB184674; 1:10,000) overnight in 1% NGS/0.5% Tx-100/TBS at 4 °C. Following the washes, sections were incubated in biotinylated secondary antibodies (1:500) against mouse (Millipore, Temecula, CA; AP124B) or rabbit IgG (Millipore, Temecula, CA; AP132B) followed by washes in TBS and 2 h incubation with Vector ABC standard detection kit (Vector Laboratories, Burlingame, CA; PK-6100). Immunolabeling for pSyn was visualized by development in 0.5 mg/ml 3,3' diaminobenzidine (DAB; Sigma-Aldrich St. Louis, MO; D5637-10G) and 0.03% H₂O₂. Slides were dehydrated in an ascending ethanol series and then xylenes before coverslipping with Cytoseal (Richard-Allan Scientific, Waltham, MA). SNpc pSyn-labeled sections were also counterstained with cresyl violet for quantification of intraneuronal pSyn inclusions (Chapter 3).

IX. Kluver–Barrera Histology

Electrode placement was verified for rats used in Experiments 2-3 (Experiment 1 rats did not receive electrode implantation surgery). Saline-perfused/PFA-postfixed brains (caudal half after hemisection) were frozen on dry ice and sectioned at 40 μ m thickness using a sliding microtome in six series. Every sixth section of the STN was stained using Kluver–Barrera histochemistry (Kluver and Barrera, 1953) to evaluate for appropriate targeting of the electrode to the STN. Only rats with correctly positioned electrodes were

included in the data analysis (see, e.g., Fig. 3.3). Electrode location was considered to be appropriate if the tip of the electrode was observed within 250 μm of the border of the STN within any of the sections based on previous estimations of current spread conducted using similar stimulation parameters [158].

X. Proteinase K Digestion

To determine whether pSyn immunoreactive inclusions were non-soluble (Lewy body-like) as previously described [420, 421], a subset of nigral sections were treated with or without 10 $\mu\text{g}/\text{mL}$ proteinase K (Invitrogen, Carlsbad, CA; #25530015) then stained for pan rabbit-anti α -syn (Abcam, Cambridge, MA; AB15530, 1:1000) as described above. Soluble α -syn is digested by Proteinase K, while non-soluble inclusions are not (Fig. 3.4).

XI. Microdissections

After brain removal, whole brains and rostral brains were flash frozen in 2-methylbutane on dry ice and stored at -80°C . Microdissections were performed by thawing brains at -20°C for 30 min, then sectioning in a Leica 305S cryostat (Leica Biosystems, Wetzlar, Germany) kept at -12°C . 2 mm^2 punches were taken bilaterally from the M1 motor cortex and striatum, and unilaterally from the frontal cortex. 1 mm^2 punches were taken bilaterally from the substantia nigra. During the procedure all brains were transferred on dry ice. Samples were stored at -80°C .

XII. ELISA

Samples were thawed on ice and 250 μ l of RIPA Lysis Buffer System was added to each sample (sc-249-48, Santa Cruz Biotechnology, Dallas, TX). Samples were sonicated, on ice, in short bursts (5-7 sec) to homogenize, followed by a 30 minute incubation. 10 μ l was taken for BCA Assay (see below) and the remaining 240 μ l was centrifuged at 10,000g for 30 minutes at 4°C and the supernatant collected. The ELISA was completed with duplicate samples, following the kit's protocol (BEK-2211, Biosensis, Thebarton, Australia).

XIII. BCA Assay

10 μ l of homogenized sample was diluted into 30 μ l of 2% SDS. Following this step, samples were handled at room temperature. Samples were loaded in 10 μ l triplicates into a 96-well plate and treated with 200 μ l of prepared BCA reagent (50 Reagent A : 1 Reagent B; 23250; ThermoFisher, Waltham, MA). Plates were incubated in the dark at 37°C for 30 minutes, then read on a Synergy H1 microplate reader (BioTek, Winooski, VT). Sample concentrations were calculated by comparing to a standard curve of known concentrations of Bovine Serum Albumin.

XIV. Statistical analyses

All statistical tests were completed using GraphPad Prism software (version 8, GraphPad, La Jolla, CA) and R (version 3.6.3; www.r-project.org). Studies utilized two-way ANOVA or multivariate linear regression to assess differences between groups. Total BDNF protein levels were analyzed with two-way ANOVA with two treatment

factors: inclusions and hemisphere (Experiment 1), or stimulation and hemisphere (Experiments 2-3). Multivariate linear regression was used to model the relationships between M1 BDNF, cortical BDNF, nigral BDNF and striatal BDNF levels in rats by experimental group. Striatal BDNF and experimental group were included as explanatory variables in the model. The linear models also included interaction terms between striatal BDNF (predictor) and experimental groups (categorical factors) to determine whether experimental treatments modified the relationship between M1/cortical/nigral and striatal BDNF. Control rats without PFF treatment or DBS stimulation were used as the reference group in the model. Due to non-normality, striatal BDNF levels were log-transformed prior to regression modeling. Statistical significance was set at p 0.05. Statistical outliers were assessed using the Absolute Deviation from the Median method using the “very conservative” criterion [422].

Results

I. Chapter 3 Recap: STN DBS does not Alter α -Syn Inclusions or TH Phenotype in SNpc Neurons.

These studies were conducted using BDNF measurements from structures in the rostral half of brains evaluated in Chapter 3. To briefly recap, the number of inclusion-bearing neurons was not changed with stimulation as measured by pSyn immunoreactivity (INACTIVE = 5580 ± 297.2 , ACTIVE = 5351 ± 249.1) or truncated pSyn* immunoreactivity (INACTIVE = 5028 ± 304.5 , ACTIVE = 4931 ± 292.5 ; Fig. 3.5). Similarly, the size and immunofluorescent intensity of individual inclusions were also not impacted by stimulation. Importantly, PFF injections result in ~18% loss of TH immunoreactivity on the ipsilateral side relative to the contralateral side, however stimulation did not alter this loss in TH phenotype (INACTIVE = 15004 ± 959.9 , ACTIVE = 11842 ± 931.2 ; Fig. 3.6). Collectively, these data suggest that any effect on BDNF levels observed in these rats as a result of stimulation is not via altered α -syn inclusion formation or TH phenotype.

II. α -Syn Inclusions do not Change Total BDNF Protein Amounts.

Measurement of BDNF protein levels in the substantia nigra, striatum, M1 cortex, and frontal cortex revealed no differences in rats treated with PFFs vs. PBS ($p > 0.05$; Fig. 5.2 A-D). There were also no differences in BDNF levels in the injected side compared to the contralateral side for any of these structures ($p > 0.05$). Specifically, in the substantia nigra BDNF levels (pg/mg protein) in PBS injected rats were 62.05 ± 8.86 (ipsilateral) and 80.28 ± 5.01 (contralateral), compared to 54.26 ± 3.83 (ipsilateral) and

72.00 ± 10.47 (contralateral). In the striatum BDNF levels in PBS injected rats were 29.54 ± 3.14 (ipsilateral) and 25.09 ± 2.75 (contralateral), compared to 28.95 ± 3.57 (ipsilateral) and 26.25 ± 3.01 (contralateral). In the M1 cortex BDNF levels in PBS injected rats were 21.13 ± 2.77 (ipsilateral) and 20.56 ± 1.13 (contralateral), compared to 18.95 ± 2.11 (ipsilateral) and 19.85 ± 0.71 (contralateral). Finally, in ipsilateral frontal cortex, BDNF levels in PBS injected rats were 44.10 ± 4.90, compared to 41.18 ± 7.21 (contralateral levels were not evaluated as they were used to verify α -syn inclusions after PFF injection).

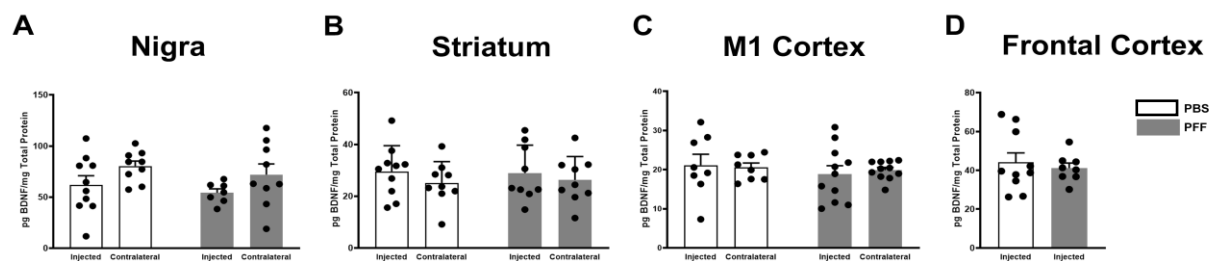


Figure 5.2: Total amount of BDNF is not impacted by inclusions

Total protein levels for rats treated with PBS or PFFs measured in the SN **(A)**, striatum **(B)**, M1 cortex **(C)**, or frontal cortex **(D)** revealed no differences ($p > 0.05$). Within each group, ipsilateral and contralateral levels also revealed no differences ($p > 0.05$).

III. α -Syn Inclusions Change BDNF Structural Relationships.

We also examined the relationship between BDNF levels in the cortex/M1/SN and the striatum by comparing BDNF levels within individual rats. Evaluation of the relationship of BDNF in these structures revealed significant positive associations in cortical- and nigrostriatal BDNF levels (Fig. 5.3A) that were disrupted with inclusions (Fig. 5.3B).

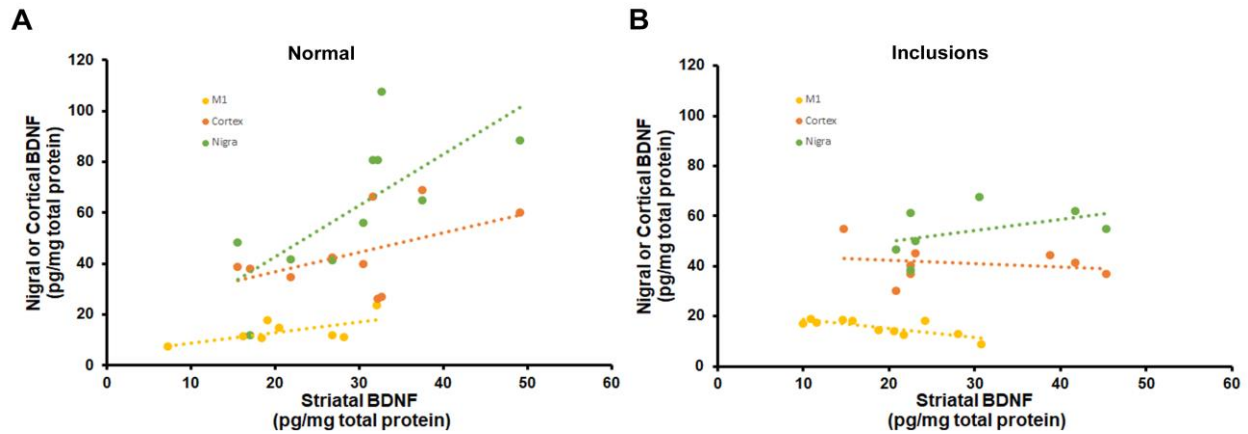


Figure 5.3: α -syn inclusions change BDNF structural relationships

Rats treated with PBS show a significant positive association ($\beta = 23.16$, $SE = 6.44$, $p < 0.001$) between nigrostriatal (green) and corticostriatal (M1, yellow; frontal cortex, red) BDNF protein levels (**A**). Rats treated with PFFs show a significantly decreased association (-17.99 , $SE = 8.26$, $p < 0.05$) between nigrostriatal (green) and corticostriatal (M1, yellow; frontal cortex, red) BDNF protein levels (**B**).

IV. STN DBS Increases Striatal BDNF in the α -Syn PFF Model.

We examined the impact of 5 days of STN DBS in a pilot cohort of naïve rats. STN DBS resulted in a 30% increase in BDNF protein in the striatum ($p < 0.05$, Fig. 5.4A). STN DBS also resulted in a 50% increase in BDNF protein in the M1 cortex ($p = 1.12$, Fig. 5.4B) although this increase did not reach significance. When analyzed together, ACTIVE and INACTIVE naïve rats show a weak positive association ($\beta = 2.63$, $p < 0.05$) between levels of BDNF protein in the M1 cortex and striatum (Fig. 5.4C). However, when factoring stimulation as a covariant, this association was no longer significant ($\beta = 2.47$, $p > 0.05$), nor is the interaction with stimulation ($\beta = 0.16$, $p > 0.05$). This is likely

due to the small sample size ($n = 4-5$). These data are from a pilot study and require replication, but they suggest that STN DBS does not interfere with the normally observed positive structural relationship in BDNF protein levels between the M1 cortex and striatum.

We next evaluated how long-term (1 month) STN DBS impacts BDNF protein in inclusion-bearing rats. One month of STN DBS resulted in a ~150% increase in BDNF protein in the ipsilateral striatum ($p < 0.01$; Fig. 5.4D). In contrast, ipsilateral BDNF levels in the M1 of α -syn inclusion bearing rats were significantly decreased ~30% by STN DBS ($p < 0.05$; Fig. 5.4E). Interestingly, contralateral striatal and BDNF protein levels were unchanged by STN DBS ($p > 0.05$, Fig. 5.4D, E).

V. STN DBS Partially Mitigates the Corticostriatal BDNF Association Disrupted by α -Syn Inclusions

Finally, we evaluated the relationship between M1 BDNF levels and striatal BDNF levels of with and without stimulation in PBS and PFF treated rats. INACTIVE PBS rats displayed a significant, positive association between M1 cortical and striatal BDNF expression (Fig. 5.4F, black; $\beta = 14.862$, $p < 0.01$). As we observed previously, the presence of inclusions in INACTIVE PFF rats reversed this relationship, resulting in a negative association (Fig. 5.4F, gray; $\beta = -38.035$, $p < 0.0001$). However, STN DBS in PFF treated rats partially mitigated this reversal caused by inclusions (Fig. 5.4F, red; $\beta = -16.820$, $p < 0.05$).

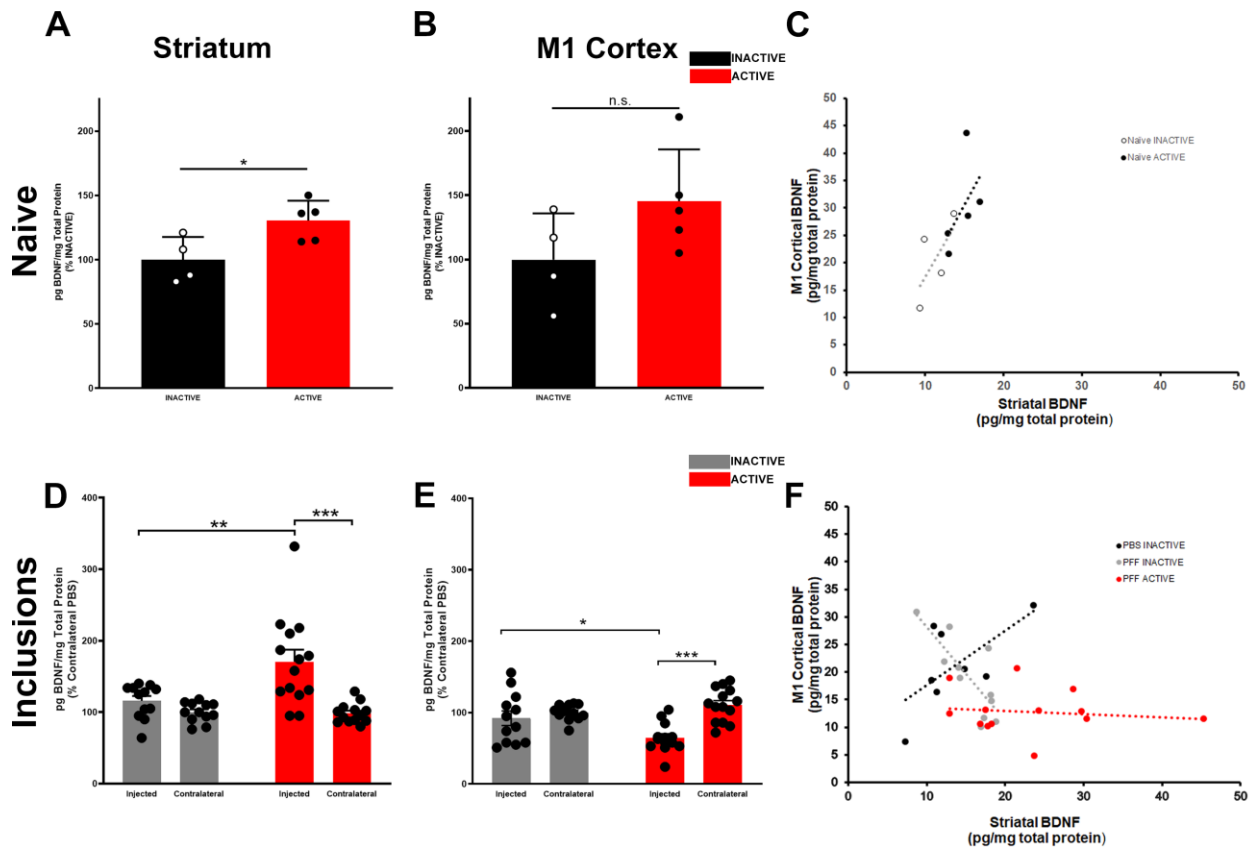


Figure 5.4: STN DBS increases striatal BDNF protein despite inclusions

A short-term pilot study (5 days, $n = 4-5$) demonstrates the typical relationship between STN DBS and BDNF protein (**A-C**). Rats receiving ACTIVE stimulation show a modest increase in striatal BDNF ($p < 0.05$, **A**), and an insignificant increase in the M1 ($p = 0.12$, **B**). Collectively, ACTIVE (black) and INACTIVE (open) naïve rats show a weak positive association ($\beta = 2.63$, $p < 0.05$) between levels of BDNF protein in the M1 cortex and striatum that is lost when factoring in stimulation ($\beta = 2.47$, $p > 0.05$), which is not a significant covariant ($\beta = 0.16$, $p > 0.05$; **C**). The relationship between cortical and striatal BDNF ACTIVE STN DBS in rats with α -syn inclusions increases ipsilateral BDNF protein in the striatum (25.74 ± 2.16 pg/mg) compared to INACTIVE (15.77 ± 0.94 pg/mg, $p < 0.001$; **D**). In contrast, BDNF protein in the ipsilateral M1 cortex (12.68 ± 1.06 pg/mg) of inclusion-bearing rats is decreased compared to INACTIVE rats ($18.26 \pm$

Figure 5.4 cont'd

2.03 pg/mg, $p < 0.05$). Neither the contralateral striatum (13.42 ± 0.52 pg/mg, $p < 0.001$) nor M1 (21.92 ± 1.23 pg/mg, $p < 0.001$) show changes in BDNF protein following ACTIVE STN DBS **(D-E)**. The relationship between BDNF protein levels in M1 Cortex and striatum are altered by PFFs and STN DBS **(F)**. Control (PBS, INACTIVE) rats show a positive association between M1 cortical and striatal BDNF expression (black; $\beta = 14.862$, $p < 0.01$). This relationship is reversed in PFF treated animals, causing a negative association (gray; $\beta = -38.035$, $p < 0.0001$). STN DBS in inclusion-bearing neurons partially mitigates this reversal caused by inclusions (red; $\beta = -16.820$, $p < 0.05$).

Discussion

In chapters 3 and 4 we looked at the ability of STN DBS to impact α -syn aggregation and gliosis in the rat α -syn preformed fibril (PFF) model of synucleinopathy. STN DBS did not impact any of these outcome measures. These findings provide important context for our present results due to the fact that observed BDNF effects cannot be attributed to differences in aggregation and neuronal survival. In the present study we investigate the impact of α -syn inclusions and STN DBS on BDNF tissue levels in the cortex, striatum and substantia nigra and BDNF corticostriatal and nigrostriatal relationships. We observed that in rats with PFF seeded nigral and cortical inclusions BDNF levels within individual structures are not impacted, however normal BDNF relationships between these structures are altered. Further, we report that despite the negative effects of α -syn inclusions on BDNF structural relationships, STN DBS in inclusion-bearing rats is capable of significantly increasing striatal BDNF levels and partially restores the normal corticostriatal BDNF relationship.

I. Inclusion Dynamics

Normally, the striatum does not produce its own BDNF; instead it is transported primarily from the cortex, and from the SNpc to lesser degree [473]; Fig. 5.5A). BDNF protein levels in the cortex/nigra and striatum are positively correlated, as such that when cortical or nigral BDNF levels are high, so are striatal BDNF levels (Fig. 5.3A, Fig. 5.4F). However this association is eliminated when α -syn inclusions are present. BDNF mRNA is decreased in neurons with inclusions seeded by PFFs [197], suggesting that BDNF protein may also be decreased. However, we did not observe any impact of

inclusions in total levels of BDNF protein in the M1 cortex, frontal cortex, substantia nigra, or striatum (Fig. 5.2), only the corticostriatal and nigrostriatal BDNF relationship is altered. At the 1 month time point of the present experiment, approximately 30% of nigral neurons contain pSynir inclusions (Chapter 3, data not shown). Perhaps with a greater cortical inclusion load, cortical, nigral, and/or striatal BDNF protein levels might be lower. Supporting this, BDNF levels are lower in the SNpc of PD patients post-mortem [276, 496].

An alternative explanation for why we observed an altered corticostriatal and nigrostriatal BDNF relationship is that anterograde transport from the cortex (and nigra) to the striatum from inclusion-bearing neurons is impaired. There is evidence *in vitro* of impaired anterograde transport of BDNF receptor, TrkB, in inclusion-bearing primary neuronal cultures [195], as well as impaired retrograde transport of BDNF itself in a α -syn overexpression model [398]. It is possible that a similar impairment of anterograde BDNF transport results in association with the formation of pSyn inclusions. Importantly, in human PD as well as in this model, only a subpopulation of nigral or cortical neurons have inclusions [514, 515]. Thus, neighboring (inclusion free or reduced) neurons may compensate for decreased BDNF production by upregulating their BDNF production, transport, and release, resulting in an overall net no change (Illustrated in Fig. 5.5B). Indeed, BDNF compensatory mechanisms have been observed in response to denervation of the nigrostriatal system, suggesting that a similar phenomenon could be occurring here [516, 517]. Finally, to account for the reversed relationship in cortical and striatal BDNF, we could imagine a third, intermediate cortical neuronal phenotype: one

lacking overt synucleinopathy, but rather some neurite pathology and resulting axonal dysfunction. In this scenario, these neurons may still have a compensatory increase in somatic BDNF production, however they also may have impaired transport. This would effectively result in BDNF protein 'getting stuck' in the soma. Rats with many of these intermediate phenotype neurons would show up on one spectrum (high cortical BDNF, low striatal BDNF) whereas animals with relatively few would show up on the other (low cortical BDNF, high striatal BDNF). In line with this idea is the fact that the number of pSynir neurons do not correlate with the negative association (data not shown), suggesting that having more somatic inclusions does not mean there is more disrupted transport. In this model the inclusion forming cascade starts in the axon, and over time spreads to the soma and dendrites [195, 197], suggesting there likely could be such a proposed intermediate level of dysfunction.

II. DBS Dynamics

STN DBS normally drives an increase in BDNF protein in the M1 cortex, striatum and substantia nigra [223]. Our pilot data suggest that the normal positive corticostriatal BDNF relationship is not altered by STN DBS (Fig. 5.5C). In the presence of α -syn inclusions, STN DBS still drives a significant BDNF increase in the striatum. While this is a tempered effect compared to what has previously been reported following chronic stimulation (~300%) [223], this suggests that STN DBS can still drive the production of BDNF from the nigrostriatal system, despite the presence of inclusions in a subpopulation of nigral neurons. In contrast, we observed that M1 cortical levels in PFF seeded rats decreased with STN DBS. This is the opposite effect than what was

previously observed in which STN DBS to naïve rats resulted in a ~50% increase in M1 BDNF protein levels [223]. The net effect of STN DBS in α -syn inclusion bearing circuitries is one of a partial restoration of the normal corticostriatal BDNF positive association. This suggests that the STN DBS-induced increase in striatal BDNF is independent of the M1 cortex. Indeed, when STN DBS is applied, BDNF mRNA is increased in the SNpc, and protein levels are increased in the striatum, unless there is a nigrostriatal lesion, in which case BDNF protein is increased in the SNpc; presumably because axonopathy induced by 6-OHDA prevents delivery of BDNF to the striatum [223]. Interestingly, cortical and striatal mRNA are not increased with STN DBS [223], further supporting the notion that STN DBS-induced increases in striatal BDNF protein are via SNpc production and release (Fig. 5.5C).

Figure 5.5D represents a possible schematic for the results we observe when STN DBS is applied to rats with inclusions in the nigrostriatal and corticostriatal system. When STN DBS is applied in conjunction with inclusions, nigrostriatal function is preserved enough to still drive increased BDNF release to the striatum. However, this increase may interfere with any compensatory increase in cortical BDNF production, resulting in a decrease in cortical BDNF (driven by inclusion-bearing neurons). In addition, high frequency stimulation of neurons can also cause dendritic release of BDNF [274], STN DBS may antidromically activate M1-STN circuitry to cause dendritic release of BDNF in the M1 cortex. Importantly, M1 neurons that innervate the striatum also innervate the STN [518], suggesting that M1-STN neurons responding to DBS may also have

inclusions. Thus, the presence of inclusions in some corticostriatal neurons may impact the ability of STN DBS to drive and increase in M1 BDNF.

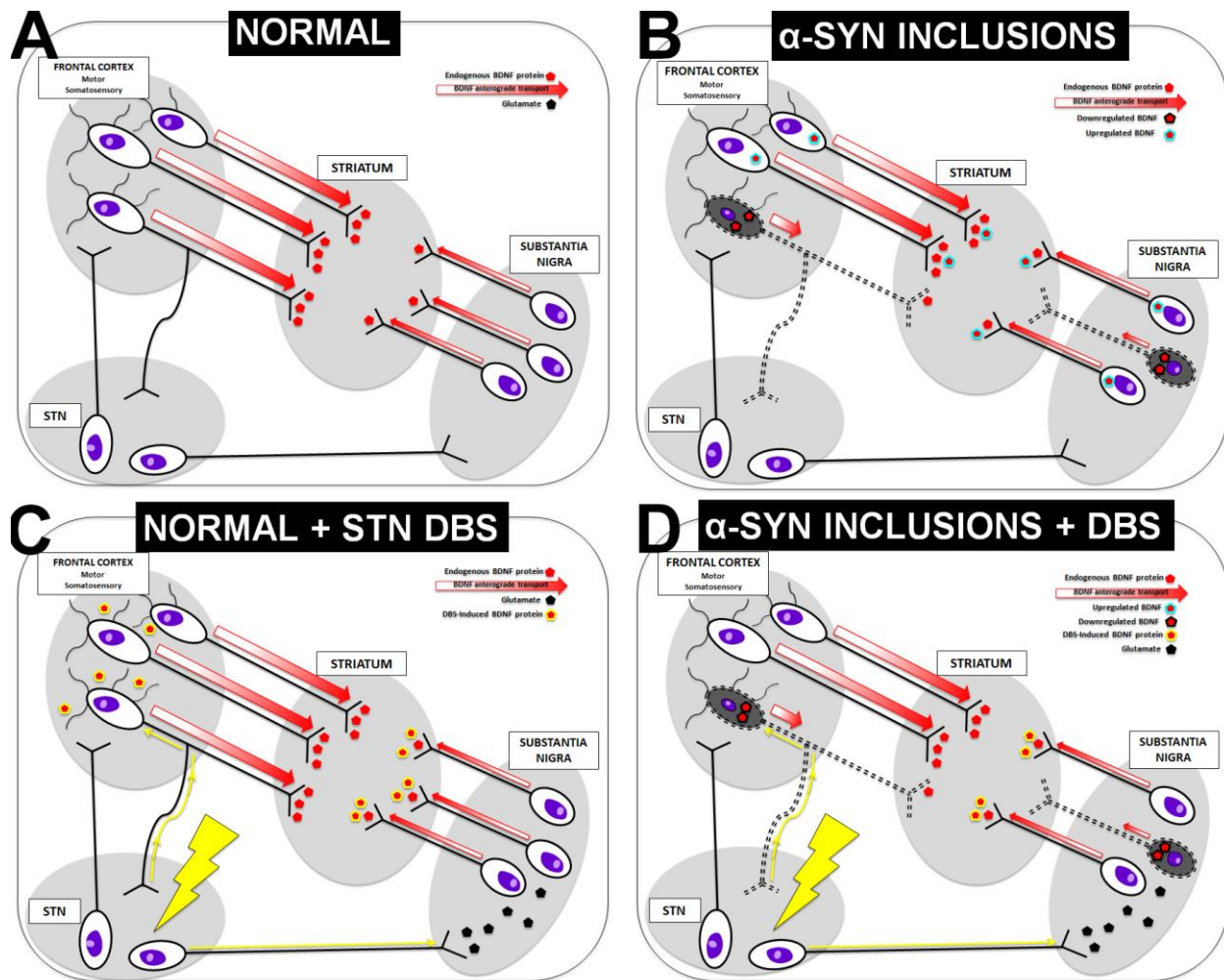


Figure 5.5: Schematic of possible mechanism

A. Under normal conditions the majority of striatal BDNF is produced and transported from the frontal cortex, with some also coming from the substantia nigra. Note that some of the layer V corticostriatal neurons also project to the STN [518]. **B.** α -syn inclusions in cortical and nigral neurons may result in decreased BDNF protein production and release, which may lead to a compensatory increase in production and release in neighboring, non-inclusion-bearing neurons. Layer V corticostriatal neurons that project to the STN are in the region of cortex that is typically seeded with inclusions, and therefore may have synuclein pathology [192]. **C.** STN DBS in a naïve animal

Figure 5.5 cont'd

results in increased BDNF protein in the cortex, substantia nigra, and striatum. Previous studies have shown that the striatal increase in BDNF is a result of increased release from the nigrostriatal system, rather than from the cortex. **D.** STN DBS applied to an inclusion-bearing rat still results in elevated striatal BDNF protein, presumably from nigrostriatal neurons that have not been compromised by α -syn inclusions, albeit to a lesser degree than reported in naïve rats. Cortical BDNF protein is decreased, perhaps as a result of decreased production (due to inclusions) and lack of compensation, as a result of the nigral-driven striatal increase in BDNF.

III. Summary

Taken together, this set of experiments add to the body of literature surrounding α -syn inclusions impacting normal physiology in the basal ganglia, and STN DBS showing potential to mitigate dysfunction. Specifically, inclusions prevent the normally positive association in BDNF protein levels in the nigrostriatal and corticostriatal circuits. Despite this, STN DBS was still able to induce striatal protein. While the mechanisms by which these phenomena are occurring are unclear given the current data, we speculate that anterograde transport of BDNF may be involved. While these findings are encouraging, in order to fully appreciate the disease-modifying potential of STN DBS in the rat PFF model, a long-term survival study must be conducted. Similarly, experiments directly measuring anterograde transport of BDNF in neurons with inclusions compared to those without are warranted. An in-depth discussion on the broader impacts and future directions of this chapter and those preceding it follows in Chapter 6.

Chapter 6: Conclusions and Future Directions

Conclusions

The present work has accomplished several goals. Chapter 1 provides an overview of the clinical and pathological aspects of Parkinson's disease (PD), current treatment strategies with an emphasis on deep brain stimulation (DBS) and brain-derived neurotrophic factor (BDNF), and the animal models used to study PD. Chapter 2 summarizes the literature surrounding synucleinopathy-associated pathogenesis, highlighting the insights derived from postmortem PD tissue and the *in vitro* α -syn pre-formed fibril (PFF) model, with a discussion on the neuroprotective potential of BDNF. Chapter 3 investigates the impact of DBS of the subthalamic nucleus (STN) on endogenous aggregation triggered by intrastriatal PFF injection. These studies revealed that STN DBS does not impact the number, size, or intensity of α -syn inclusions in the substantia nigra pars compacta (SNpc). Chapter 4 extends this work to evaluate the impact of STN DBS on inclusion-associated neuroinflammation in the SNpc, and found that neither markers of microglial (MHC-II) nor astrocytic (GFAP) activation were altered. Chapter 5 demonstrates that α -syn inclusions in the nigrostriatal and corticostriatal system alter the normally positive relationship in BDNF protein levels between those structures. However, despite this impact of α -syn inclusions, STN DBS is able to significantly increase striatal BDNF protein, suggesting that STN DBS applied early in disease progression may retain neuroprotective potential within the context of synucleinopathy. Collectively, these studies reinforce the therapeutic potential of STN DBS for Parkinson's disease. Importantly, these studies suggest that any symptomatic or disease modifying effects of STN DBS is unlikely to be the result of changes in

aggregation or neuroinflammation in the nigra, however could be related to increased BDNF expression.

There are many possible mechanisms by which BDNF could be neuroprotective in PD beyond preservation of nigrostriatal projections [494]. We now appreciate that prior to neurodegeneration, there is dysfunction at the terminals of nigral neurons, and mitigating this dysfunction is a promising disease-modifying approach to PD [497-500]. BDNF signaling increases dopamine release, tyrosine hydroxylase synthesis, dopamine turnover, and dopamine neuron activity, all of which are decreased in PD [80, 501-507]. This is supported by evidence that STN DBS alters dopaminergic neurotransmission [508], perhaps via increased BDNF signaling. Beyond nigrostriatal dopaminergic neurons, BDNF is critical in maintaining gamma aminobutyric acid-ergic (GABAergic) and glutamatergic synapses by facilitating long-term potentiation and plasticity [492, 509, 510]. In the striatum, BDNF helps maintain postsynaptic spine density [511], which is decreased in postmortem PD brains [512]. Collectively, these data present a strong argument for BDNF having the ability to mitigate cellular dysfunction in PD, prior to neurodegeneration.

Clinical Implications

Collectively, these findings present a strong argument in favor of BDNF as a therapeutic strategy to combat synucleinopathy-associated pathogenesis. This is important for several reasons: **1. STN DBS offers both therapeutic efficacy and neuroprotective potential.** It has already been established that STN DBS offers therapeutic benefits to

patients [130, 519, 520]. Thus, if STN DBS applied early in disease progression proves to be disease-modifying, as suggested [216, 298, 299], and increased BDNF is the mechanism, as shown in preclinical studies [223, 411], patients electing STN DBS could benefit two-fold. **2. BDNF as a target for disease modification.** BDNF may provide neuroprotection for neurons that degenerate in PD as well as positively impacting neurotransmitter synthesis, protecting spine density, or promoting motor cortex excitability. Therapeutic approaches could shift towards pharmacologically activating BDNF, avoiding the process of an involved brain surgery. However, *in vivo* data suggests that STN DBS provides symptomatic relief through mechanisms both dependent and independent of BDNF-TrkB [411], therefore pharmacologically targeting either BDNF or TrkB might not capture the full therapeutic potential that DBS offers. Moreover, STN DBS is targeted specifically to the basal ganglia circuitry and allows for appropriate physiological release of BDNF at the right time, by the right mechanisms, reducing off-target effects. **3. Broadening to other synucleinopathies.** Aberrant, α -syn inclusions are common among all synucleinopathies (Multiple System Atrophy, Lewy Body Dementia), and the pathology associated may have commonalities as well. Indeed, there is evidence suggesting that decreased trophic factor transport may be relevant to other synucleinopathies [521-524]. Understanding the mechanism responsible for inclusion-associated changes in BDNF protein could prove useful beyond PD.

Future Directions

I. Does STN DBS Spare SNpc Neurons from Degeneration?

While the finding that BDNF is increased in the striatum as a result of STN DBS is encouraging, we still have not determined whether this would result in neuroprotection of SNpc neurons. Conducting a long-term (6 month) continuous STN DBS study with outcome measures that include the quantification of THir and total neurons (HuC) in the SNpc is critical for understanding the neuroprotective potential of STN DBS in the context of synucleinopathy. Additionally, this work models an early intervention, prior to diagnosis. It is estimated that at the time of clinical diagnosis, there is already a 60% or more loss of striatal DA caused by a 50% loss of nigrostriatal dopamine neuron cell bodies [27, 28], thus STN DBS administered post diagnosis could yield different results.

II. Do Inclusions Interfere with Anterograde Transport of BDNF?

Another important follow-up study is to directly investigate the impact of α -syn inclusions on BDNF transport. Our findings in Chapter 5 suggest that anterograde transport from the cortex and nigra to the striatum may be impacted by inclusions, however we did not directly examine this mechanism. Using primary cultures and green fluorescent protein (GFP)-tagged BDNF, transport from the soma towards the axon terminal in both α -syn inclusion and non- α -syn inclusion bearing neurons could be visualized and quantified in real time. This experiment would provide data that would help support or refute the idea that inclusions decrease anterograde transport of BDNF.

III. Characterization of Cortical α -syn Inclusions and the Impact of STN DBS

Inclusions in our rat PFF model have been well-characterized in the SNpc. While we know that intrastriatal PFF injections result in widespread pSyn pathology [193], we

have not quantified the phenotype and number of inclusion-bearing neurons, or the pathological consequences of inclusions in the cortex. This is primarily due to a lack of a developed stereology protocol for specific cortical regions. For example, Chapters 3-4 and previous findings [193, 198] reveal that ~30% of nigral neurons have pSyn^{ir} inclusions, and ~50% of nigral neurons degenerate. Understanding the magnitude of cortical pSyn accumulation and whether there is associated neurodegeneration is a logical extension to this work. Developing a protocol to assess these outcome measures could help understand the non-nigrostriatal contributions to PD pathology and the effect of STN DBS.

IV. Neuroinflammation

Finally, Chapter 4 revealed that STN DBS had no impact on the number of MHC-II^{ir} microglia, or GFAP immunofluorescence intensity, and morphometric analysis of GFAP^{ir} astrocytic processes. However, while these specific neuroinflammatory markers were not impacted by STN DBS, they represent a limited analysis of potential neuroinflammatory effects of both α -syn inclusions and STN DBS. Future studies could undertake a more comprehensive investigation including other neuroinflammatory markers and could reveal differences missed in this initial study. Conducting a broader neuroinflammatory sweep could identify important α -syn inclusion associated and/or STN DBS-induced changes in glial functional phenotypes, or further support the idea that neuroinflammation is not involved in STN DBS-induced changes.

Final Remarks

This work has demonstrated that STN DBS increases BDNF in the context of nigrostriatal synucleinopathy. These experiments have provided a foundation for investigating the aspects of α -syn pathology that may be modulated by STN DBS. Specifically, aggregation and neuroinflammation do not seem to be impacted by stimulation. However, production and/or transport of BDNF may be impaired as a result of inclusions, and STN DBS might be able to partially restore these functions.

REFERENCES

REFERENCES

1. Parkinson, J., *An essay on the shaking palsy*. 1817. *J Neuropsychiatry Clin Neurosci*, 2002. **14**(2): p. 223-36; discussion 222.
2. Chen, J.J., *Parkinson's disease: health-related quality of life, economic cost, and implications of early treatment*. *Am J Manag Care*, 2010. **16 Suppl Implications**: p. S87-93.
3. Horn, S. and H. Hurtig, *The Many Faces of Parkinson's Disease*. Cerebrum, 2019. **2019**.
4. Hirtz, D., et al., *How common are the "common" neurologic disorders?* *Neurology*, 2007. **68**(5): p. 326-37.
5. Kowal, S.L., et al., *The current and projected economic burden of Parkinson's disease in the United States*. *Mov Disord*, 2013. **28**(3): p. 311-8.
6. Hirsch, L., et al., *The Incidence of Parkinson's Disease: A Systematic Review and Meta-Analysis*. *Neuroepidemiology*, 2016. **46**(4): p. 292-300.
7. Ishihara, L.S., et al., *Estimated life expectancy of Parkinson's patients compared with the UK population*. *J Neurol Neurosurg Psychiatry*, 2007. **78**(12): p. 1304-9.
8. Pahwa, R. and K.E. Lyons, *Early diagnosis of Parkinson's disease: recommendations from diagnostic clinical guidelines*. *Am J Manag Care*, 2010. **16 Suppl Implications**: p. S94-9.
9. Postuma, R.B., et al., *MDS clinical diagnostic criteria for Parkinson's disease*. *Mov Disord*, 2015. **30**(12): p. 1591-601.
10. Seifert, K.D. and J.I. Wiener, *The impact of DaTscan on the diagnosis and management of movement disorders: A retrospective study*. *Am J Neurodegener Dis*, 2013. **2**(1): p. 29-34.
11. Hughes, A.J., et al., *Accuracy of clinical diagnosis of idiopathic Parkinson's disease: a clinico-pathological study of 100 cases*. *J Neurol Neurosurg Psychiatry*, 1992. **55**(3): p. 181-4.
12. Marinus, J. and J.J. van Hilten, *The significance of motor (a)symmetry in Parkinson's disease*. *Mov Disord*, 2015. **30**(3): p. 379-85.
13. Nandhagopal, R., et al., *Longitudinal progression of sporadic Parkinson's disease: a multi-tracer positron emission tomography study*. *Brain*, 2009. **132**(Pt 11): p. 2970-9.

14. Gallagher, D.A., A.J. Lees, and A. Schrag, *What are the most important nonmotor symptoms in patients with Parkinson's disease and are we missing them?* *Mov Disord*, 2010. **25**(15): p. 2493-500.
15. Lyons, K.E. and R. Pahwa, *The impact and management of nonmotor symptoms of Parkinson's disease*. *Am J Manag Care*, 2011. **17 Suppl 12**: p. S308-14.
16. Biundo, R., L. Weis, and A. Antonini, *Cognitive decline in Parkinson's disease: the complex picture*. *NPJ Parkinsons Dis*, 2016. **2**: p. 16018.
17. Schwarz, J., et al., *Depression in Parkinson's disease*. *J Neurol*, 2011. **258**(Suppl 2): p. S336-8.
18. Soh, S.E., M.E. Morris, and J.L. McGinley, *Determinants of health-related quality of life in Parkinson's disease: a systematic review*. *Parkinsonism Relat Disord*, 2011. **17**(1): p. 1-9.
19. Alexander, G.E., M.R. DeLong, and P.L. Strick, *Parallel organization of functionally segregated circuits linking basal ganglia and cortex*. *Annu Rev Neurosci*, 1986. **9**: p. 357-81.
20. Fazl, A. and J. Fleisher, *Anatomy, Physiology, and Clinical Syndromes of the Basal Ganglia: A Brief Review*. *Semin Pediatr Neurol*, 2018. **25**: p. 2-9.
21. Bolam, J.P., et al., *Synaptic organisation of the basal ganglia*. *J Anat*, 2000. **196 (Pt 4)**: p. 527-42.
22. Redgrave, P., et al., *Goal-directed and habitual control in the basal ganglia: implications for Parkinson's disease*. *Nat Rev Neurosci*, 2010. **11**(11): p. 760-72.
23. Albin, R.L., A.B. Young, and J.B. Penney, *The functional anatomy of basal ganglia disorders*. *Trends Neurosci*, 1989. **12**(10): p. 366-75.
24. Lewis, S.J., M.A. Caldwell, and R.A. Barker, *Modern therapeutic approaches in Parkinson's disease*. *Expert Rev Mol Med*, 2003. **5**(10): p. 1-20.
25. Chevalier, G. and J.M. Deniau, *Disinhibition as a basic process in the expression of striatal functions*. *Trends Neurosci*, 1990. **13**(7): p. 277-80.
26. Shink, E., et al., *The subthalamic nucleus and the external pallidum: two tightly interconnected structures that control the output of the basal ganglia in the monkey*. *Neuroscience*, 1996. **73**(2): p. 335-57.
27. Kordower, J.H., et al., *Disease duration and the integrity of the nigrostriatal system in Parkinson's disease*. *Brain*, 2013. **136**(Pt 8): p. 2419-31.

28. Kurowska, Z., et al., *Is Axonal Degeneration a Key Early Event in Parkinson's Disease?* J Parkinsons Dis, 2016. **6**(4): p. 703-707.
29. Bernheimer, H., et al., *Brain dopamine and the syndromes of Parkinson and Huntington. Clinical, morphological and neurochemical correlations.* J Neurol Sci, 1973. **20**(4): p. 415-55.
30. Hornykiewicz, O., *Chemical neuroanatomy of the basal ganglia--normal and in Parkinson's disease.* J Chem Neuroanat, 2001. **22**(1-2): p. 3-12.
31. Agid, Y., *Parkinson's disease: pathophysiology.* Lancet, 1991. **337**(8753): p. 1321-4.
32. Gibb, W.R. and A.J. Lees, *Anatomy, pigmentation, ventral and dorsal subpopulations of the substantia nigra, and differential cell death in Parkinson's disease.* J Neurol Neurosurg Psychiatry, 1991. **54**(5): p. 388-96.
33. Shults, C.W., *Lewy bodies.* Proc Natl Acad Sci U S A, 2006. **103**(6): p. 1661-8.
34. Wakabayashi, K., et al., *The Lewy body in Parkinson's disease and related neurodegenerative disorders.* Mol Neurobiol, 2013. **47**(2): p. 495-508.
35. Chan, C.S., T.S. Gertler, and D.J. Surmeier, *A molecular basis for the increased vulnerability of substantia nigra dopamine neurons in aging and Parkinson's disease.* Mov Disord, 2010. **25 Suppl 1**: p. S63-70.
36. Hirsch, E., A.M. Graybiel, and Y.A. Agid, *Melanized dopaminergic neurons are differentially susceptible to degeneration in Parkinson's disease.* Nature, 1988. **334**(6180): p. 345-8.
37. Holdorff, B., *Friedrich Heinrich Lewy (1885-1950) and his work.* J Hist Neurosci, 2002. **11**(1): p. 19-28.
38. Spillantini, M.G., et al., *Alpha-synuclein in Lewy bodies.* Nature, 1997. **388**(6645): p. 839-40.
39. Braak, H., et al., *Staging of brain pathology related to sporadic Parkinson's disease.* Neurobiol Aging, 2003. **24**(2): p. 197-211.
40. Braak, H., et al., *Stages in the development of Parkinson's disease-related pathology.* Cell Tissue Res, 2004. **318**(1): p. 121-34.
41. Braak, H. and K. Del Tredici, *Neuroanatomy and pathology of sporadic Parkinson's disease.* Adv Anat Embryol Cell Biol, 2009. **201**: p. 1-119.

42. Steiner, J.A., E. Angot, and P. Brundin, *A deadly spread: cellular mechanisms of alpha-synuclein transfer*. *Cell Death Differ*, 2011. **18**(9): p. 1425-33.
43. Jellinger, K.A., *A critical reappraisal of current staging of Lewy-related pathology in human brain*. *Acta Neuropathol*, 2008. **116**(1): p. 1-16.
44. Kalaitzakis, M.E., et al., *The dorsal motor nucleus of the vagus is not an obligatory trigger site of Parkinson's disease: a critical analysis of alpha-synuclein staging*. *Neuropathol Appl Neurobiol*, 2008. **34**(3): p. 284-95.
45. Ohnmacht, J., et al., *Missing heritability in Parkinson's disease: the emerging role of non-coding genetic variation*. *J Neural Transm (Vienna)*, 2020.
46. Lill, C.M., *Genetics of Parkinson's disease*. *Mol Cell Probes*, 2016. **30**(6): p. 386-396.
47. Polymeropoulos, M.H., et al., *Mutation in the alpha-synuclein gene identified in families with Parkinson's disease*. *Science*, 1997. **276**(5321): p. 2045-7.
48. Chartier-Harlin, M.C., et al., *Alpha-synuclein locus duplication as a cause of familial Parkinson's disease*. *Lancet*, 2004. **364**(9440): p. 1167-9.
49. Ibanez, P., et al., *Causal relation between alpha-synuclein gene duplication and familial Parkinson's disease*. *Lancet*, 2004. **364**(9440): p. 1169-71.
50. Kruger, R., et al., *Ala30Pro mutation in the gene encoding alpha-synuclein in Parkinson's disease*. *Nat Genet*, 1998. **18**(2): p. 106-8.
51. Singleton, A.B., et al., *alpha-Synuclein locus triplication causes Parkinson's disease*. *Science*, 2003. **302**(5646): p. 841.
52. Zarranz, J.J., et al., *The new mutation, E46K, of alpha-synuclein causes Parkinson and Lewy body dementia*. *Ann Neurol*, 2004. **55**(2): p. 164-73.
53. Conway, K.A., J.D. Harper, and P.T. Lansbury, *Accelerated in vitro fibril formation by a mutant alpha-synuclein linked to early-onset Parkinson disease*. *Nat Med*, 1998. **4**(11): p. 1318-20.
54. Flagmeier, P., et al., *Mutations associated with familial Parkinson's disease alter the initiation and amplification steps of alpha-synuclein aggregation*. *Proc Natl Acad Sci U S A*, 2016. **113**(37): p. 10328-33.
55. Oliveira, L.M., et al., *Elevated alpha-synuclein caused by SNCA gene triplication impairs neuronal differentiation and maturation in Parkinson's patient-derived induced pluripotent stem cells*. *Cell Death Dis*, 2015. **6**: p. e1994.

56. Zimprich, A., et al., *Mutations in LRRK2 cause autosomal-dominant parkinsonism with pleomorphic pathology*. *Neuron*, 2004. **44**(4): p. 601-7.
57. Paisan-Ruiz, C., et al., *Cloning of the gene containing mutations that cause PARK8-linked Parkinson's disease*. *Neuron*, 2004. **44**(4): p. 595-600.
58. Blauwendraat, C., M.A. Nalls, and A.B. Singleton, *The genetic architecture of Parkinson's disease*. *Lancet Neurol*, 2020. **19**(2): p. 170-178.
59. Rahman, A.A. and B.E. Morrison, *Contributions of VPS35 Mutations to Parkinson's Disease*. *Neuroscience*, 2019. **401**: p. 1-10.
60. Gasser, T., J. Hardy, and Y. Mizuno, *Milestones in PD genetics*. *Mov Disord*, 2011. **26**(6): p. 1042-8.
61. Lees, A.J., J. Hardy, and T. Revesz, *Parkinson's disease*. *Lancet*, 2009. **373**(9680): p. 2055-66.
62. Giasson, B.I., et al., *Biochemical and pathological characterization of Lrrk2*. *Ann Neurol*, 2006. **59**(2): p. 315-22.
63. Ross, O.A., et al., *Lrrk2 and Lewy body disease*. *Ann Neurol*, 2006. **59**(2): p. 388-93.
64. Kitada, T., et al., *Mutations in the parkin gene cause autosomal recessive juvenile parkinsonism*. *Nature*, 1998. **392**(6676): p. 605-8.
65. Lucking, C.B., et al., *Association between early-onset Parkinson's disease and mutations in the parkin gene*. *N Engl J Med*, 2000. **342**(21): p. 1560-7.
66. Houlden, H. and A.B. Singleton, *The genetics and neuropathology of Parkinson's disease*. *Acta Neuropathol*, 2012. **124**(3): p. 325-38.
67. Trempe, J.F. and E.A. Fon, *Structure and Function of Parkin, PINK1, and DJ-1, the Three Musketeers of Neuroprotection*. *Front Neurol*, 2013. **4**: p. 38.
68. Shendelman, S., et al., *DJ-1 is a redox-dependent molecular chaperone that inhibits alpha-synuclein aggregate formation*. *PLoS Biol*, 2004. **2**(11): p. e362.
69. Steenland, K., et al., *Polychlorinated biphenyls and neurodegenerative disease mortality in an occupational cohort*. *Epidemiology*, 2006. **17**(1): p. 8-13.
70. Noyce, A.J., et al., *Meta-analysis of early nonmotor features and risk factors for Parkinson disease*. *Ann Neurol*, 2012. **72**(6): p. 893-901.

71. Mortimer, J.A., A.R. Borenstein, and L.M. Nelson, *Associations of welding and manganese exposure with Parkinson disease: review and meta-analysis*. *Neurology*, 2012. **79**(11): p. 1174-80.
72. Palin, O., et al., *Systematic review and meta-analysis of hydrocarbon exposure and the risk of Parkinson's disease*. *Parkinsonism Relat Disord*, 2015. **21**(3): p. 243-8.
73. Pezzoli, G. and E. Cereda, *Exposure to pesticides or solvents and risk of Parkinson disease*. *Neurology*, 2013. **80**(22): p. 2035-41.
74. Goldman, S.M., *Trichloroethylene and Parkinson's disease: dissolving the puzzle*. *Expert Rev Neurother*, 2010. **10**(6): p. 835-7.
75. Caudle, W.M., et al., *Industrial toxicants and Parkinson's disease*. *Neurotoxicology*, 2012. **33**(2): p. 178-88.
76. Cannon, J.R. and J.T. Greenamyre, *Gene-environment interactions in Parkinson's disease: specific evidence in humans and mammalian models*. *Neurobiol Dis*, 2013. **57**: p. 38-46.
77. Brown, T.P., et al., *Pesticides and Parkinson's disease--is there a link?* *Environ Health Perspect*, 2006. **114**(2): p. 156-64.
78. Maroteaux, L., J.T. Campanelli, and R.H. Scheller, *Synuclein: a neuron-specific protein localized to the nucleus and presynaptic nerve terminal*. *J Neurosci*, 1988. **8**(8): p. 2804-15.
79. Iwai, A., et al., *The precursor protein of non-A beta component of Alzheimer's disease amyloid is a presynaptic protein of the central nervous system*. *Neuron*, 1995. **14**(2): p. 467-75.
80. Benskey, M.J., R.G. Perez, and F.P. Manfredsson, *The contribution of alpha synuclein to neuronal survival and function - Implications for Parkinson's disease*. *J Neurochem*, 2016. **137**(3): p. 331-59.
81. Weinreb, P.H., et al., *NACP, a protein implicated in Alzheimer's disease and learning, is natively unfolded*. *Biochemistry*, 1996. **35**(43): p. 13709-15.
82. Bobela, W., P. Aebischer, and B.L. Schneider, *Alphalpa-Synuclein as a Mediator in the Interplay between Aging and Parkinson's Disease*. *Biomolecules*, 2015. **5**(4): p. 2675-700.
83. Sulzer, D., *Multiple hit hypotheses for dopamine neuron loss in Parkinson's disease*. *Trends Neurosci*, 2007. **30**(5): p. 244-50.

84. Collier, T.J., N.M. Kanaan, and J.H. Kordower, *Aging and Parkinson's disease: Different sides of the same coin?* *Mov Disord*, 2017. **32**(7): p. 983-990.
85. Collier, T.J., N.M. Kanaan, and J.H. Kordower, *Ageing as a primary risk factor for Parkinson's disease: evidence from studies of non-human primates.* *Nat Rev Neurosci*, 2011. **12**(6): p. 359-66.
86. Kanaan, N.M., J.H. Kordower, and T.J. Collier, *Age-related changes in glial cells of dopamine midbrain subregions in rhesus monkeys.* *Neurobiol Aging*, 2010. **31**(6): p. 937-52.
87. Bardou, I., et al., *Age and duration of inflammatory environment differentially affect the neuroimmune response and catecholaminergic neurons in the midbrain and brainstem.* *Neurobiol Aging*, 2014. **35**(5): p. 1065-73.
88. Collier, T.J., et al., *Aging-related changes in the nigrostriatal dopamine system and the response to MPTP in nonhuman primates: diminished compensatory mechanisms as a prelude to parkinsonism.* *Neurobiol Dis*, 2007. **26**(1): p. 56-65.
89. Ross, J.M., L. Olson, and G. Coppotelli, *Mitochondrial and Ubiquitin Proteasome System Dysfunction in Ageing and Disease: Two Sides of the Same Coin?* *Int J Mol Sci*, 2015. **16**(8): p. 19458-76.
90. Filiano, A.J., S.P. Gadani, and J. Kipnis, *Interactions of innate and adaptive immunity in brain development and function.* *Brain Res*, 2015. **1617**: p. 18-27.
91. Doorn, K.J., et al., *Brain region-specific gene expression profiles in freshly isolated rat microglia.* *Front Cell Neurosci*, 2015. **9**: p. 84.
92. De Biase, L.M., et al., *Local Cues Establish and Maintain Region-Specific Phenotypes of Basal Ganglia Microglia.* *Neuron*, 2017. **95**(2): p. 341-356 e6.
93. Kettenmann, H., et al., *Physiology of microglia.* *Physiol Rev*, 2011. **91**(2): p. 461-553.
94. Nimmerjahn, A., *Two-photon imaging of microglia in the mouse cortex in vivo.* *Cold Spring Harb Protoc*, 2012. **2012**(5).
95. Kim, S., et al., *Alpha-synuclein induces migration of BV-2 microglial cells by up-regulation of CD44 and MT1-MMP.* *J Neurochem*, 2009. **109**(5): p. 1483-96.
96. Wang, S., et al., *alpha-Synuclein, a chemoattractant, directs microglial migration via H2O2-dependent Lyn phosphorylation.* *Proc Natl Acad Sci U S A*, 2015. **112**(15): p. E1926-35.

97. Gunther, E. and L. Walter, *The major histocompatibility complex of the rat (Rattus norvegicus)*. Immunogenetics, 2001. **53**(7): p. 520-42.
98. Croisier, E., et al., *Microglial inflammation in the parkinsonian substantia nigra: relationship to alpha-synuclein deposition*. J Neuroinflammation, 2005. **2**: p. 14.
99. Imamura, K., et al., *Distribution of major histocompatibility complex class II-positive microglia and cytokine profile of Parkinson's disease brains*. Acta Neuropathol, 2003. **106**(6): p. 518-26.
100. McGeer, P.L., et al., *Reactive microglia are positive for HLA-DR in the substantia nigra of Parkinson's and Alzheimer's disease brains*. Neurology, 1988. **38**(8): p. 1285-91.
101. Gagne, J.J. and M.C. Power, *Anti-inflammatory drugs and risk of Parkinson disease: a meta-analysis*. Neurology, 2010. **74**(12): p. 995-1002.
102. Gao, H.M., et al., *Neuroinflammation and alpha-synuclein dysfunction potentiate each other, driving chronic progression of neurodegeneration in a mouse model of Parkinson's disease*. Environ Health Perspect, 2011. **119**(6): p. 807-14.
103. Doody, R.S., *We should not distinguish between symptomatic and disease-modifying treatments in Alzheimer's disease drug development*. Alzheimers Dement, 2008. **4**(1 Suppl 1): p. S21-5.
104. Morant, A.V., V. Jagalski, and H.T. Vestergaard, *Labeling of Disease-Modifying Therapies for Neurodegenerative Disorders*. Front Med (Lausanne), 2019. **6**: p. 223.
105. Cheng, H.C., C.M. Ulane, and R.E. Burke, *Clinical progression in Parkinson disease and the neurobiology of axons*. Ann Neurol, 2010. **67**(6): p. 715-25.
106. DeMaagd, G. and A. Philip, *Part 2: Introduction to the Pharmacotherapy of Parkinson's Disease, With a Focus on the Use of Dopaminergic Agents*. P T, 2015. **40**(9): p. 590-600.
107. Khor, S.P. and A. Hsu, *The pharmacokinetics and pharmacodynamics of levodopa in the treatment of Parkinson's disease*. Curr Clin Pharmacol, 2007. **2**(3): p. 234-43.
108. Zhang, J. and L.C. Tan, *Revisiting the Medical Management of Parkinson's Disease: Levodopa versus Dopamine Agonist*. Curr Neuropharmacol, 2016. **14**(4): p. 356-63.
109. LeWitt, P.A., *Levodopa therapy for Parkinson's disease: Pharmacokinetics and pharmacodynamics*. Mov Disord, 2015. **30**(1): p. 64-72.

110. Prashanth, L.K., S. Fox, and W.G. Meissner, *L-Dopa-induced dyskinesia-clinical presentation, genetics, and treatment*. *Int Rev Neurobiol*, 2011. **98**: p. 31-54.
111. Porras, G., et al., *L-dopa-induced dyskinesia: beyond an excessive dopamine tone in the striatum*. *Sci Rep*, 2014. **4**: p. 3730.
112. Parashos, S.A., et al., *Measuring disease progression in early Parkinson disease: the National Institutes of Health Exploratory Trials in Parkinson Disease (NET-PD) experience*. *JAMA Neurol*, 2014. **71**(6): p. 710-6.
113. Weintraub, D., et al., *Impulse control disorders in Parkinson disease: a cross-sectional study of 3090 patients*. *Arch Neurol*, 2010. **67**(5): p. 589-95.
114. Etminan, M., et al., *Risk of Gambling Disorder and Impulse Control Disorder With Aripiprazole, Pramipexole, and Ropinirole: A Pharmacoepidemiologic Study*. *J Clin Psychopharmacol*, 2017. **37**(1): p. 102-104.
115. Schrag, A. and N. Quinn, *Dyskinesias and motor fluctuations in Parkinson's disease. A community-based study*. *Brain*, 2000. **123 (Pt 11)**: p. 2297-305.
116. Hely, M.A., et al., *The sydney multicentre study of Parkinson's disease: progression and mortality at 10 years*. *J Neurol Neurosurg Psychiatry*, 1999. **67**(3): p. 300-7.
117. Pahwa, R., et al., *Practice Parameter: treatment of Parkinson disease with motor fluctuations and dyskinesia (an evidence-based review): report of the Quality Standards Subcommittee of the American Academy of Neurology*. *Neurology*, 2006. **66**(7): p. 983-95.
118. Collins, K.L., E.M. Lehmann, and P.G. Patil, *Deep brain stimulation for movement disorders*. *Neurobiol Dis*, 2010. **38**(3): p. 338-45.
119. Larson, P.S., *Deep brain stimulation for movement disorders*. *Neurotherapeutics*, 2014. **11**(3): p. 465-74.
120. Wagle Shukla, A. and M.S. Okun, *Surgical treatment of Parkinson's disease: patients, targets, devices, and approaches*. *Neurotherapeutics*, 2014. **11**(1): p. 47-59.
121. Graat, I., M. Figeet, and D. Denys, *The application of deep brain stimulation in the treatment of psychiatric disorders*. *Int Rev Psychiatry*, 2017. **29**(2): p. 178-190.
122. Limousin, P. and I. Martinez-Torres, *Deep brain stimulation for Parkinson's disease*. *Neurotherapeutics*, 2008. **5**(2): p. 309-19.

123. Chang, V.C. and K.L. Chou, *Deep brain stimulation for Parkinson's disease: patient selection and motor outcomes*. Med Health R I, 2006. **89**(4): p. 142-4.
124. Espay, A.J., G.T. Mandybur, and F.J. Revilla, *Surgical treatment of movement disorders*. Clin Geriatr Med, 2006. **22**(4): p. 813-25, vi.
125. Neimat, J.S., C. Hamani, and A.M. Lozano, *Neural stimulation for Parkinson's disease: current therapies and future directions*. Expert Rev Neurother, 2006. **6**(1): p. 101-9.
126. Volkmann, J., *Deep brain stimulation for the treatment of Parkinson's disease*. J Clin Neurophysiol, 2004. **21**(1): p. 6-17.
127. Angeli, A., et al., *Genotype and phenotype in Parkinson's disease: lessons in heterogeneity from deep brain stimulation*. Mov Disord, 2013. **28**(10): p. 1370-5.
128. Rezai, A.R., et al., *Surgery for movement disorders*. Neurosurgery, 2008. **62 Suppl 2**: p. 809-38; discussion 838-9.
129. Shih, L.C. and D. Tarsy, *Deep brain stimulation for the treatment of atypical parkinsonism*. Mov Disord, 2007. **22**(15): p. 2149-55.
130. Okun, M.S. and K.D. Foote, *Parkinson's disease DBS: what, when, who and why? The time has come to tailor DBS targets*. Expert Rev Neurother, 2010. **10**(12): p. 1847-57.
131. Follett, K.A., et al., *Pallidal versus subthalamic deep-brain stimulation for Parkinson's disease*. N Engl J Med, 2010. **362**(22): p. 2077-91.
132. Krack, P., et al., *Five-year follow-up of bilateral stimulation of the subthalamic nucleus in advanced Parkinson's disease*. N Engl J Med, 2003. **349**(20): p. 1925-34.
133. Herzog, E.D. and R.M. Huckfeldt, *Circadian entrainment to temperature, but not light, in the isolated suprachiasmatic nucleus*. J Neurophysiol, 2003. **90**(2): p. 763-70.
134. Rodriguez-Oroz, M.C., et al., *Efficacy of deep brain stimulation of the subthalamic nucleus in Parkinson's disease 4 years after surgery: double blind and open label evaluation*. J Neurol Neurosurg Psychiatry, 2004. **75**(10): p. 1382-5.
135. Schupbach, W.M., et al., *Stimulation of the subthalamic nucleus in Parkinson's disease: a 5 year follow up*. J Neurol Neurosurg Psychiatry, 2005. **76**(12): p. 1640-4.

136. Ostergaard, K. and N. Aa Sunde, *Evolution of Parkinson's disease during 4 years of bilateral deep brain stimulation of the subthalamic nucleus*. *Mov Disord*, 2006. **21**(5): p. 624-31.
137. Deuschl, G., et al., *A randomized trial of deep-brain stimulation for Parkinson's disease*. *N Engl J Med*, 2006. **355**(9): p. 896-908.
138. Charles, P.D., et al., *Deep brain stimulation of the subthalamic nucleus reduces antiparkinsonian medication costs*. *Parkinsonism Relat Disord*, 2004. **10**(8): p. 475-9.
139. Meissner, W., et al., *Deep brain stimulation in late stage Parkinson's disease: a retrospective cost analysis in Germany*. *J Neurol*, 2005. **252**(2): p. 218-23.
140. Martinez-Martin, P. and G. Deuschl, *Effect of medical and surgical interventions on health-related quality of life in Parkinson's disease*. *Mov Disord*, 2007. **22**(6): p. 757-65.
141. Mow, S.J., et al., *Effects of STN and GPi deep brain stimulation on impulse control disorders and dopamine dysregulation syndrome*. *PLoS One*, 2012. **7**(1): p. e29768.
142. Bronstein, J.M., et al., *Deep brain stimulation for Parkinson disease: an expert consensus and review of key issues*. *Arch Neurol*, 2011. **68**(2): p. 165.
143. Moro, E., et al., *Long-term results of a multicenter study on subthalamic and pallidal stimulation in Parkinson's disease*. *Mov Disord*, 2010. **25**(5): p. 578-86.
144. Andrade, P., J.D. Carrillo-Ruiz, and F. Jimenez, *A systematic review of the efficacy of globus pallidus stimulation in the treatment of Parkinson's disease*. *J Clin Neurosci*, 2009. **16**(7): p. 877-81.
145. Zheng, F., et al., *Axonal failure during high frequency stimulation of rat subthalamic nucleus*. *J Physiol*, 2011. **589**(Pt 11): p. 2781-93.
146. Garcia, L., et al., *Dual effect of high-frequency stimulation on subthalamic neuron activity*. *J Neurosci*, 2003. **23**(25): p. 8743-51.
147. Shi, L.H., et al., *Basal ganglia neural responses during behaviorally effective deep brain stimulation of the subthalamic nucleus in rats performing a treadmill locomotion test*. *Synapse*, 2006. **59**(7): p. 445-57.
148. Brown, P., et al., *Effects of stimulation of the subthalamic area on oscillatory pallidal activity in Parkinson's disease*. *Exp Neurol*, 2004. **188**(2): p. 480-90.

149. Meissner, W., et al., *Subthalamic high frequency stimulation resets subthalamic firing and reduces abnormal oscillations*. Brain, 2005. **128**(Pt 10): p. 2372-82.
150. Silberstein, P., et al., *Cortico-cortical coupling in Parkinson's disease and its modulation by therapy*. Brain, 2005. **128**(Pt 6): p. 1277-91.
151. Wingeier, B., et al., *Intra-operative STN DBS attenuates the prominent beta rhythm in the STN in Parkinson's disease*. Exp Neurol, 2006. **197**(1): p. 244-51.
152. Bronte-Stewart, H., et al., *The STN beta-band profile in Parkinson's disease is stationary and shows prolonged attenuation after deep brain stimulation*. Exp Neurol, 2009. **215**(1): p. 20-8.
153. Blumenfeld, Z., et al., *Sixty hertz neurostimulation amplifies subthalamic neural synchrony in Parkinson's disease*. PLoS One, 2015. **10**(3): p. e0121067.
154. Bove, J., et al., *Toxin-induced models of Parkinson's disease*. NeuroRx, 2005. **2**(3): p. 484-94.
155. Ungerstedt, U. and G.W. Arbuthnott, *Quantitative recording of rotational behavior in rats after 6-hydroxy-dopamine lesions of the nigrostriatal dopamine system*. Brain Res, 1970. **24**(3): p. 485-93.
156. Simola, N., M. Morelli, and A.R. Carta, *The 6-hydroxydopamine model of Parkinson's disease*. Neurotox Res, 2007. **11**(3-4): p. 151-67.
157. Cohen, G., *Oxy-radical toxicity in catecholamine neurons*. Neurotoxicology, 1984. **5**(1): p. 77-82.
158. Spieles-Engemann, A.L., et al., *Stimulation of the rat subthalamic nucleus is neuroprotective following significant nigral dopamine neuron loss*. Neurobiol Dis, 2010. **39**(1): p. 105-15.
159. Langston, J.W., *The MPTP Story*. J Parkinsons Dis, 2017. **7**(s1): p. S11-S19.
160. Lewin, R., *Trail of ironies to Parkinson's disease*. Science, 1984. **224**(4653): p. 1083-5.
161. Ballard, P.A., J.W. Tetrad, and J.W. Langston, *Permanent human parkinsonism due to 1-methyl-4-phenyl-1,2,3,6-tetrahydropyridine (MPTP): seven cases*. Neurology, 1985. **35**(7): p. 949-56.
162. Langston, J.W. and P.A. Ballard, Jr., *Parkinson's disease in a chemist working with 1-methyl-4-phenyl-1,2,5,6-tetrahydropyridine*. N Engl J Med, 1983. **309**(5): p. 310.

163. Burns, R.S., et al., *The neurotoxicity of 1-methyl-4-phenyl-1,2,3,6-tetrahydropyridine in the monkey and man*. Can J Neurol Sci, 1984. **11**(1 Suppl): p. 166-8.
164. Langston, J.W., E.B. Langston, and I. Irwin, *MPTP-induced parkinsonism in human and non-human primates--clinical and experimental aspects*. Acta Neurol Scand Suppl, 1984. **100**: p. 49-54.
165. Riachi, N.J., J.C. LaManna, and S.I. Harik, *Entry of 1-methyl-4-phenyl-1,2,3,6-tetrahydropyridine into the rat brain*. J Pharmacol Exp Ther, 1989. **249**(3): p. 744-8.
166. Przedborski, S., et al., *The parkinsonian toxin MPTP: action and mechanism*. Restor Neurol Neurosci, 2000. **16**(2): p. 135-142.
167. Jackson-Lewis, V. and S. Przedborski, *Protocol for the MPTP mouse model of Parkinson's disease*. Nat Protoc, 2007. **2**(1): p. 141-51.
168. Meredith, G.E. and D.J. Rademacher, *MPTP mouse models of Parkinson's disease: an update*. J Parkinsons Dis, 2011. **1**(1): p. 19-33.
169. Betarbet, R., et al., *Chronic systemic pesticide exposure reproduces features of Parkinson's disease*. Nat Neurosci, 2000. **3**(12): p. 1301-6.
170. Day, B.J., et al., *A mechanism of paraquat toxicity involving nitric oxide synthase*. Proc Natl Acad Sci U S A, 1999. **96**(22): p. 12760-5.
171. Gao, H.M., B. Liu, and J.S. Hong, *Critical role for microglial NADPH oxidase in rotenone-induced degeneration of dopaminergic neurons*. J Neurosci, 2003. **23**(15): p. 6181-7.
172. Wu, F., et al., *Rotenone impairs autophagic flux and lysosomal functions in Parkinson's disease*. Neuroscience, 2015. **284**: p. 900-11.
173. Brooks, A.I., et al., *Paraquat elicited neurobehavioral syndrome caused by dopaminergic neuron loss*. Brain Res, 1999. **823**(1-2): p. 1-10.
174. McCormack, A.L., et al., *Environmental risk factors and Parkinson's disease: selective degeneration of nigral dopaminergic neurons caused by the herbicide paraquat*. Neurobiol Dis, 2002. **10**(2): p. 119-27.
175. van der Putten, H., et al., *Neuropathology in mice expressing human alpha-synuclein*. J Neurosci, 2000. **20**(16): p. 6021-9.

176. Giasson, B.I., et al., *Neuronal alpha-synucleinopathy with severe movement disorder in mice expressing A53T human alpha-synuclein*. *Neuron*, 2002. **34**(4): p. 521-33.
177. Gispert, S., et al., *Transgenic mice expressing mutant A53T human alpha-synuclein show neuronal dysfunction in the absence of aggregate formation*. *Mol Cell Neurosci*, 2003. **24**(2): p. 419-29.
178. Gomez-Isla, T., et al., *Motor dysfunction and gliosis with preserved dopaminergic markers in human alpha-synuclein A30P transgenic mice*. *Neurobiol Aging*, 2003. **24**(2): p. 245-58.
179. Lo Bianco, C., et al., *alpha-Synucleinopathy and selective dopaminergic neuron loss in a rat lentiviral-based model of Parkinson's disease*. *Proc Natl Acad Sci U S A*, 2002. **99**(16): p. 10813-8.
180. Kirik, D., et al., *Parkinson-like neurodegeneration induced by targeted overexpression of alpha-synuclein in the nigrostriatal system*. *J Neurosci*, 2002. **22**(7): p. 2780-91.
181. Klein, R.L., et al., *Dopaminergic cell loss induced by human A30P alpha-synuclein gene transfer to the rat substantia nigra*. *Hum Gene Ther*, 2002. **13**(5): p. 605-12.
182. Chung, C.Y., et al., *Dynamic changes in presynaptic and axonal transport proteins combined with striatal neuroinflammation precede dopaminergic neuronal loss in a rat model of AAV alpha-synucleinopathy*. *J Neurosci*, 2009. **29**(11): p. 3365-73.
183. Lundblad, M., et al., *Impaired neurotransmission caused by overexpression of alpha-synuclein in nigral dopamine neurons*. *Proc Natl Acad Sci U S A*, 2012. **109**(9): p. 3213-9.
184. Yamada, M., et al., *Overexpression of alpha-synuclein in rat substantia nigra results in loss of dopaminergic neurons, phosphorylation of alpha-synuclein and activation of caspase-9: resemblance to pathogenetic changes in Parkinson's disease*. *J Neurochem*, 2004. **91**(2): p. 451-61.
185. Decressac, M., et al., *Progressive neurodegenerative and behavioural changes induced by AAV-mediated overexpression of alpha-synuclein in midbrain dopamine neurons*. *Neurobiol Dis*, 2012. **45**(3): p. 939-53.
186. Sanchez-Guajardo, V., et al., *Neuroimmunological processes in Parkinson's disease and their relation to alpha-synuclein: microglia as the referee between neuronal processes and peripheral immunity*. *ASN Neuro*, 2013. **5**(2): p. 113-39.

187. Sanchez-Guajardo, V., et al., *Microglia acquire distinct activation profiles depending on the degree of alpha-synuclein neuropathology in a rAAV based model of Parkinson's disease*. PLoS One, 2010. **5**(1): p. e8784.
188. Theodore, S., et al., *Targeted overexpression of human alpha-synuclein triggers microglial activation and an adaptive immune response in a mouse model of Parkinson disease*. J Neuropathol Exp Neurol, 2008. **67**(12): p. 1149-58.
189. Su, X., et al., *Alpha-Synuclein mRNA Is Not Increased in Sporadic PD and Alpha-Synuclein Accumulation Does Not Block GDNF Signaling in Parkinson's Disease and Disease Models*. Mol Ther, 2017. **25**(10): p. 2231-2235.
190. Luk, K.C., et al., *Exogenous alpha-synuclein fibrils seed the formation of Lewy body-like intracellular inclusions in cultured cells*. Proc Natl Acad Sci U S A, 2009. **106**(47): p. 20051-6.
191. Luk, K.C., et al., *Pathological alpha-synuclein transmission initiates Parkinson-like neurodegeneration in nontransgenic mice*. Science, 2012. **338**(6109): p. 949-53.
192. Paumier, K.L., et al., *Intrastriatal injection of pre-formed mouse alpha-synuclein fibrils into rats triggers alpha-synuclein pathology and bilateral nigrostriatal degeneration*. Neurobiol Dis, 2015. **82**: p. 185-199.
193. Patterson, J.R., et al., *Time course and magnitude of alpha-synuclein inclusion formation and nigrostriatal degeneration in the rat model of synucleinopathy triggered by intrastriatal alpha-synuclein preformed fibrils*. Neurobiol Dis, 2019. **130**: p. 104525.
194. Patterson, J.R., et al., *Generation of Alpha-Synuclein Preformed Fibrils from Monomers and Use In Vivo*. J Vis Exp, 2019(148).
195. Volpicelli-Daley, L.A., K.C. Luk, and V.M. Lee, *Addition of exogenous alpha-synuclein preformed fibrils to primary neuronal cultures to seed recruitment of endogenous alpha-synuclein to Lewy body and Lewy neurite-like aggregates*. Nat Protoc, 2014. **9**(9): p. 2135-46.
196. Volpicelli-Daley, L.A., et al., *Exogenous alpha-synuclein fibrils induce Lewy body pathology leading to synaptic dysfunction and neuron death*. Neuron, 2011. **72**(1): p. 57-71.
197. Mahul-Mellier, A.L., et al., *The process of Lewy body formation, rather than simply alpha-synuclein fibrillization, is one of the major drivers of neurodegeneration*. Proc Natl Acad Sci U S A, 2020. **117**(9): p. 4971-4982.

198. Duffy, M.F., et al., *Lewy body-like alpha-synuclein inclusions trigger reactive microgliosis prior to nigral degeneration*. J Neuroinflammation, 2018. **15**(1): p. 129.
199. Mogi, M., et al., *Interleukin-1 beta, interleukin-6, epidermal growth factor and transforming growth factor-alpha are elevated in the brain from parkinsonian patients*. Neurosci Lett, 1994. **180**(2): p. 147-50.
200. Mogi, M., et al., *Tumor necrosis factor-alpha (TNF-alpha) increases both in the brain and in the cerebrospinal fluid from parkinsonian patients*. Neurosci Lett, 1994. **165**(1-2): p. 208-10.
201. McGeer, P.L., S. Itagaki, and E.G. McGeer, *Expression of the histocompatibility glycoprotein HLA-DR in neurological disease*. Acta Neuropathol, 1988. **76**(6): p. 550-7.
202. Gerhard, A., et al., *In vivo imaging of microglial activation with [11C](R)-PK11195 PET in idiopathic Parkinson's disease*. Neurobiol Dis, 2006. **21**(2): p. 404-12.
203. Doorn, K.J., et al., *Microglial phenotypes and toll-like receptor 2 in the substantia nigra and hippocampus of incidental Lewy body disease cases and Parkinson's disease patients*. Acta Neuropathol Commun, 2014. **2**: p. 90.
204. Rodrigues, R.W., V.C. Gomide, and G. Chadi, *Astroglial and microglial reaction after a partial nigrostriatal degeneration induced by the striatal injection of different doses of 6-hydroxydopamine*. Int J Neurosci, 2001. **109**(1-2): p. 91-126.
205. Cicchetti, F., et al., *Neuroinflammation of the nigrostriatal pathway during progressive 6-OHDA dopamine degeneration in rats monitored by immunohistochemistry and PET imaging*. Eur J Neurosci, 2002. **15**(6): p. 991-8.
206. Na, S.J., et al., *Molecular profiling of a 6-hydroxydopamine model of Parkinson's disease*. Neurochem Res, 2010. **35**(5): p. 761-72.
207. Duffy, M.F., et al., *Quality Over Quantity: Advantages of Using Alpha-Synuclein Preformed Fibril Triggered Synucleinopathy to Model Idiopathic Parkinson's Disease*. Front Neurosci, 2018. **12**: p. 621.
208. Ceballos-Baumann, A.O., et al., *A positron emission tomographic study of subthalamic nucleus stimulation in Parkinson disease: enhanced movement-related activity of motor-association cortex and decreased motor cortex resting activity*. Arch Neurol, 1999. **56**(8): p. 997-1003.
209. Hershey, T., et al., *Cortical and subcortical blood flow effects of subthalamic nucleus stimulation in PD*. Neurology, 2003. **61**(6): p. 816-21.

210. Windels, F., et al., *Effects of high frequency stimulation of subthalamic nucleus on extracellular glutamate and GABA in substantia nigra and globus pallidus in the normal rat*. Eur J Neurosci, 2000. **12**(11): p. 4141-6.
211. Boulet, S., et al., *Subthalamic stimulation-induced forelimb dyskinesias are linked to an increase in glutamate levels in the substantia nigra pars reticulata*. J Neurosci, 2006. **26**(42): p. 10768-76.
212. Krack, P., et al., *Subthalamic nucleus or internal pallidal stimulation in young onset Parkinson's disease*. Brain, 1998. **121 (Pt 3)**: p. 451-7.
213. Rodriguez-Oroz, M.C., et al., *Bilateral deep brain stimulation in Parkinson's disease: a multicentre study with 4 years follow-up*. Brain, 2005. **128**(Pt 10): p. 2240-9.
214. Tagliati, M., C. Martin, and R. Alterman, *Lack of motor symptoms progression in Parkinson's disease patients with long-term bilateral subthalamic deep brain stimulation*. Int J Neurosci, 2010. **120**(11): p. 717-23.
215. Charles, D., et al., *Subthalamic nucleus deep brain stimulation in early stage Parkinson's disease*. Parkinsonism Relat Disord, 2014. **20**(7): p. 731-7.
216. Hacker, M.L., et al., *Effects of deep brain stimulation on rest tremor progression in early stage Parkinson disease*. Neurology, 2018. **91**(5): p. e463-e471.
217. Maesawa, S., et al., *Long-term stimulation of the subthalamic nucleus in hemiparkinsonian rats: neuroprotection of dopaminergic neurons*. J Neurosurg, 2004. **100**(4): p. 679-87.
218. Temel, Y., et al., *Protection of nigral cell death by bilateral subthalamic nucleus stimulation*. Brain Res, 2006. **1120**(1): p. 100-5.
219. Harnack, D., et al., *Placebo-controlled chronic high-frequency stimulation of the subthalamic nucleus preserves dopaminergic nigral neurons in a rat model of progressive Parkinsonism*. Exp Neurol, 2008. **210**(1): p. 257-60.
220. Wallace, B.A., et al., *Survival of midbrain dopaminergic cells after lesion or deep brain stimulation of the subthalamic nucleus in MPTP-treated monkeys*. Brain, 2007. **130**(Pt 8): p. 2129-45.
221. Musacchio, T., et al., *Subthalamic nucleus deep brain stimulation is neuroprotective in the A53T alpha-synuclein Parkinson's disease rat model*. Ann Neurol, 2017. **81**(6): p. 825-836.

222. Fischer, D.L., et al., *Subthalamic Nucleus Deep Brain Stimulation Does Not Modify the Functional Deficits or Axonopathy Induced by Nigrostriatal alpha-Synuclein Overexpression*. Sci Rep, 2017. **7**(1): p. 16356.
223. Spieles-Engemann, A.L., et al., *Subthalamic nucleus stimulation increases brain derived neurotrophic factor in the nigrostriatal system and primary motor cortex*. J Parkinsons Dis, 2011. **1**(1): p. 123-36.
224. Friedman, A., et al., *Programmed acute electrical stimulation of ventral tegmental area alleviates depressive-like behavior*. Neuropsychopharmacology, 2009. **34**(4): p. 1057-66.
225. Hamani, C., et al., *Deep brain stimulation reverses anhedonic-like behavior in a chronic model of depression: role of serotonin and brain derived neurotrophic factor*. Biol Psychiatry, 2012. **71**(1): p. 30-5.
226. Gersner, R., et al., *Site-specific antidepressant effects of repeated subconvulsive electrical stimulation: potential role of brain-derived neurotrophic factor*. Biol Psychiatry, 2010. **67**(2): p. 125-32.
227. Lang, A.E., et al., *Randomized controlled trial of intraputamenal glial cell line-derived neurotrophic factor infusion in Parkinson disease*. Ann Neurol, 2006. **59**(3): p. 459-66.
228. Whone, A., et al., *Randomized trial of intermittent intraputamenal glial cell line-derived neurotrophic factor in Parkinson's disease*. Brain, 2019. **142**(3): p. 512-525.
229. Warren Olanow, C., et al., *Gene delivery of neurturin to putamen and substantia nigra in Parkinson disease: A double-blind, randomized, controlled trial*. Ann Neurol, 2015. **78**(2): p. 248-57.
230. Bartus, R.T., et al., *Post-mortem assessment of the short and long-term effects of the trophic factor neurturin in patients with α -synucleinopathies*. Neurobiol Dis, 2015. **78**: p. 162-71.
231. Marks, W.J., et al., *Gene delivery of AAV2-neurturin for Parkinson's disease: a double-blind, randomised, controlled trial*. Lancet Neurol, 2010. **9**(12): p. 1164-1172.
232. Paul, G. and A.M. Sullivan, *Trophic factors for Parkinson's disease: Where are we and where do we go from here?* Eur J Neurosci, 2019. **49**(4): p. 440-452.
233. Leibrock, J., et al., *Molecular cloning and expression of brain-derived neurotrophic factor*. Nature, 1989. **341**(6238): p. 149-52.

234. Levi-Montalcini, R. and B. Booker, *Destruction of the Sympathetic Ganglia in Mammals by an Antiserum to a Nerve-Growth Protein*. Proc Natl Acad Sci U S A, 1960. **46**(3): p. 384-91.
235. Crowley, C., et al., *Mice lacking nerve growth factor display perinatal loss of sensory and sympathetic neurons yet develop basal forebrain cholinergic neurons*. Cell, 1994. **76**(6): p. 1001-11.
236. Oppenheim, R.W., *Pathways in the emergence of developmental neuroethology: antecedents to current views of neurobehavioral ontogeny*. J Neurobiol, 1992. **23**(10): p. 1370-403.
237. Ernfors, P., K.F. Lee, and R. Jaenisch, *Mice lacking brain-derived neurotrophic factor develop with sensory deficits*. Nature, 1994. **368**(6467): p. 147-50.
238. Ernfors, P., et al., *Complementary roles of BDNF and NT-3 in vestibular and auditory development*. Neuron, 1995. **14**(6): p. 1153-64.
239. Wetmore, C., et al., *Localization of brain-derived neurotrophic factor mRNA to neurons in the brain by in situ hybridization*. Exp Neurol, 1990. **109**(2): p. 141-52.
240. Hofer, M., et al., *Regional distribution of brain-derived neurotrophic factor mRNA in the adult mouse brain*. EMBO J, 1990. **9**(8): p. 2459-64.
241. Yamamoto, H. and M.E. Gurney, *Human platelets contain brain-derived neurotrophic factor*. J Neurosci, 1990. **10**(11): p. 3469-78.
242. Acheson, A., et al., *Detection of brain-derived neurotrophic factor-like activity in fibroblasts and Schwann cells: inhibition by antibodies to NGF*. Neuron, 1991. **7**(2): p. 265-75.
243. Seroogy, K.B. and C.M. Gall, *Expression of neurotrophins by midbrain dopaminergic neurons*. Exp Neurol, 1993. **124**(1): p. 119-28.
244. Lessmann, V., K. Gottmann, and M. Malcangio, *Neurotrophin secretion: current facts and future prospects*. Prog Neurobiol, 2003. **69**(5): p. 341-74.
245. Yang, J., et al., *Neuronal release of proBDNF*. Nat Neurosci, 2009. **12**(2): p. 113-5.
246. Mowla, S.J., et al., *Biosynthesis and post-translational processing of the precursor to brain-derived neurotrophic factor*. J Biol Chem, 2001. **276**(16): p. 12660-6.
247. Teng, H.K., et al., *ProBDNF induces neuronal apoptosis via activation of a receptor complex of p75NTR and sortilin*. J Neurosci, 2005. **25**(22): p. 5455-63.

248. Pang, P.T., et al., *Cleavage of proBDNF by tPA/plasmin is essential for long-term hippocampal plasticity*. Science, 2004. **306**(5695): p. 487-91.
249. Sasi, M., et al., *Neurobiology of local and intercellular BDNF signaling*. Pflugers Arch, 2017. **469**(5-6): p. 593-610.
250. Barde, Y.A., D. Edgar, and H. Thoenen, *Purification of a new neurotrophic factor from mammalian brain*. EMBO J, 1982. **1**(5): p. 549-53.
251. Balkowiec, A. and D.M. Katz, *Activity-dependent release of endogenous brain-derived neurotrophic factor from primary sensory neurons detected by ELISA in situ*. J Neurosci, 2000. **20**(19): p. 7417-23.
252. Martínez-Levy, G.A. and C.S. Cruz-Fuentes, *Genetic and epigenetic regulation of the brain-derived neurotrophic factor in the central nervous system*. Yale J Biol Med, 2014. **87**(2): p. 173-86.
253. Tao, X., et al., *A calcium-responsive transcription factor, CaRF, that regulates neuronal activity-dependent expression of BDNF*. Neuron, 2002. **33**(3): p. 383-95.
254. Aid, T., et al., *Mouse and rat BDNF gene structure and expression revisited*. J Neurosci Res, 2007. **85**(3): p. 525-35.
255. Karpova, N.N., *Role of BDNF epigenetics in activity-dependent neuronal plasticity*. Neuropharmacology, 2014. **76 Pt C**: p. 709-18.
256. Pruunsild, P., et al., *Identification of cis-elements and transcription factors regulating neuronal activity-dependent transcription of human BDNF gene*. J Neurosci, 2011. **31**(9): p. 3295-308.
257. Björkholm, C. and L.M. Monteggia, *BDNF - a key transducer of antidepressant effects*. Neuropharmacology, 2016. **102**: p. 72-9.
258. Gomez-Pinilla, F., et al., *Exercise impacts brain-derived neurotrophic factor plasticity by engaging mechanisms of epigenetic regulation*. Eur J Neurosci, 2011. **33**(3): p. 383-90.
259. Tsankova, N.M., A. Kumar, and E.J. Nestler, *Histone modifications at gene promoter regions in rat hippocampus after acute and chronic electroconvulsive seizures*. J Neurosci, 2004. **24**(24): p. 5603-10.
260. Tongiorgi, E., M. Righi, and A. Cattaneo, *Activity-dependent dendritic targeting of BDNF and TrkB mRNAs in hippocampal neurons*. J Neurosci, 1997. **17**(24): p. 9492-505.

261. Tongiorgi, E., *Activity-dependent expression of brain-derived neurotrophic factor in dendrites: facts and open questions*. *Neurosci Res*, 2008. **61**(4): p. 335-46.
262. Tongiorgi, E. and G. Baj, *Functions and mechanisms of BDNF mRNA trafficking*. *Novartis Found Symp*, 2008. **289**: p. 136-47; discussion 147-51, 193-5.
263. Lewin, G.R. and B.D. Carter, *Neurotrophic factors. Preface*. *Handb Exp Pharmacol*, 2014. **220**: p. v-vi.
264. Cobb, M.H., *MAP kinase pathways*. *Prog Biophys Mol Biol*, 1999. **71**(3-4): p. 479-500.
265. Airaksinen, M.S. and M. Saarma, *The GDNF family: signalling, biological functions and therapeutic value*. *Nat Rev Neurosci*, 2002. **3**(5): p. 383-94.
266. Chao, M.V. and M. Bothwell, *Neurotrophins: to cleave or not to cleave*. *Neuron*, 2002. **33**(1): p. 9-12.
267. Chen, W., et al., *BDNF released during neuropathic pain potentiates NMDA receptors in primary afferent terminals*. *Eur J Neurosci*, 2014. **39**(9): p. 1439-54.
268. Nakai, T., et al., *Girdin phosphorylation is crucial for synaptic plasticity and memory: a potential role in the interaction of BDNF/TrkB/Akt signaling with NMDA receptor*. *J Neurosci*, 2014. **34**(45): p. 14995-5008.
269. Li, J., et al., *Experimental colitis modulates the functional properties of NMDA receptors in dorsal root ganglia neurons*. *Am J Physiol Gastrointest Liver Physiol*, 2006. **291**(2): p. G219-28.
270. Wetmore, C., et al., *Brain-derived neurotrophic factor: subcellular compartmentalization and interneuronal transfer as visualized with anti-peptide antibodies*. *Proc Natl Acad Sci U S A*, 1991. **88**(21): p. 9843-7.
271. Conner, J.M., et al., *Distribution of brain-derived neurotrophic factor (BDNF) protein and mRNA in the normal adult rat CNS: evidence for anterograde axonal transport*. *J Neurosci*, 1997. **17**(7): p. 2295-313.
272. Altar, C.A., et al., *Anterograde transport of brain-derived neurotrophic factor and its role in the brain*. *Nature*, 1997. **389**(6653): p. 856-60.
273. Balkowiec, A. and D.M. Katz, *Cellular mechanisms regulating activity-dependent release of native brain-derived neurotrophic factor from hippocampal neurons*. *J Neurosci*, 2002. **22**(23): p. 10399-407.
274. Hartmann, M., R. Heumann, and V. Lessmann, *Synaptic secretion of BDNF after high-frequency stimulation of glutamatergic synapses*. *EMBO J*, 2001. **20**(21): p. 5887-97.

275. Griesbeck, O., et al., *Are there differences between the secretion characteristics of NGF and BDNF? Implications for the modulatory role of neurotrophins in activity-dependent neuronal plasticity.* Microsc Res Tech, 1999. **45**(4-5): p. 262-75.
276. Howells, D.W., et al., *Reduced BDNF mRNA expression in the Parkinson's disease substantia nigra.* Exp Neurol, 2000. **166**(1): p. 127-35.
277. Mogi, M., et al., *Brain-derived growth factor and nerve growth factor concentrations are decreased in the substantia nigra in Parkinson's disease.* Neurosci Lett, 1999. **270**(1): p. 45-8.
278. Imamura, K., et al., *Cytokine production of activated microglia and decrease in neurotrophic factors of neurons in the hippocampus of Lewy body disease brains.* Acta Neuropathol, 2005. **109**(2): p. 141-50.
279. Scalzo, P., et al., *Serum levels of brain-derived neurotrophic factor correlate with motor impairment in Parkinson's disease.* J Neurol, 2010. **257**(4): p. 540-5.
280. Hyman, C., et al., *BDNF is a neurotrophic factor for dopaminergic neurons of the substantia nigra.* Nature, 1991. **350**(6315): p. 230-2.
281. Spina, M.B., et al., *Brain-derived neurotrophic factor protects dopaminergic cells from 6-hydroxydopamine toxicity.* Ann N Y Acad Sci, 1992. **648**: p. 348-50.
282. Frim, D.M., et al., *Implanted fibroblasts genetically engineered to produce brain-derived neurotrophic factor prevent 1-methyl-4-phenylpyridinium toxicity to dopaminergic neurons in the rat.* Proc Natl Acad Sci U S A, 1994. **91**(11): p. 5104-8.
283. Yoshimoto, Y., et al., *Astrocytes retrovirally transduced with BDNF elicit behavioral improvement in a rat model of Parkinson's disease.* Brain Res, 1995. **691**(1-2): p. 25-36.
284. Tsukahara, T., et al., *Effects of brain-derived neurotrophic factor on 1-methyl-4-phenyl-1,2,3,6-tetrahydropyridine-induced parkinsonism in monkeys.* Neurosurgery, 1995. **37**(4): p. 733-9; discussion 739-41.
285. Nagappan, G., et al., *Control of extracellular cleavage of ProBDNF by high frequency neuronal activity.* Proc Natl Acad Sci U S A, 2009. **106**(4): p. 1267-72.
286. Rizzone, M., et al., *Deep brain stimulation of the subthalamic nucleus in Parkinson's disease: effects of variation in stimulation parameters.* J Neurol Neurosurg Psychiatry, 2001. **71**(2): p. 215-9.

287. Moro, E., et al., *The impact on Parkinson's disease of electrical parameter settings in STN stimulation*. *Neurology*, 2002. **59**(5): p. 706-13.
288. Garcia, L., et al., *High-frequency stimulation in Parkinson's disease: more or less?* *Trends Neurosci*, 2005. **28**(4): p. 209-16.
289. Vidal-Martínez, G., et al., *FTY720/Fingolimod Reduces Synucleinopathy and Improves Gut Motility in A53T Mice: CONTRIBUTIONS OF PRO-BRAIN-DERIVED NEUROTROPHIC FACTOR (PRO-BDNF) AND MATURE BDNF*. *J Biol Chem*, 2016. **291**(39): p. 20811-21.
290. Sathiya, S., et al., *Telmisartan attenuates MPTP induced dopaminergic degeneration and motor dysfunction through regulation of α -synuclein and neurotrophic factors (BDNF and GDNF) expression in C57BL/6J mice*. *Neuropharmacology*, 2013. **73**: p. 98-110.
291. Katila, N., et al., *Metformin lowers α -synuclein phosphorylation and upregulates neurotrophic factor in the MPTP mouse model of Parkinson's disease*. *Neuropharmacology*, 2017. **125**: p. 396-407.
292. Zhou, W., J.C. Barkow, and C.R. Freed, *Running wheel exercise reduces α -synuclein aggregation and improves motor and cognitive function in a transgenic mouse model of Parkinson's disease*. *PLoS One*, 2017. **12**(12): p. e0190160.
293. Almeida, M.F., et al., *Effects of mild running on substantia nigra during early neurodegeneration*. *J Sports Sci*, 2018. **36**(12): p. 1363-1370.
294. Hsueh, S.C., et al., *Voluntary Physical Exercise Improves Subsequent Motor and Cognitive Impairments in a Rat Model of Parkinson's Disease*. *Int J Mol Sci*, 2018. **19**(2).
295. Tuon, T., et al., *Physical training exerts neuroprotective effects in the regulation of neurochemical factors in an animal model of Parkinson's disease*. *Neuroscience*, 2012. **227**: p. 305-12.
296. Siracusa, R., et al., *Neuroprotective Effects of Temsirolimus in Animal Models of Parkinson's Disease*. *Mol Neurobiol*, 2018. **55**(3): p. 2403-2419.
297. Li, Y., et al., *D-Ala²-GIP-glu-PAL is neuroprotective in a chronic Parkinson's disease mouse model and increases BDNF expression while reducing neuroinflammation and lipid peroxidation*. *Eur J Pharmacol*, 2017. **797**: p. 162-172.
298. Charles, D., et al., *Deep brain stimulation in early stage Parkinson's disease*. *Parkinsonism Relat Disord*, 2015. **21**(3): p. 347-8.

299. Hacker, M., D. Charles, and S. Finder, *Deep brain stimulation in early stage Parkinson's disease may reduce the relative risk of symptom worsening*. *Parkinsonism Relat Disord*, 2016. **22**: p. 112-3.
300. Marsili, L., G. Rizzo, and C. Colosimo, *Diagnostic Criteria for Parkinson's Disease: From James Parkinson to the Concept of Prodromal Disease*. *Front Neurol*, 2018. **9**: p. 156.
301. Lunati, A., S. Lesage, and A. Brice, *The genetic landscape of Parkinson's disease*. *Rev Neurol (Paris)*, 2018. **174**(9): p. 628-643.
302. Obeso, J.A., et al., *Past, present, and future of Parkinson's disease: A special essay on the 200th Anniversary of the Shaking Palsy*. *Mov Disord*, 2017. **32**(9): p. 1264-1310.
303. Surguchov, A., *Molecular and cellular biology of synucleins*. *Int Rev Cell Mol Biol*, 2008. **270**: p. 225-317.
304. Bussell, R., Jr. and D. Eliezer, *A structural and functional role for 11-mer repeats in alpha-synuclein and other exchangeable lipid binding proteins*. *J Mol Biol*, 2003. **329**(4): p. 763-78.
305. Ueda, K., T. Saitoh, and H. Mori, *Tissue-dependent alternative splicing of mRNA for NACP, the precursor of non-A beta component of Alzheimer's disease amyloid*. *Biochem Biophys Res Commun*, 1994. **205**(2): p. 1366-72.
306. Periquet, M., et al., *Aggregated alpha-synuclein mediates dopaminergic neurotoxicity in vivo*. *J Neurosci*, 2007. **27**(12): p. 3338-46.
307. Waxman, E.A., J.R. Mazzulli, and B.I. Giasson, *Characterization of hydrophobic residue requirements for alpha-synuclein fibrillization*. *Biochemistry*, 2009. **48**(40): p. 9427-36.
308. Hasegawa, M., et al., *Phosphorylated alpha-synuclein is ubiquitinated in alpha-synucleinopathy lesions*. *J Biol Chem*, 2002. **277**(50): p. 49071-6.
309. Oueslati, A., M. Fournier, and H.A. Lashuel, *Role of post-translational modifications in modulating the structure, function and toxicity of alpha-synuclein: implications for Parkinson's disease pathogenesis and therapies*. *Prog Brain Res*, 2010. **183**: p. 115-45.
310. Krumova, P., et al., *Sumoylation inhibits alpha-synuclein aggregation and toxicity*. *J Cell Biol*, 2011. **194**(1): p. 49-60.
311. Chandra, S., et al., *A broken alpha-helix in folded alpha-Synuclein*. *J Biol Chem*, 2003. **278**(17): p. 15313-8.

312. Davidson, W.S., et al., *Stabilization of alpha-synuclein secondary structure upon binding to synthetic membranes*. J Biol Chem, 1998. **273**(16): p. 9443-9.
313. Jao, C.C., et al., *Structure of membrane-bound alpha-synuclein studied by site-directed spin labeling*. Proc Natl Acad Sci U S A, 2004. **101**(22): p. 8331-6.
314. Burré, J., et al., *Alpha-synuclein promotes SNARE-complex assembly in vivo and in vitro*. Science, 2010. **329**(5999): p. 1663-7.
315. Burré, J., M. Sharma, and T.C. Südhof, *Systematic mutagenesis of α -synuclein reveals distinct sequence requirements for physiological and pathological activities*. J Neurosci, 2012. **32**(43): p. 15227-42.
316. Vargas, K.J., et al., *Synucleins regulate the kinetics of synaptic vesicle endocytosis*. J Neurosci, 2014. **34**(28): p. 9364-76.
317. Fortin, D.L., et al., *Neural activity controls the synaptic accumulation of alpha-synuclein*. J Neurosci, 2005. **25**(47): p. 10913-21.
318. Burre, J., et al., *Alpha-synuclein promotes SNARE-complex assembly in vivo and in vitro*. Science, 2010. **329**(5999): p. 1663-7.
319. Perez, R.G., et al., *A role for alpha-synuclein in the regulation of dopamine biosynthesis*. J Neurosci, 2002. **22**(8): p. 3090-9.
320. Perez, R.G. and T.G. Hastings, *Could a loss of alpha-synuclein function put dopaminergic neurons at risk?* J Neurochem, 2004. **89**(6): p. 1318-24.
321. Yu, S., et al., *Inhibition of tyrosine hydroxylase expression in alpha-synuclein-transfected dopaminergic neuronal cells*. Neurosci Lett, 2004. **367**(1): p. 34-9.
322. Lee, F.J., et al., *Direct binding and functional coupling of alpha-synuclein to the dopamine transporters accelerate dopamine-induced apoptosis*. FASEB J, 2001. **15**(6): p. 916-26.
323. Dauer, W., et al., *Resistance of alpha -synuclein null mice to the parkinsonian neurotoxin MPTP*. Proc Natl Acad Sci U S A, 2002. **99**(22): p. 14524-9.
324. Wersinger, C. and A. Sidhu, *Attenuation of dopamine transporter activity by alpha-synuclein*. Neurosci Lett, 2003. **340**(3): p. 189-92.
325. Wersinger, C., et al., *Modulation of dopamine transporter function by alpha-synuclein is altered by impairment of cell adhesion and by induction of oxidative stress*. FASEB J, 2003. **17**(14): p. 2151-3.

326. Fountaine, T.M. and R. Wade-Martins, *RNA interference-mediated knockdown of alpha-synuclein protects human dopaminergic neuroblastoma cells from MPP(+)
toxicity and reduces dopamine transport*. J Neurosci Res, 2007. **85**(2): p. 351-63.
327. Fountaine, T.M., et al., *The effect of alpha-synuclein knockdown on MPP+
toxicity in models of human neurons*. Eur J Neurosci, 2008. **28**(12): p. 2459-73.
328. Abeliovich, A., et al., *Mice lacking alpha-synuclein display functional deficits in
the nigrostriatal dopamine system*. Neuron, 2000. **25**(1): p. 239-52.
329. Cabin, D.E., et al., *Synaptic vesicle depletion correlates with attenuated synaptic
responses to prolonged repetitive stimulation in mice lacking alpha-synuclein*. J
Neurosci, 2002. **22**(20): p. 8797-807.
330. Unni, V.K., et al., *In vivo imaging of alpha-synuclein in mouse cortex
demonstrates stable expression and differential subcellular compartment
mobility*. PLoS One, 2010. **5**(5): p. e10589.
331. Uversky, V.N., et al., *Accelerated alpha-synuclein fibrillation in crowded milieu*.
FEBS Lett, 2002. **515**(1-3): p. 99-103.
332. Breydo, L., J.W. Wu, and V.N. Uversky, *A-synuclein misfolding and Parkinson's
disease*. Biochim Biophys Acta, 2012. **1822**(2): p. 261-85.
333. Bartels, T., J.G. Choi, and D.J. Selkoe, *alpha-Synuclein occurs physiologically as
a helically folded tetramer that resists aggregation*. Nature, 2011. **477**(7362): p.
107-10.
334. Dettmer, U., et al., *In vivo cross-linking reveals principally oligomeric forms of
alpha-synuclein and beta-synuclein in neurons and non-neural cells*. J Biol
Chem, 2013. **288**(9): p. 6371-85.
335. Dettmer, U., et al., *KTKEGV repeat motifs are key mediators of normal alpha-
synuclein tetramerization: Their mutation causes excess monomers and
neurotoxicity*. Proc Natl Acad Sci U S A, 2015. **112**(31): p. 9596-601.
336. Serpell, L.C., et al., *Fiber diffraction of synthetic alpha-synuclein filaments shows
amyloid-like cross-beta conformation*. Proc Natl Acad Sci U S A, 2000. **97**(9): p.
4897-902.
337. Caughey, B. and P.T. Lansbury, *Protofibrils, pores, fibrils, and
neurodegeneration: separating the responsible protein aggregates from the
innocent bystanders*. Annu Rev Neurosci, 2003. **26**: p. 267-98.
338. Bengoa-Vergniory, N., et al., *Alpha-synuclein oligomers: a new hope*. Acta
Neuropathol, 2017. **134**(6): p. 819-838.

339. Sharon, R., et al., *The formation of highly soluble oligomers of alpha-synuclein is regulated by fatty acids and enhanced in Parkinson's disease*. *Neuron*, 2003. **37**(4): p. 583-95.
340. Tofaris, G.K., et al., *Ubiquitination of alpha-synuclein in Lewy bodies is a pathological event not associated with impairment of proteasome function*. *J Biol Chem*, 2003. **278**(45): p. 44405-11.
341. Chen, L., et al., *Oligomeric alpha-synuclein inhibits tubulin polymerization*. *Biochem Biophys Res Commun*, 2007. **356**(3): p. 548-53.
342. Danzer, K.M., et al., *Different species of alpha-synuclein oligomers induce calcium influx and seeding*. *J Neurosci*, 2007. **27**(34): p. 9220-32.
343. Nasstrom, T., et al., *The lipid peroxidation products 4-oxo-2-nonenal and 4-hydroxy-2-nonenal promote the formation of alpha-synuclein oligomers with distinct biochemical, morphological, and functional properties*. *Free Radic Biol Med*, 2011. **50**(3): p. 428-37.
344. Tetzlaff, J.E., et al., *CHIP targets toxic alpha-Synuclein oligomers for degradation*. *J Biol Chem*, 2008. **283**(26): p. 17962-8.
345. Pieri, L., K. Madiona, and R. Melki, *Structural and functional properties of prefibrillar alpha-synuclein oligomers*. *Sci Rep*, 2016. **6**: p. 24526.
346. Karpinar, D.P., et al., *Pre-fibrillar alpha-synuclein variants with impaired beta-structure increase neurotoxicity in Parkinson's disease models*. *EMBO J*, 2009. **28**(20): p. 3256-68.
347. Dimant, H., et al., *Direct detection of alpha synuclein oligomers in vivo*. *Acta Neuropathol Commun*, 2013. **1**: p. 6.
348. Winner, B., et al., *In vivo demonstration that alpha-synuclein oligomers are toxic*. *Proc Natl Acad Sci U S A*, 2011. **108**(10): p. 4194-9.
349. Wood, S.J., et al., *alpha-synuclein fibrillogenesis is nucleation-dependent. Implications for the pathogenesis of Parkinson's disease*. *J Biol Chem*, 1999. **274**(28): p. 19509-12.
350. Uversky, V.N. and D. Eliezer, *Biophysics of Parkinson's disease: structure and aggregation of alpha-synuclein*. *Curr Protein Pept Sci*, 2009. **10**(5): p. 483-99.
351. Volpicelli-Daley, L.A., et al., *Exogenous alpha-synuclein fibrils induce Lewy body pathology leading to synaptic dysfunction and neuron death*. *Neuron*, 2011. **72**(1): p. 57-71.

352. Braak, H., et al., *Staging of brain pathology related to sporadic Parkinson's disease*. Neurobiol Aging, 2003. **24**(2): p. 197-211.
353. Fujiwara, H., et al., *alpha-Synuclein is phosphorylated in synucleinopathy lesions*. Nat Cell Biol, 2002. **4**(2): p. 160-4.
354. Volpicelli-Daley, L.A., K.C. Luk, and V.M. Lee, *Addition of exogenous α -synuclein preformed fibrils to primary neuronal cultures to seed recruitment of endogenous α -synuclein to Lewy body and Lewy neurite-like aggregates*. Nat Protoc, 2014. **9**(9): p. 2135-46.
355. Chu, Y., et al., *Alterations in lysosomal and proteasomal markers in Parkinson's disease: relationship to alpha-synuclein inclusions*. Neurobiol Dis, 2009. **35**(3): p. 385-98.
356. Chu, Y., A.L. Mickiewicz, and J.H. Kordower, *alpha-synuclein aggregation reduces nigral myocyte enhancer factor-2D in idiopathic and experimental Parkinson's disease*. Neurobiol Dis, 2011. **41**(1): p. 71-82.
357. Chu, Y., et al., *Alterations in axonal transport motor proteins in sporadic and experimental Parkinson's disease*. Brain, 2012. **135**(Pt 7): p. 2058-73.
358. Schaser, A.J., et al., *Alpha-synuclein is a DNA binding protein that modulates DNA repair with implications for Lewy body disorders*. Sci Rep, 2019. **9**(1): p. 10919.
359. Dzamko, N., et al., *Toll-like receptor 2 is increased in neurons in Parkinson's disease brain and may contribute to alpha-synuclein pathology*. Acta Neuropathol, 2017. **133**(2): p. 303-319.
360. Grunblatt, E., et al., *Gene expression profiling of parkinsonian substantia nigra pars compacta; alterations in ubiquitin-proteasome, heat shock protein, iron and oxidative stress regulated proteins, cell adhesion/cellular matrix and vesicle trafficking genes*. J Neural Transm (Vienna), 2004. **111**(12): p. 1543-73.
361. Hauser, M.A., et al., *Expression profiling of substantia nigra in Parkinson disease, progressive supranuclear palsy, and frontotemporal dementia with parkinsonism*. Arch Neurol, 2005. **62**(6): p. 917-21.
362. Duke, D.C., et al., *Transcriptome analysis reveals link between proteasomal and mitochondrial pathways in Parkinson's disease*. Neurogenetics, 2006. **7**(3): p. 139-48.
363. Elstner, M., et al., *Single-cell expression profiling of dopaminergic neurons combined with association analysis identifies pyridoxal kinase as Parkinson's disease gene*. Ann Neurol, 2009. **66**(6): p. 792-8.

364. Botta-Orfila, T., et al., *Microarray expression analysis in idiopathic and LRRK2-associated Parkinson's disease*. *Neurobiol Dis*, 2012. **45**(1): p. 462-8.
365. Dijkstra, A.A., et al., *Evidence for Immune Response, Axonal Dysfunction and Reduced Endocytosis in the Substantia Nigra in Early Stage Parkinson's Disease*. *PLoS One*, 2015. **10**(6): p. e0128651.
366. Lu, L., et al., *Gene expression profiling of Lewy body-bearing neurons in Parkinson's disease*. *Exp Neurol*, 2005. **195**(1): p. 27-39.
367. Cantuti-Castelvetri, I., et al., *Effects of gender on nigral gene expression and parkinson disease*. *Neurobiol Dis*, 2007. **26**(3): p. 606-14.
368. Elstner, M., et al., *Neuromelanin, neurotransmitter status and brainstem location determine the differential vulnerability of catecholaminergic neurons to mitochondrial DNA deletions*. *Mol Brain*, 2011. **4**: p. 43.
369. Lin, M.T., et al., *Somatic mitochondrial DNA mutations in early Parkinson and incidental Lewy body disease*. *Ann Neurol*, 2012. **71**(6): p. 850-4.
370. Grunewald, A., et al., *Mitochondrial DNA Depletion in Respiratory Chain-Deficient Parkinson Disease Neurons*. *Ann Neurol*, 2016. **79**(3): p. 366-78.
371. Duda, J., et al., *Cell-Specific RNA Quantification in Human SN DA Neurons from Heterogeneous Post-mortem Midbrain Samples by UV-Laser Microdissection and RT-qPCR*. *Methods Mol Biol*, 2018. **1723**: p. 335-360.
372. Grundemann, J., F. Schlaudraff, and B. Liss, *UV-laser microdissection and mRNA expression analysis of individual neurons from postmortem Parkinson's disease brains*. *Methods Mol Biol*, 2011. **755**: p. 363-74.
373. Matsuoka, Y., et al., *Lack of nigral pathology in transgenic mice expressing human alpha-synuclein driven by the tyrosine hydroxylase promoter*. *Neurobiol Dis*, 2001. **8**(3): p. 535-9.
374. Kahle, P.J., et al., *Hyperphosphorylation and insolubility of alpha-synuclein in transgenic mouse oligodendrocytes*. *EMBO Rep*, 2002. **3**(6): p. 583-8.
375. Rockenstein, E., et al., *Differential neuropathological alterations in transgenic mice expressing alpha-synuclein from the platelet-derived growth factor and Thy-1 promoters*. *J Neurosci Res*, 2002. **68**(5): p. 568-78.
376. Fernagut, P.O. and M.F. Chesselet, *Alpha-synuclein and transgenic mouse models*. *Neurobiol Dis*, 2004. **17**(2): p. 123-30.

377. Osterberg, V.R., et al., *Progressive aggregation of alpha-synuclein and selective degeneration of lewy inclusion-bearing neurons in a mouse model of parkinsonism*. Cell Rep, 2015. **10**(8): p. 1252-60.
378. Abdelmotilib, H., et al., *alpha-Synuclein fibril-induced inclusion spread in rats and mice correlates with dopaminergic Neurodegeneration*. Neurobiol Dis, 2017. **105**: p. 84-98.
379. Tapias, V., et al., *Synthetic alpha-synuclein fibrils cause mitochondrial impairment and selective dopamine neurodegeneration in part via iNOS-mediated nitric oxide production*. Cell Mol Life Sci, 2017. **74**(15): p. 2851-2874.
380. Grassi, D., et al., *Identification of a highly neurotoxic alpha-synuclein species inducing mitochondrial damage and mitophagy in Parkinson's disease*. Proc Natl Acad Sci U S A, 2018. **115**(11): p. E2634-E2643.
381. Wang, X., et al., *Pathogenic alpha-synuclein aggregates preferentially bind to mitochondria and affect cellular respiration*. Acta Neuropathol Commun, 2019. **7**(1): p. 41.
382. Froula, J.M., et al., *alpha-Synuclein fibril-induced paradoxical structural and functional defects in hippocampal neurons*. Acta Neuropathol Commun, 2018. **6**(1): p. 35.
383. Wu, Q., et al., *alpha-Synuclein (alphaSyn) Preformed Fibrils Induce Endogenous alphaSyn Aggregation, Compromise Synaptic Activity and Enhance Synapse Loss in Cultured Excitatory Hippocampal Neurons*. J Neurosci, 2019. **39**(26): p. 5080-5094.
384. Hofer, M.M. and Y.A. Barde, *Brain-derived neurotrophic factor prevents neuronal death in vivo*. Nature, 1988. **331**(6153): p. 261-2.
385. Kalcheim, C. and M. Gendreau, *Brain-derived neurotrophic factor stimulates survival and neuronal differentiation in cultured avian neural crest*. Brain Res, 1988. **469**(1-2): p. 79-86.
386. Barde, Y.A., *The nerve growth factor family*. Prog Growth Factor Res, 1990. **2**(4): p. 237-48.
387. Snider, W.D. and E.M. Johnson, *Neurotrophic molecules*. Ann Neurol, 1989. **26**(4): p. 489-506.
388. Kowiański, P., et al., *BDNF: A Key Factor with Multipotent Impact on Brain Signaling and Synaptic Plasticity*. Cell Mol Neurobiol, 2018. **38**(3): p. 579-593.

389. Chen, S.D., et al., *More Insight into BDNF against Neurodegeneration: Anti-Apoptosis, Anti-Oxidation, and Suppression of Autophagy*. Int J Mol Sci, 2017. **18**(3).
390. Patapoutian, A. and L.F. Reichardt, *Trk receptors: mediators of neurotrophin action*. Curr Opin Neurobiol, 2001. **11**(3): p. 272-80.
391. Hempstead, B.L., *Deciphering proneurotrophin actions*. Handb Exp Pharmacol, 2014. **220**: p. 17-32.
392. Middlemas, D.S., R.A. Lindberg, and T. Hunter, *trkB, a neural receptor protein-tyrosine kinase: evidence for a full-length and two truncated receptors*. Mol Cell Biol, 1991. **11**(1): p. 143-53.
393. Klein, R., et al., *The trkB tyrosine protein kinase gene codes for a second neurogenic receptor that lacks the catalytic kinase domain*. Cell, 1990. **61**(4): p. 647-56.
394. Haapasalo, A., et al., *Regulation of TRKB surface expression by brain-derived neurotrophic factor and truncated TRKB isoforms*. J Biol Chem, 2002. **277**(45): p. 43160-7.
395. Yoshii, A. and M. Constantine-Paton, *Postsynaptic BDNF-TrkB signaling in synapse maturation, plasticity, and disease*. Dev Neurobiol, 2010. **70**(5): p. 304-22.
396. Yoshii, A. and M. Constantine-Paton, *Postsynaptic localization of PSD-95 is regulated by all three pathways downstream of TrkB signaling*. Front Synaptic Neurosci, 2014. **6**: p. 6.
397. Bosse, K.E., et al., *Aberrant striatal dopamine transmitter dynamics in brain-derived neurotrophic factor-deficient mice*. J Neurochem, 2012. **120**(3): p. 385-95.
398. Fang, F., et al., *Synuclein impairs trafficking and signaling of BDNF in a mouse model of Parkinson's disease*. Sci Rep, 2017. **7**(1): p. 3868.
399. Yuan, Y., et al., *Overexpression of alpha-synuclein down-regulates BDNF expression*. Cell Mol Neurobiol, 2010. **30**(6): p. 939-46.
400. Wang, Y.C., et al., *Knockdown of α -synuclein in cerebral cortex improves neural behavior associated with apoptotic inhibition and neurotrophin expression in spinal cord transected rats*. Apoptosis, 2016. **21**(4): p. 404-20.

401. Decressac, M., et al., *α -Synuclein-induced down-regulation of Nurr1 disrupts GDNF signaling in nigral dopamine neurons*. *Sci Transl Med*, 2012. **4**(163): p. 163ra156.
402. Kang, S.S., et al., *TrkB neurotrophic activities are blocked by α -synuclein, triggering dopaminergic cell death in Parkinson's disease*. *Proc Natl Acad Sci U S A*, 2017. **114**(40): p. 10773-10778.
403. Markham, A., et al., *BDNF increases rat brain mitochondrial respiratory coupling at complex I, but not complex II*. *Eur J Neurosci*, 2004. **20**(5): p. 1189-96.
404. Su, B., et al., *Brain-derived neurotrophic factor (BDNF)-induced mitochondrial motility arrest and presynaptic docking contribute to BDNF-enhanced synaptic transmission*. *J Biol Chem*, 2014. **289**(3): p. 1213-26.
405. Leal, G., D. Comprido, and C.B. Duarte, *BDNF-induced local protein synthesis and synaptic plasticity*. *Neuropharmacology*, 2014. **76 Pt C**: p. 639-56.
406. von Bohlen Und Halbach, O. and V. von Bohlen Und Halbach, *BDNF effects on dendritic spine morphology and hippocampal function*. *Cell Tissue Res*, 2018. **373**(3): p. 729-741.
407. Spina, M.B., et al., *Brain-derived neurotrophic factor protects dopamine neurons against 6-hydroxydopamine and N-methyl-4-phenylpyridinium ion toxicity: involvement of the glutathione system*. *J Neurochem*, 1992. **59**(1): p. 99-106.
408. Zhang, X., P.E. Andren, and P. Svenningsson, *Repeated L-DOPA treatment increases c-fos and BDNF mRNAs in the subthalamic nucleus in the 6-OHDA rat model of Parkinson's disease*. *Brain Res*, 2006. **1095**(1): p. 207-10.
409. Sauer, H., V. Wong, and A. Björklund, *Brain-derived neurotrophic factor and neurotrophin-4/5 modify neurotransmitter-related gene expression in the 6-hydroxydopamine-lesioned rat striatum*. *Neuroscience*, 1995. **65**(4): p. 927-33.
410. Friedman, W.J., L. Olson, and H. Persson, *Cells that Express Brain-Derived Neurotrophic Factor mRNA in the Developing Postnatal Rat Brain*. *Eur J Neurosci*, 1991. **3**(7): p. 688-697.
411. Fischer, D.L., et al., *Subthalamic Nucleus Deep Brain Stimulation Employs trkB Signaling for Neuroprotection and Functional Restoration*. *J Neurosci*, 2017. **37**(28): p. 6786-6796.
412. Hilker, R., et al., *Disease progression continues in patients with advanced Parkinson's disease and effective subthalamic nucleus stimulation*. *J Neurol Neurosurg Psychiatry*, 2005. **76**(9): p. 1217-21.

413. Lilleeng, B., et al., *Progression and survival in Parkinson's disease with subthalamic nucleus stimulation*. Acta Neurol Scand, 2014. **130**(5): p. 292-8.
414. Wichmann, T. and M.R. Delong, *Deep-Brain Stimulation for Basal Ganglia Disorders*. Basal Ganglia, 2011. **1**(2): p. 65-77.
415. Miller, D.W., et al., *Alpha-synuclein in blood and brain from familial Parkinson disease with SNCA locus triplication*. Neurology, 2004. **62**(10): p. 1835-8.
416. Tan, E.K., et al., *Alpha-synuclein mRNA expression in sporadic Parkinson's disease*. Mov Disord, 2005. **20**(5): p. 620-3.
417. Quinn, J.G., et al., *alpha-Synuclein mRNA and soluble alpha-synuclein protein levels in post-mortem brain from patients with Parkinson's disease, dementia with Lewy bodies, and Alzheimer's disease*. Brain Res, 2012. **1459**: p. 71-80.
418. Polinski, N.K., et al., *Best Practices for Generating and Using Alpha-Synuclein Pre-Formed Fibrils to Model Parkinson's Disease in Rodents*. J Parkinsons Dis, 2018. **8**(2): p. 303-322.
419. Tarutani, A., et al., *The Effect of Fragmented Pathogenic alpha-Synuclein Seeds on Prion-like Propagation*. J Biol Chem, 2016. **291**(36): p. 18675-88.
420. Li, J.Y., et al., *Characterization of Lewy body pathology in 12- and 16-year-old intrastriatal mesencephalic grafts surviving in a patient with Parkinson's disease*. Mov Disord, 2010. **25**(8): p. 1091-6.
421. Tanji, K., et al., *Proteinase K-resistant alpha-synuclein is deposited in presynapses in human Lewy body disease and A53T alpha-synuclein transgenic mice*. Acta Neuropathol, 2010. **120**(2): p. 145-54.
422. Leys, C., Klein, O., Bernard, P., Licata, L. , *Detecting outliers: Do not use standard deviation around the mean, use absolute deviation around the median*. Journal of Experimental Social Psychology, 2013. **49** p. 764–766.
423. Schuepbach, W.M., et al., *Neurostimulation for Parkinson's disease with early motor complications*. N Engl J Med, 2013. **368**(7): p. 610-22.
424. Hacker, M.L., et al., *Deep brain stimulation may reduce the relative risk of clinically important worsening in early stage Parkinson's disease*. Parkinsonism Relat Disord, 2015. **21**(10): p. 1177-83.
425. Karpowicz, R.J., Jr., et al., *Selective imaging of internalized proteopathic alpha-synuclein seeds in primary neurons reveals mechanistic insight into transmission of synucleinopathies*. J Biol Chem, 2017. **292**(32): p. 13482-13497.

426. Luk, K.C., et al., *Intracerebral inoculation of pathological alpha-synuclein initiates a rapidly progressive neurodegenerative alpha-synucleinopathy in mice*. J Exp Med, 2012. **209**(5): p. 975-86.
427. Muntane, G., I. Ferrer, and M. Martinez-Vicente, *alpha-synuclein phosphorylation and truncation are normal events in the adult human brain*. Neuroscience, 2012. **200**: p. 106-19.
428. Anderson, J.P., et al., *Phosphorylation of Ser-129 is the dominant pathological modification of alpha-synuclein in familial and sporadic Lewy body disease*. J Biol Chem, 2006. **281**(40): p. 29739-52.
429. Zhou, J., et al., *Changes in the solubility and phosphorylation of alpha-synuclein over the course of Parkinson's disease*. Acta Neuropathol, 2011. **121**(6): p. 695-704.
430. Raghunathan, R., et al., *Glycomic and Proteomic Changes in Aging Brain Nigrostriatal Pathway*. Mol Cell Proteomics, 2018. **17**(9): p. 1778-1787.
431. Tansey, M.G. and M. Romero-Ramos, *Immune system responses in Parkinson's disease: Early and dynamic*. Eur J Neurosci, 2019. **49**(3): p. 364-383.
432. Chu, K., X. Zhou, and B.Y. Luo, *Cytokine gene polymorphisms and Parkinson's disease: a meta-analysis*. Can J Neurol Sci, 2012. **39**(1): p. 58-64.
433. Hamza, T.H., et al., *Common genetic variation in the HLA region is associated with late-onset sporadic Parkinson's disease*. Nat Genet, 2010. **42**(9): p. 781-5.
434. Kannarkat, G.T., et al., *Common Genetic Variant Association with Altered HLA Expression, Synergy with Pyrethroid Exposure, and Risk for Parkinson's Disease: An Observational and Case-Control Study*. NPJ Parkinsons Dis, 2015. **1**.
435. Barkholt, P., et al., *Long-term polarization of microglia upon alpha-synuclein overexpression in nonhuman primates*. Neuroscience, 2012. **208**: p. 85-96.
436. Watson, M.B., et al., *Regionally-specific microglial activation in young mice over-expressing human wildtype alpha-synuclein*. Exp Neurol, 2012. **237**(2): p. 318-34.
437. Iannaccone, S., et al., *In vivo microglia activation in very early dementia with Lewy bodies, comparison with Parkinson's disease*. Parkinsonism Relat Disord, 2013. **19**(1): p. 47-52.
438. Ouchi, Y., et al., *Microglial activation and dopamine terminal loss in early Parkinson's disease*. Ann Neurol, 2005. **57**(2): p. 168-75.

439. Braak, H., M. Sastre, and K. Del Tredici, *Development of alpha-synuclein immunoreactive astrocytes in the forebrain parallels stages of intraneuronal pathology in sporadic Parkinson's disease*. *Acta Neuropathol*, 2007. **114**(3): p. 231-41.
440. Hishikawa, N., et al., *Widespread occurrence of argyrophilic glial inclusions in Parkinson's disease*. *Neuropathol Appl Neurobiol*, 2001. **27**(5): p. 362-72.
441. Wakabayashi, K., et al., *NACP/alpha-synuclein-positive filamentous inclusions in astrocytes and oligodendrocytes of Parkinson's disease brains*. *Acta Neuropathol*, 2000. **99**(1): p. 14-20.
442. Tavares, G., et al., *Employing an open-source tool to assess astrocyte tridimensional structure*. *Brain Struct Funct*, 2017. **222**(4): p. 1989-1999.
443. Harms, A.S., et al., *MHCII is required for alpha-synuclein-induced activation of microglia, CD4 T cell proliferation, and dopaminergic neurodegeneration*. *J Neurosci*, 2013. **33**(23): p. 9592-600.
444. Ouchi, Y., et al., *Neuroinflammation in the living brain of Parkinson's disease*. *Parkinsonism Relat Disord*, 2009. **15 Suppl 3**: p. S200-4.
445. Koprach, J.B., et al., *Expression of human A53T alpha-synuclein in the rat substantia nigra using a novel AAV1/2 vector produces a rapidly evolving pathology with protein aggregation, dystrophic neurite architecture and nigrostriatal degeneration with potential to model the pathology of Parkinson's disease*. *Mol Neurodegener*, 2010. **5**: p. 43.
446. Ulusoy, A., et al., *Viral vector-mediated overexpression of alpha-synuclein as a progressive model of Parkinson's disease*. *Prog Brain Res*, 2010. **184**: p. 89-111.
447. Oliveras-Salva, M., et al., *rAAV2/7 vector-mediated overexpression of alpha-synuclein in mouse substantia nigra induces protein aggregation and progressive dose-dependent neurodegeneration*. *Mol Neurodegener*, 2013. **8**: p. 44.
448. Gombash, S.E., et al., *Morphological and behavioral impact of AAV2/5-mediated overexpression of human wildtype alpha-synuclein in the rat nigrostriatal system*. *PLoS One*, 2013. **8**(11): p. e81426.
449. Fischer, D.L., et al., *Viral Vector-Based Modeling of Neurodegenerative Disorders: Parkinson's Disease*. *Methods Mol Biol*, 2016. **1382**: p. 367-82.
450. Ip, C.W., et al., *AAV1/2-induced overexpression of A53T-alpha-synuclein in the substantia nigra results in degeneration of the nigrostriatal system with Lewy-like pathology and motor impairment: a new mouse model for Parkinson's disease*. *Acta Neuropathol Commun*, 2017. **5**(1): p. 11.

451. Thakur, P., et al., *Modeling Parkinson's disease pathology by combination of fibril seeds and alpha-synuclein overexpression in the rat brain*. Proc Natl Acad Sci U S A, 2017. **114**(39): p. E8284-E8293.
452. Farrer, M., et al., *Comparison of kindreds with parkinsonism and alpha-synuclein genomic multiplications*. Ann Neurol, 2004. **55**(2): p. 174-9.
453. Oberheim, N.A., S.A. Goldman, and M. Nedergaard, *Heterogeneity of astrocytic form and function*. Methods Mol Biol, 2012. **814**: p. 23-45.
454. Oberheim, N.A., et al., *Uniquely hominid features of adult human astrocytes*. J Neurosci, 2009. **29**(10): p. 3276-87.
455. Sofroniew, M.V. and H.V. Vinters, *Astrocytes: biology and pathology*. Acta Neuropathol, 2010. **119**(1): p. 7-35.
456. Clarke, L.E., et al., *Normal aging induces A1-like astrocyte reactivity*. Proc Natl Acad Sci U S A, 2018. **115**(8): p. E1896-E1905.
457. Chung, W.S., et al., *Astrocytes mediate synapse elimination through MEGF10 and MERTK pathways*. Nature, 2013. **504**(7480): p. 394-400.
458. Liddelow, S. and B. Barres, *SnapShot: Astrocytes in Health and Disease*. Cell, 2015. **162**(5): p. 1170-1170 e1.
459. Booth, H.D.E., W.D. Hirst, and R. Wade-Martins, *The Role of Astrocyte Dysfunction in Parkinson's Disease Pathogenesis*. Trends Neurosci, 2017. **40**(6): p. 358-370.
460. Liddelow, S.A., et al., *Neurotoxic reactive astrocytes are induced by activated microglia*. Nature, 2017. **541**(7638): p. 481-487.
461. Zamanian, J.L., et al., *Genomic analysis of reactive astrogliosis*. J Neurosci, 2012. **32**(18): p. 6391-410.
462. Anderson, M.A., et al., *Astrocyte scar formation aids central nervous system axon regeneration*. Nature, 2016. **532**(7598): p. 195-200.
463. Yun, S.P., et al., *Block of A1 astrocyte conversion by microglia is neuroprotective in models of Parkinson's disease*. Nat Med, 2018. **24**(7): p. 931-938.
464. Eng, L.F., R.S. Ghirnikar, and Y.L. Lee, *Glial fibrillary acidic protein: GFAP-thirty-one years (1969-2000)*. Neurochem Res, 2000. **25**(9-10): p. 1439-51.

465. Yang, Z. and K.K. Wang, *Glial fibrillary acidic protein: from intermediate filament assembly and gliosis to neurobiomarker*. Trends Neurosci, 2015. **38**(6): p. 364-74.
466. Matias, I., J. Morgado, and F.C.A. Gomes, *Astrocyte Heterogeneity: Impact to Brain Aging and Disease*. Front Aging Neurosci, 2019. **11**: p. 59.
467. Vedam-Mai, V., et al., *Tissue Response to Deep Brain Stimulation and Microlesion: A Comparative Study*. Neuromodulation, 2016. **19**(5): p. 451-8.
468. Vedam-Mai, V., et al., *Deep Brain Stimulation associated gliosis: A post-mortem study*. Parkinsonism Relat Disord, 2018. **54**: p. 51-55.
469. Amorim, B.O., et al., *Deep brain stimulation induces antiapoptotic and anti-inflammatory effects in epileptic rats*. J Neuroinflammation, 2015. **12**: p. 162.
470. Lai, S.W., et al., *Regulatory Effects of Neuroinflammatory Responses Through Brain-Derived Neurotrophic Factor Signaling in Microglial Cells*. Mol Neurobiol, 2018. **55**(9): p. 7487-7499.
471. Liddelow, S.A. and B.A. Barres, *Reactive Astrocytes: Production, Function, and Therapeutic Potential*. Immunity, 2017. **46**(6): p. 957-967.
472. Rodriguez, J.J., et al., *Complex and region-specific changes in astroglial markers in the aging brain*. Neurobiol Aging, 2014. **35**(1): p. 15-23.
473. Altar, C.A. and P.S. DiStefano, *Neurotrophin trafficking by anterograde transport*. Trends Neurosci, 1998. **21**(10): p. 433-7.
474. Radka, S.F., et al., *Presence of brain-derived neurotrophic factor in brain and human and rat but not mouse serum detected by a sensitive and specific immunoassay*. Brain Res, 1996. **709**(1): p. 122-301.
475. Pollock, G.S., et al., *Effects of early visual experience and diurnal rhythms on BDNF mRNA and protein levels in the visual system, hippocampus, and cerebellum*. J Neurosci, 2001. **21**(11): p. 3923-31.
476. Nawa, H., J. Carnahan, and C. Gall, *BDNF protein measured by a novel enzyme immunoassay in normal brain and after seizure: partial disagreement with mRNA levels*. Eur J Neurosci, 1995. **7**(7): p. 1527-35.
477. von Bartheld, C.S., et al., *Anterograde transport of neurotrophins and axodendritic transfer in the developing visual system*. Nature, 1996. **379**(6568): p. 830-3.

478. von Bartheld, C.S., X. Wang, and R. Butowt, *Anterograde axonal transport, transcytosis, and recycling of neurotrophic factors: the concept of trophic currencies in neural networks*. Mol Neurobiol, 2001. **24**(1-3): p. 1-28.
479. Conner, J.M., J.C. Lauterborn, and C.M. Gall, *Anterograde transport of neurotrophin proteins in the CNS--a reassessment of the neurotrophic hypothesis*. Rev Neurosci, 1998. **9**(2): p. 91-103.
480. Farhadi, H.F., et al., *Neurotrophin-3 sorts to the constitutive secretory pathway of hippocampal neurons and is diverted to the regulated secretory pathway by coexpression with brain-derived neurotrophic factor*. J Neurosci, 2000. **20**(11): p. 4059-68.
481. Johnson, F., et al., *Neurotrophins suppress apoptosis induced by deafferentation of an avian motor-cortical region*. J Neurosci, 1997. **17**(6): p. 2101-11.
482. Mowla, S.J., et al., *Differential sorting of nerve growth factor and brain-derived neurotrophic factor in hippocampal neurons*. J Neurosci, 1999. **19**(6): p. 2069-80.
483. Nieto-Bona, M.P., L.M. Garcia-Segura, and I. Torres-Aleman, *Orthograde transport and release of insulin-like growth factor I from the inferior olive to the cerebellum*. J Neurosci Res, 1993. **36**(5): p. 520-7.
484. Adachi, N., K. Kohara, and T. Tsumoto, *Difference in trafficking of brain-derived neurotrophic factor between axons and dendrites of cortical neurons, revealed by live-cell imaging*. BMC Neurosci, 2005. **6**: p. 42.
485. Butowt, R. and C.S. von Bartheld, *Conventional kinesin-I motors participate in the anterograde axonal transport of neurotrophins in the visual system*. J Neurosci Res, 2007. **85**(12): p. 2546-56.
486. Colin, E., et al., *Huntingtin phosphorylation acts as a molecular switch for anterograde/retrograde transport in neurons*. EMBO J, 2008. **27**(15): p. 2124-34.
487. Kokaia, Z., et al., *Rapid alterations of BDNF protein levels in the rat brain after focal ischemia: evidence for increased synthesis and anterograde axonal transport*. Exp Neurol, 1998. **154**(2): p. 289-301.
488. Michael, G.J., et al., *Axotomy results in major changes in BDNF expression by dorsal root ganglion cells: BDNF expression in large *trkB* and *trkC* cells, in pericellular baskets, and in projections to deep dorsal horn and dorsal column nuclei*. Eur J Neurosci, 1999. **11**(10): p. 3539-51.
489. Tonra, J.R., *Classical and novel directions in neurotrophin transport and research: anterograde transport of brain-derived neurotrophic factor by sensory neurons*. Microsc Res Tech, 1999. **45**(4-5): p. 225-32.

490. Tonra, J.R., et al., *Axotomy upregulates the anterograde transport and expression of brain-derived neurotrophic factor by sensory neurons*. J Neurosci, 1998. **18**(11): p. 4374-83.
491. Kohara, K., et al., *Activity-dependent transfer of brain-derived neurotrophic factor to postsynaptic neurons*. Science, 2001. **291**(5512): p. 2419-23.
492. Gottmann, K., T. Mittmann, and V. Lessmann, *BDNF signaling in the formation, maturation and plasticity of glutamatergic and GABAergic synapses*. Exp Brain Res, 2009. **199**(3-4): p. 203-34.
493. Bustos, G., et al., *Functional interactions between somatodendritic dopamine release, glutamate receptors and brain-derived neurotrophic factor expression in mesencephalic structures of the brain*. Brain Res Brain Res Rev, 2004. **47**(1-3): p. 126-44.
494. Fischer, D.L. and C.E. Sortwell, *BDNF provides many routes toward STN DBS-mediated disease modification*. Mov Disord, 2019. **34**(1): p. 22-34.
495. Yurek, D.M., et al., *BDNF enhances the functional reinnervation of the striatum by grafted fetal dopamine neurons*. Exp Neurol, 1996. **137**(1): p. 105-18.
496. Parain, K., et al., *Reduced expression of brain-derived neurotrophic factor protein in Parkinson's disease substantia nigra*. Neuroreport, 1999. **10**(3): p. 557-61.
497. Burke, R.E. and K. O'Malley, *Axon degeneration in Parkinson's disease*. Exp Neurol, 2013. **246**: p. 72-83.
498. O'Malley, K.L., *The role of axonopathy in Parkinson's disease*. Exp Neurobiol, 2010. **19**(3): p. 115-9.
499. Tagliaferro, P. and R.E. Burke, *Retrograde Axonal Degeneration in Parkinson Disease*. J Parkinsons Dis, 2016. **6**(1): p. 1-15.
500. Nordstroma, U., et al., *Progressive nigrostriatal terminal dysfunction and degeneration in the engrailed1 heterozygous mouse model of Parkinson's disease*. Neurobiol Dis, 2015. **73**: p. 70-82.
501. Altar, C.A., et al., *Efficacy of brain-derived neurotrophic factor and neurotrophin-3 on neurochemical and behavioral deficits associated with partial nigrostriatal dopamine lesions*. J Neurochem, 1994. **63**(3): p. 1021-32.
502. Knusel, B., et al., *Promotion of central cholinergic and dopaminergic neuron differentiation by brain-derived neurotrophic factor but not neurotrophin 3*. Proc Natl Acad Sci U S A, 1991. **88**(3): p. 961-5.

503. Beck, K.D., B. Knusel, and F. Hefti, *The nature of the trophic action of brain-derived neurotrophic factor, des(1-3)-insulin-like growth factor-1, and basic fibroblast growth factor on mesencephalic dopaminergic neurons developing in culture*. Neuroscience, 1993. **52**(4): p. 855-66.
504. Hyman, C., et al., *Overlapping and distinct actions of the neurotrophins BDNF, NT-3, and NT-4/5 on cultured dopaminergic and GABAergic neurons of the ventral mesencephalon*. J Neurosci, 1994. **14**(1): p. 335-47.
505. Zhou, J., H.F. Bradford, and G.M. Stern, *The stimulatory effect of brain-derived neurotrophic factor on dopaminergic phenotype expression of embryonic rat cortical neurons in vitro*. Brain Res Dev Brain Res, 1994. **81**(2): p. 318-24.
506. Blochl, A. and C. Sirrenberg, *Neurotrophins stimulate the release of dopamine from rat mesencephalic neurons via Trk and p75Lntnr receptors*. J Biol Chem, 1996. **271**(35): p. 21100-7.
507. Shen, R.Y., C.A. Altar, and L.A. Chiodo, *Brain-derived neurotrophic factor increases the electrical activity of pars compacta dopamine neurons in vivo*. Proc Natl Acad Sci U S A, 1994. **91**(19): p. 8920-4.
508. Stefani, A., et al., *Subthalamic nucleus deep brain stimulation on motor-symptoms of Parkinson's disease: Focus on neurochemistry*. Prog Neurobiol, 2017. **151**: p. 157-174.
509. Cirillo, J., et al., *Differential modulation of motor cortex excitability in BDNF Met allele carriers following experimentally induced and use-dependent plasticity*. Eur J Neurosci, 2012. **36**(5): p. 2640-9.
510. Schinder, A.F. and M. Poo, *The neurotrophin hypothesis for synaptic plasticity*. Trends Neurosci, 2000. **23**(12): p. 639-45.
511. Rauskolb, S., et al., *Global deprivation of brain-derived neurotrophic factor in the CNS reveals an area-specific requirement for dendritic growth*. J Neurosci, 2010. **30**(5): p. 1739-49.
512. McNeill, T.H., et al., *Atrophy of medium spiny I striatal dendrites in advanced Parkinson's disease*. Brain Res, 1988. **455**(1): p. 148-52.
513. Spieles-Engemann, A.L., T.J. Collier, and C.E. Sortwell, *A functionally relevant and long-term model of deep brain stimulation of the rat subthalamic nucleus: advantages and considerations*. Eur J Neurosci, 2010. **32**(7): p. 1092-9.
514. Milber, J.M., et al., *Lewy pathology is not the first sign of degeneration in vulnerable neurons in Parkinson disease*. Neurology, 2012. **79**(24): p. 2307-14.

515. Greffard, S., et al., *A stable proportion of Lewy body bearing neurons in the substantia nigra suggests a model in which the Lewy body causes neuronal death*. Neurobiol Aging, 2010. **31**(1): p. 99-103.
516. Collier, T.J., et al., *Striatal trophic factor activity in aging monkeys with unilateral MPTP-induced parkinsonism*. Exp Neurol, 2005. **191 Suppl 1**: p. S60-7.
517. Yurek, D.M. and A. Fletcher-Turner, *Lesion-induced increase of BDNF is greater in the striatum of young versus old rat brain*. Exp Neurol, 2000. **161**(1): p. 392-6.
518. Kita, T. and H. Kita, *The subthalamic nucleus is one of multiple innervation sites for long-range corticofugal axons: a single-axon tracing study in the rat*. J Neurosci, 2012. **32**(17): p. 5990-9.
519. Okun, M.S., et al., *Development and initial validation of a screening tool for Parkinson disease surgical candidates*. Neurology, 2004. **63**(1): p. 161-3.
520. Moro, E., et al., *A decision tool to support appropriate referral for deep brain stimulation in Parkinson's disease*. J Neurol, 2009. **256**(1): p. 83-8.
521. May, V.E., et al., *alpha-Synuclein impairs oligodendrocyte progenitor maturation in multiple system atrophy*. Neurobiol Aging, 2014. **35**(10): p. 2357-68.
522. Segura-Ulate, I., et al., *FTY720 (Fingolimod) reverses alpha-synuclein-induced downregulation of brain-derived neurotrophic factor mRNA in OLN-93 oligodendroglial cells*. Neuropharmacology, 2017. **117**: p. 149-157.
523. Vargas-Medrano, J., et al., *FTY720-Mitoxy reduces toxicity associated with MSA-like alpha-synuclein and oxidative stress by increasing trophic factor expression and myelin protein in OLN-93 oligodendroglia cell cultures*. Neuropharmacology, 2019. **158**: p. 107701.
524. Ventriglia, M., et al., *Serum brain-derived neurotrophic factor levels in different neurological diseases*. Biomed Res Int, 2013. **2013**: p. 901082.